Trends in Auckland's air quality 2006-2018

Nick Talbot and Paul Crimmins

February 2020 Technical Report 2020/004

Research and Evaluation Unit | RIMU

Auckland Council
Te Kaunihera o Tāmaki Makaurau

Trends in Auckland's air quality 2006-2018

February 2020 Technical Report 2020/004

Nick Talbot

Paul Crimmins

Auckland Council
Technical Report 2020/004

ISSN 2230-4525 (Print)
ISSN 2230-4533 (Online)

ISBN 978-1-99-002204-3 (Print)
ISBN 978-1-99-002205-0 (PDF)

This report has been peer reviewed by the Peer Review Panel.
Review completed on 3 February 2020 Reviewed by two reviewers
Approved for Auckland Council publication by: Name: Eva McLaren Position: Manager, Research and Evaluation (RIMU)
Name: Megan Carbines Position: Manager, Air, Land and Biodiversity (RIMU
Date: 3 February 2020

Recommended citation

Talbot, N and P Crimmins (2020). Trends in Auckland's air quality 2006-2018. Auckland Council technical report, TR2020/004

Cover image: Air quality monitoring shed Penrose, Auckland. Photograph by Woodrow Pattinson, Mote Ltd

Executive summary

Pollutants in the air cause adverse health effects and reduced visibility. Air pollution in the Auckland region has been monitored by Auckland Council since the late 1990s at representative monitoring sites using high-accuracy equipment in accordance with applicable Australian and New Zealand standards. The purpose of the regional air quality monitoring programme is to ensure that there is good scientific understanding of pollutant levels, trends and sources, in order for Auckland Council to manage air quality. In addition, regional councils have a responsibility to monitor and manage outdoor air quality under the Resource Management Act 1991.

Trends in air pollution across the Auckland air quality network between 2006 and 2018 (inclusive) are reported here. Statistical analysis has been split into two separate time considerations, long-term (2006-2018) and short-term (2013-2018). Seasonal and deseasonalised statistics are provided for both time periods and for all measured variables across the Auckland network. Source apportionment data for fine particulate matter (PM_{10} and $PM_{2.5}$) has been included in the analysis where available to identify emission sources.

In most locations, PM_{10} and $PM_{2.5}$ had statistically significant decreasing monotonic trends for both short- and long-term timeframes. Queen Street is not following this trend. This city centre site has shown significant increases in $PM_{2.5}$ and PM_{10} for the short-term analysis ($P<0.001$ and $P<0.1$, respectively).

Nitrogen dioxide (NO_2) shows marked decreases in concentration over the long-term; however, short-term trends are starting to show increases in concentration at several sites near major roads. Queen Street has shown a statistically significant increase in NO_2 since 2013 ($P<0.001$) and has for the past two years exceeded Auckland's ambient air quality target for NO_2 of 40 $\mu g/m^3$ per annum.

This report provides an analysis of air quality across Auckland, changes over time, key factors driving the observed patterns and how policy and regulatory responses impact the quality of Auckland's air. The need for more city centre monitoring is apparent to further investigate recently increasing trends.

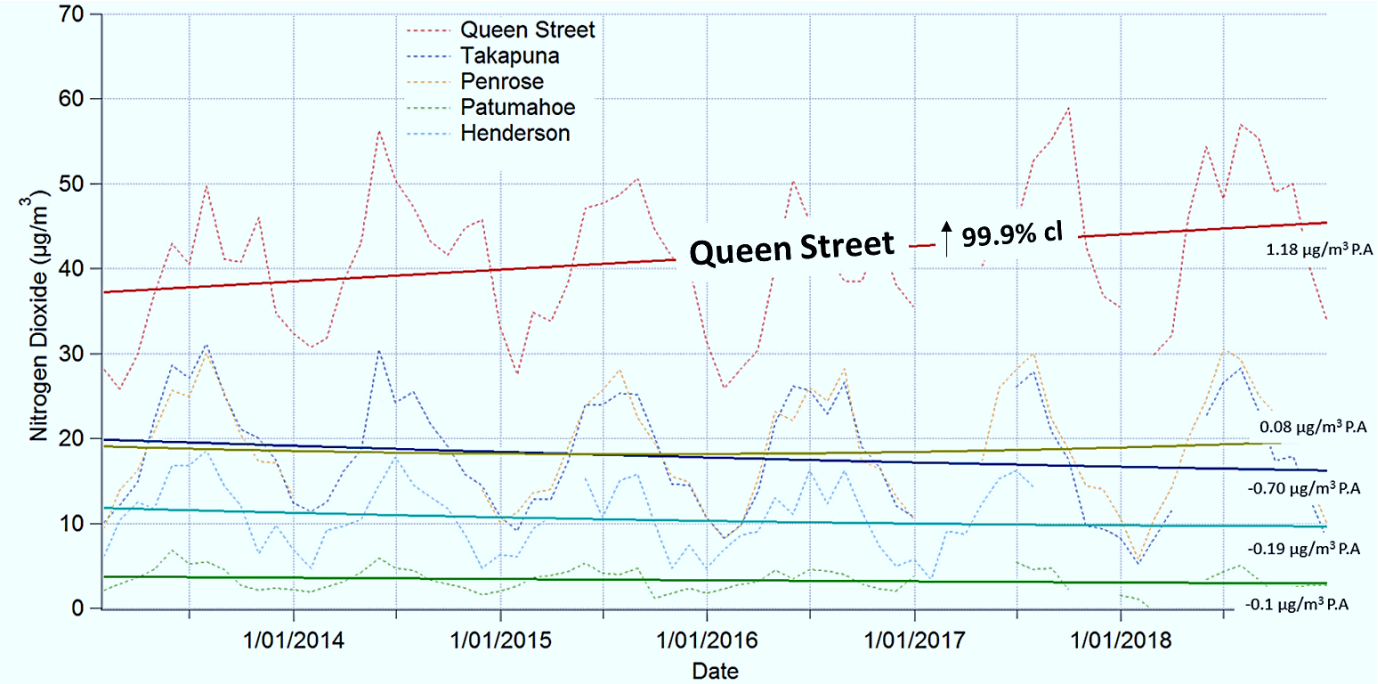

Figure 1 Monthly NO_2 concentrations and trends across Auckland's ambient air quality network, 2013-2018.

Acknowledgement

The air quality monitoring data for this report was collected on contract to Auckland Council by Watercare Laboratory Services Ltd and Mote Ltd with thanks from the authors for its accuracy and completeness.

Thank you to the peer reviewers of this report for useful comments and recommendations.

Table of contents

List of figures

Appendix figures

List of tables

1.0 Introduction

Auckland sits on an isthmus between the Tasman Sea and the South Pacific. With no landmass close to the east or west of the city, a relatively clean and reliable airflow is enjoyed by Auckland, helping remove air pollutants emitted across the region. Despite this, Auckland still manages to self-pollute to levels which can exceed national and international standards and to a degree which impacts people's health (Kuschel et al., 2012; Dirks et al., 2017) .

Auckland's urban setting means that emissions from transport, domestic heating (the use of solid fuels such as wood and coal) and industry combine to add pressure upon the environment and degrade air quality, particularly during winter. This mixture of gases and particles impacts human health and well-being.

The World Health Organisation (2013) has identified that exposure to outdoor air pollution is a leading cause of global mortality and morbidity and that exposure to urban air pollution is carcinogenic to humans. Therefore, it is important to minimise air pollution levels as far as practicable.

The purpose of the regional air quality monitoring programme is to ensure that there is good scientific understanding of pollutant levels, trends and sources, in order for Auckland Council to manage air quality and reduce pollutant levels. In addition, regional councils have a responsibility to monitor and manage outdoor air quality under the Resource Management Act 1991 (RMA) and the National Environmental Standards for Air Quality (NESAQ) are mandatory environmental standards (see section 1.2).

Auckland Council has monitored air pollution at representative sites using high-accuracy continuous ambient air quality monitoring equipment for more than two decades (Figure 2). This monitoring data is used to infer typical air pollution exposure levels experienced by Auckland's citizens and assess compliance with regulatory standards. The monitoring programme covers key air pollutants that come from a variety of emission sources (monitored pollutants are outlined in Section 1.1).Transport emissions are the main source of air pollutants in Auckland (Davy et al., 2017; Xie et al., 2014). Residential wood burning and industry also make important contributions to air pollutant levels. Combustion emissions include fine particulate matter (including black carbon), volatile organic compounds (such as benzene) and nitrogen dioxide. Nitrogen dioxide can occur directly from combustion processes and because of the conversion of nitric oxide gas (also produced from combustion processes) reacting in the atmosphere in the presence of ozone.

Other gases (such as sulphur dioxide and ozone) and secondary particulate (sulphates and nitrates) can form in the atmosphere from reactions involving some of these primary emissions.

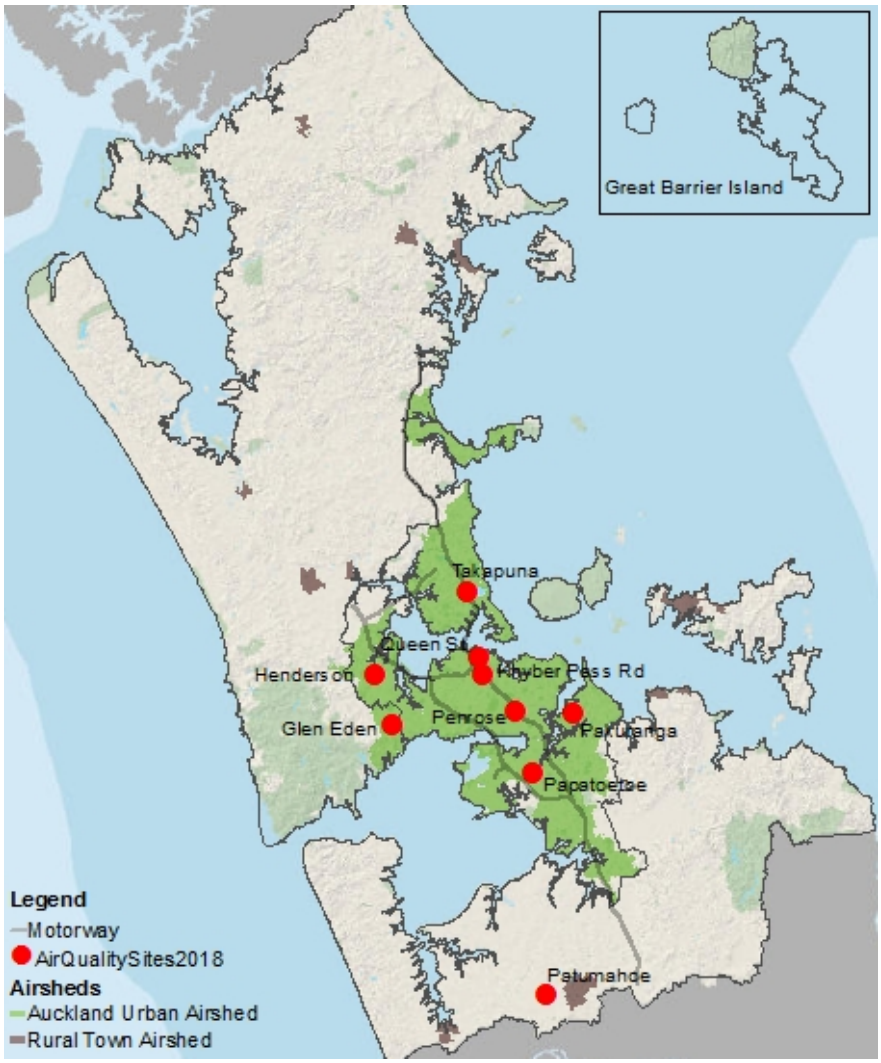

Figure 2 Map of the current air quality monitoring sites across Auckland.

1.1 Monitored air pollutants

1.1.1 PM_{10} and coarse particulate

Particulates (liquid and solid particles) in the atmosphere that have an aerodynamic diameter of 10 microns (μm) and smaller are measured and reported as PM_{10}. Although PM_{10} includes all particle sizes up to 10 μm, including 'ultra-fine particles' less than 0.1 μm, the 'coarse mode' particulates (2.5-10μm) tend to contribute disproportionately to the PM_{10} mass. PM_{10} is a Hazardous Air Pollutant owing to its significant risks to human health (particularly to the respiratory system) (WHO, 2013). Combustion derived particulate makes up 44% of total particulate concentrations ($PM_{2.5}$ and PM_{10}, combined) (Davy et al., 2017). The PM_{10} size fraction is predominantly released from

biogenic (natural) sources such as soil and rock abrasion released as dust (Carslaw et al., 2010). There is also a notable contribution across the Auckland region from sea salt, which can make up the majority of PM_{10} mass during summertime (Davy et al., 2017). Non-exhaust transport sources of PM_{10}, brake and tyre wear and unsealed road dust, are deposited rapidly due to gravitational force but are often resuspended into the atmosphere through vehicle induced air turbulence alongside roads (Xie et al., 2016).

1.1.2 Fine particulate ($PM_{2.5}$)

Fine particulates are smaller than 2.5 microns in diameter ($PM_{2.5}$). These are also counted as part of the PM_{10} data but are investigated separately due to their ability to penetrate deeper into the airways and blood stream and therefore increase the risks and range of negative health impacts (Karagulian et al., 2015). The WHO (2013) notes that $PM_{2.5}$ acts as a delivery mechanism into the bloodstream for hazardous semi-volatile pollutants and that there are no safe exposure thresholds below which health risks are not present.

Transport emissions are the major source of $PM_{2.5}$ across the Auckland region, most notably within urban centres and alongside major arterial routes (Talbot & Lehn 2018). The burning of wood for home heating is another major contributor to particulate concentrations across Auckland. These are identified in winter peaks in PM_{10} and $PM_{2.5}$ concentrations and in bottom up emission inventories (Xie et al., 2014; Metcalfe et al., 2018). Secondary sulphates are also a significant particulate source across the region. For Auckland, these will generally originate from oceanic biogenic gas emissions such as dimethyl sulphate, that then stabilise as fine particulates within the atmosphere (Davy et al., 2017).

1.1.3 Black carbon

Soot generated from combustion processes is a common type of $PM_{2.5}$ particle in urban areas. These ‘black carbon’ particles (BC) can be emitted from combustion sources (particularly diesel, coal and wood) and are known to be hazardous to human health (Janssen et al., 2011). As solar energy is absorbed by the dark particles, BC is also an atmospheric warming pollutant and has been identified as having the second greatest global warming impact (to carbon dioxide) over the industrial era (Bond et al., 2013). The major contributors to black carbon in Auckland are from diesel transport modes such as buses and trucks and wood combustion for home heating (Crimmins et al., 2019).

1.1.4 Nitrogen dioxide (NO_2)

Unlike PM_{10}, NO_2 is emitted almost entirely from human activities (except for a small contribution from volcanic emissions) (Xie et al., 2014). This makes NO_2 a particularly useful parameter in understanding manmade impacts on Auckland's air quality. NO_2 is a respiratory restrictor (WHO 2013). Concentrations of NO_2 are highest along busy road corridors, especially routes which are used by buses and heavy goods vehicles (Longely et al., 2014).

1.1.5 Sulphur dioxide (SO_2)

SO_2 is typically associated with combustion of fuels containing high levels of sulphur commonly found in heavy fuel oils used in shipping (Talbot et al., 2017). Levels of SO_2 have rapidly declined across the Auckland airshed since national regulations reduced the sulphur content of diesel and petrol. The positive impacts of this regulation are discussed by Davy et al., 2017.

1.2 Regulatory requirements

In New Zealand, monitoring and management of air quality is undertaken within defined gazetted air quality management Airsheds that are officially identified by regional councils and approved are made public by the Ministry for the Environment (MfE).

Regional councils have a responsibility to monitor and manage outdoor air quality under the Resource Management Act 1991 (RMA). The National Environmental Standards for Air Quality (NESAQ) are mandatory environmental regulations made under the RMA that:

- Include ambient air quality standards for PM_{10}, NO_2, carbon monoxide, SO_2 and ozone to protect human health (Table 1).
- Require regional councils to monitor air quality if it is likely that the ambient air quality standard for a contaminant will be breached in an airshed.
- State that an airshed is classified as polluted if it has more than one exceedance of the PM_{10} standard per 12-month period.
- State that an airshed ceases to be polluted when the PM_{10} standard has not been breached in the airshed for five years.

In accordance with these conditions, the Auckland Urban area is not currently considered to be a polluted airshed.

Table 1 National Environmental Standards for Air Quality.

Contaminant	Standard Concentration	Standard Averaging period	Allowable exceedances per year
Carbon monoxide	10 mg/m^3	8-hour	1
Particles (PM_{10})	50 µg/m^3	24-hour	1
Nitrogen dioxide	200 µg/m^3	1-hour	9
Sulphur dioxide	350 µg/m^3	1-hour	9[a]
Sulphur dioxide	570 µg/m^3	1-hour	0[a]
Ozone	150 µg/m^3	1-hour	0

Further ambient air quality targets are scheduled by the Auckland Unitary Plan (Operative in Part) (Table 2). Objectives and policies of the Auckland Unitary Plan require council to have regard to these targets to minimise potential health risks. The targets are generally in accordance with the recommendations of the World Health Organisation (2013) and include a broad range of hazardous air pollutants, and those of the NES:AQ at differing averaging periods. A full list of monitored contaminants is provided in the Appendix (Table A1), along with a chart showing the number of exceedances of the standards and targets recorded for short-term PM_{10}, $PM_{2.5}$ and NO_2 (Figure A1).

Table 2 Ambient air quality guidelines relevant to this report (Auckland Unitary Plan (Operative in Part)).

Contaminant	Target concentration	Target averaging period
Particles $PM_{2.5}$	25 µg/m^3	24-hour
Particles $PM_{2.5}$	10 µg/m^3	Annual
Particles PM_{10}	20 µg/m^3	Annual
Nitrogen dioxide	40	Annual
Nitrogen dioxide	100	24-hour
Sulphur Dioxide	120 µg/m^3	24-hour
Ozone	100 µg/m^3	8-hour

This report details air quality trends at seven of the nine currently active air quality monitoring site in Auckland. Khyber Pass and Papatoetoe are not included in this trend report due to fragmented (Khyber Pass) and short (Papatoetoe) datasets.

1.3 Data analysis methods

All quality assured datasets were compiled into a complete database, beginning at the start of the data period for each site. This formed the 'master' database for the project, on which usual descriptive tools (data period, percentage of valid data, annual averages) were calculated. The data for Auckland is captured using a Kisters software package.

Trend analysis and most plotting was completed using the Openair package for R, including the Theil-Sen tool (Carslaw & Ropkins 2012). The Openair package was specifically designed for ambient air quality data analysis and is freely available from CRAN (Comprehensive R Archive Network (www.cran.r-project.org)).

The Theil-Sen technique is an extension of the non-parametric Mann-Kendall method, and is commonly used for environmental analysis (Helsel & Hirsh, 2002). This deseasonalising statistical technique was used so comparisons could be made with the source apportionment dataset created for Auckland Council by GNS Ltd (Davy et al., 2017).

To allow comparisons with other regional council trends, seasonalised statistics for each parameter measured at each site are also provided. These statistics were calculated in the NIWA trends and analysis tool employing Mann-Kendell analysis in line with other councils air quality trend analysis (Wilton & Caldwell, 2017).

The seasonal method performs trend analysis for each season through the record and provides aggregated trends for each season. The seasons are split as follows: Summer (December, January and February), Autumn (March, April and May), Winter (June, July and August), Spring (September, October and November). This allows assessment of trends in each season to be made. For seasonal analysis, one season will only be compared to that same season in a different year. For example, Spring would be only be compared with Spring and Summer would only be compared with Summer.

Seasonal statistical techniques allow for better identification of monotonic trends from seasonal sources of pollutants (such as woodsmoke from home heating). By deseasonalising with Theil Sen, the seasonal variability is not separated within the dataset; this technique shows statistical patterns from consistent pollution sources such as on-road vehicles or natural sources such as sea salt.

PM_{10} and $PM_{2.5}$ source contributions are detailed in elemental analysis carried out since 2006 across the Auckland network (Davy et al., 2017). The results of this analysis are referred to where available to assess the causes of observed trends.

2.0 Air trends analysis across Auckland

2.1 Henderson

2.1.1 Site description

The Henderson air quality monitoring site was established at the end of 1993 and is classified as a residential peak site. Pollutants monitored at the site considered here are NO_2 and PM_{10} as well as meteorological parameters. In late 2017 a real time black carbon monitor (Aethalometer) was installed; the first in the Auckland region.

The Henderson site is located within Henderson Intermediate School set back about 10 metres from Lincoln Rd, a busy arterial route linking western suburbs to the north-western motorway (Figure 3). The land use in the area is a mixture of residential and commercial activities with Te Pai Park industrial area (mainly warehousing and light industrial activities) 500 m to the northeast and Waitakere Hospital 300 m southeast of the site. Meteorology for Henderson is provided in the appendix (Figure A2).

Figure 3 Map of the location of Henderson air quality monitoring site (Google Maps 2018).

2.1.2 PM_{10} trends and analysis

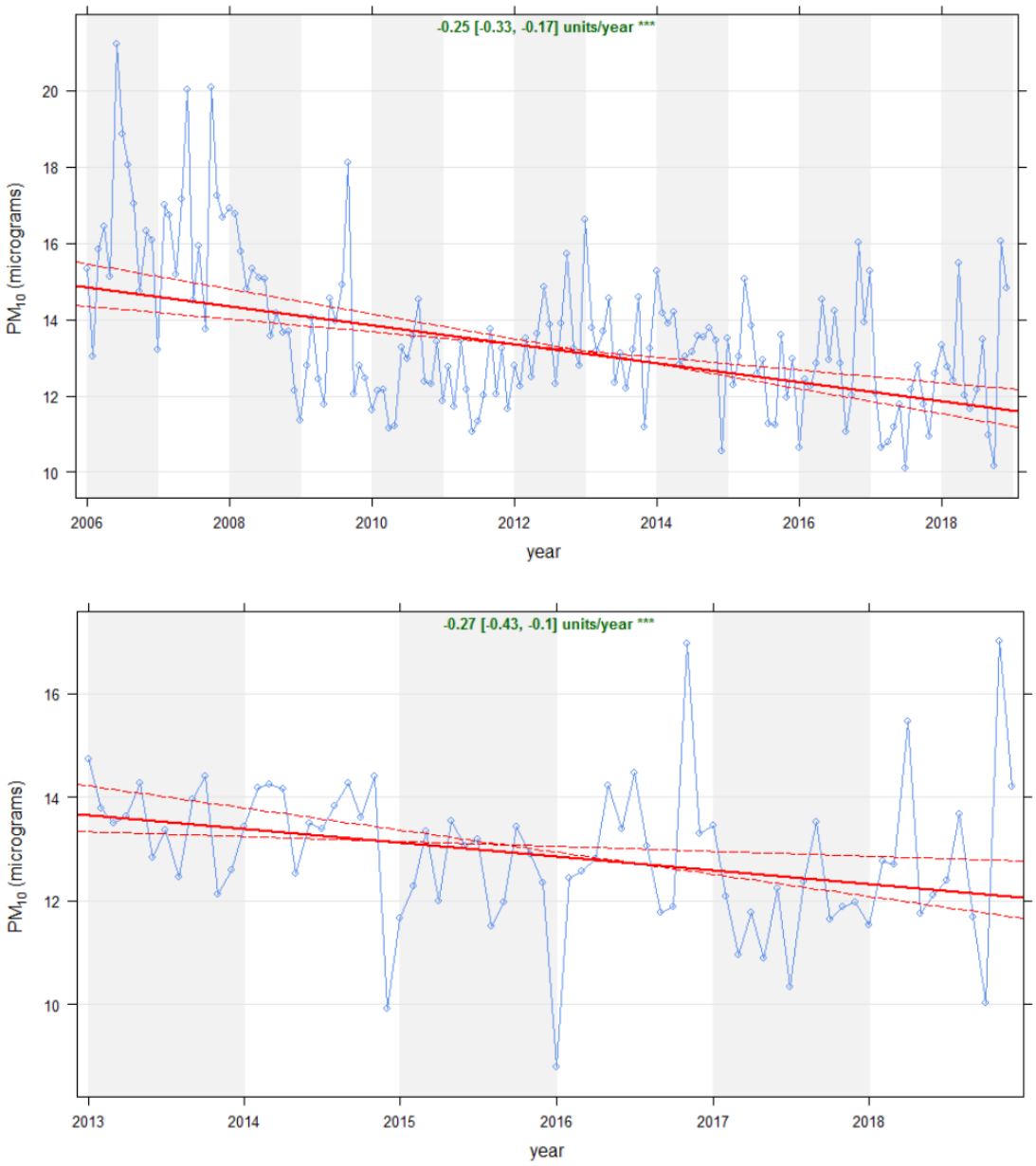

Figure 4 Theil-Sen deseasonalised trends for PM_{10} at Henderson, 2006-2018 (top) and 2013-2018 (bottom).

The deseasonalised long-term trend analysis show a 0.25 µg/m^3 year on year reduction in PM_{10} (P=<0.001), as shown by the solid red line in Figure 4, with the upper (-0.17) and lower (-0.33) variability shown by the hatched lines. There appears to be a step change in daily PM_{10} concentrations observed at Henderson during 2008 (Figure 4). This may be due to a slight relocation of the monitoring hut. Also, regulatory reductions of sulphur in fuel were introduced around this time and a reconfiguration of Lincoln Rd occurred with the inclusion of extra lanes reducing vehicle idling alongside the monitor.

In the 2013-2018 period there is still a significant downward trend in concentrations (P=<0.001). The seasonal trends shown in Table 3 agree with the long term deseasonalised trend, however, no statistically significant seasonal trend is observed for the period 2013-2018. Seasonal variability within the PM_{10} dataset is shown although not as pronounced as with NO_2 (Figure 5).

Table 3 Mann-Kendall seasonal statistical test for PM_{10} at Henderson.

Henderson: Mann-Kendell Seasonal						
Statistical Period: 2006- 2018				*Statistical Period: 2013 - 2018*		
Stats		***PM10***		***Stats***		***PM10***
probability		1		probability		0.954
Z		-3.539		Z		-1.605
p		0.000		p		0.108
Theil-Sen deseasonal p		<0.001		Theil-Sen deseasonal p		<0.001

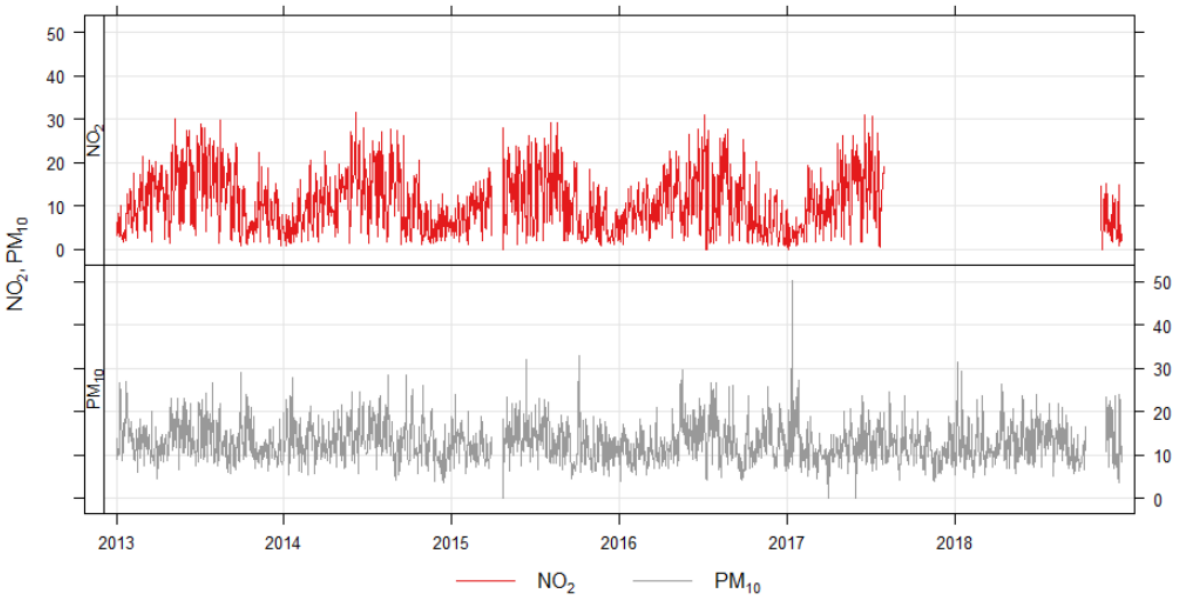

Figure 5 Time trend plot for PM_{10} and NO_2 at Henderson, 2013-2018.

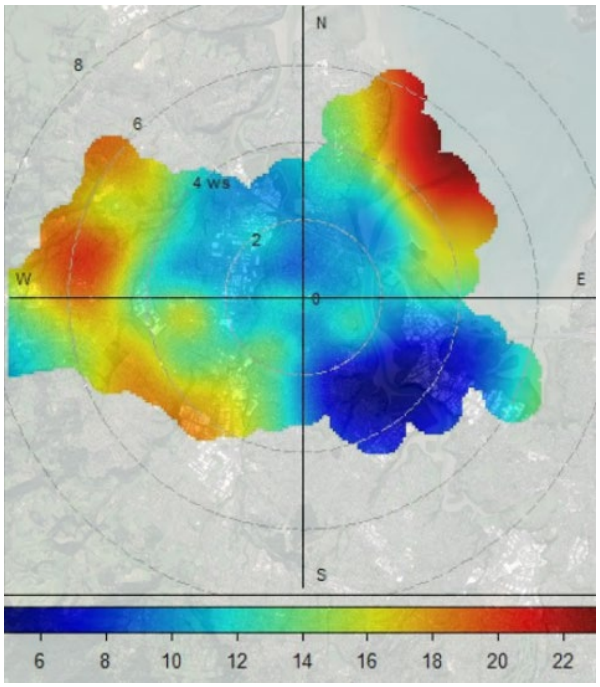

Figure 6 Polar plot showing PM_{10} concentrations at Henderson in relation to wind speed and direction, 2018.

The polar plot in Figure 6 describes PM_{10} concentrations in relation to wind speed, as defined by the circular contours across the plot, and wind direction. The plot is overlaid on a map of Henderson to indicate source-location information. During 2018, there was no dominant local source for PM_{10} in Henderson. This is indicated by low PM_{10} concentrations at low wind speeds (rings close to the centre) (Figure 6). Rather, PM_{10} concentrations predominantly originate from further afield, typically from the west and north-east with peak concentrations originating from the northeast. There are notably lower concentrations from the southeast. This pattern reflects the prevailing wind directions and highest wind speeds for this site (Figure A2). Higher concentrations transported by higher winds indicate that sea salt originating from the Tasman sea to the west and southwest, and from the Waitemata Harbour to the north-east is the dominant source of PM_{10} at this site.

Figure 7 shows that the peak PM_{10} concentrations arise during winds from the north east, supporting results shown in Figure 6. These peaks are concentrated to January (maybe due to post tropical cyclone influences delivering an abundance of sea salt from the Pacific). Baseline PM_{10} concentrations at the Henderson air quality site mostly come from the southwest of the monitoring site signalling a year-round source. The highest concentrations occurred overnight, however there is also a strong afternoon increase in concentrations. Midweek shows the highest concentrations.

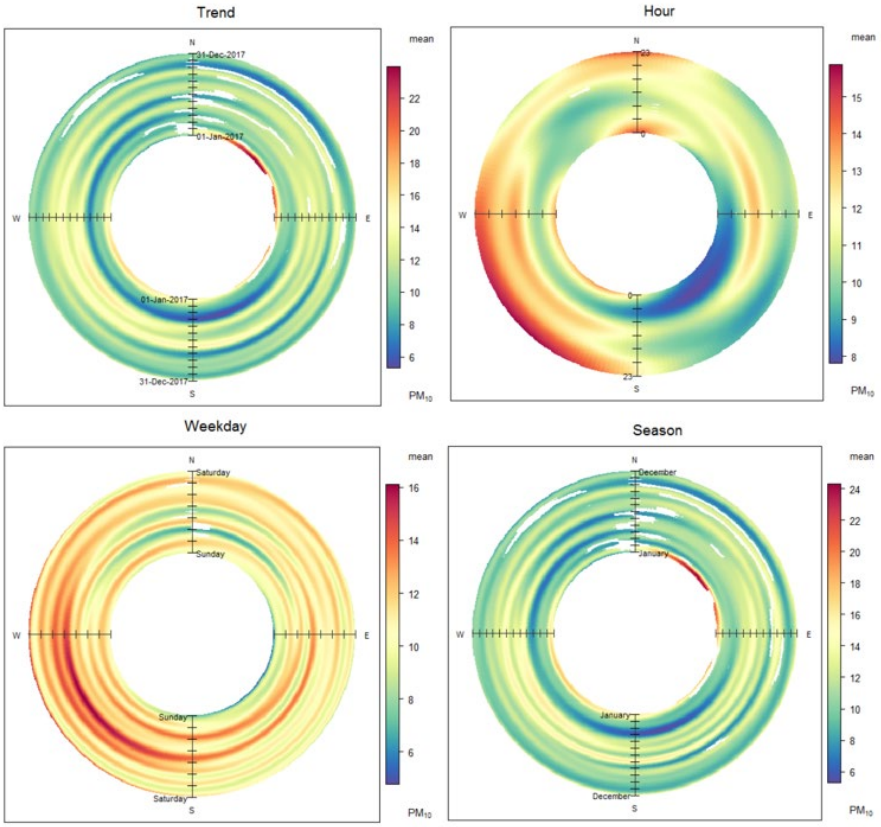

Figure 7 PolarAnnulus plots for PM_{10} at Henderson, 2017.

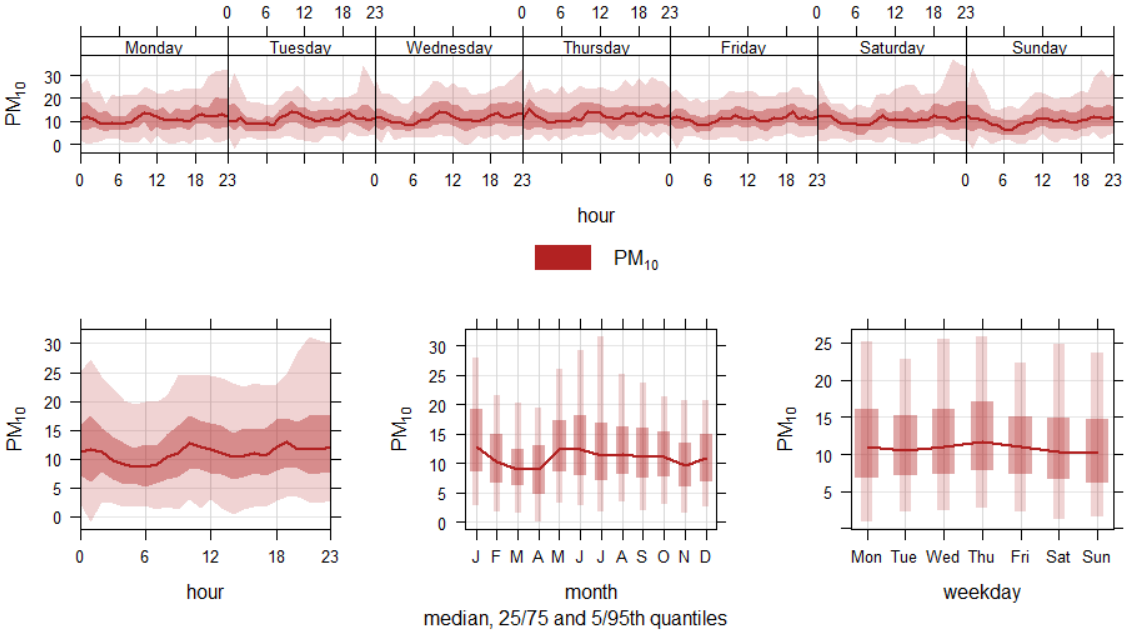

Figure 8 Temporal variability for PM_{10} at Henderson, including hourly, weekday and monthly plots, 2017.

The plots in Figure 8 provide further analysis of temporal trends based on 1-hour PM_{10} data. PM_{10} show peak concentrations occurring during mid-morning and late evening peaks, this is denoted by the shaded areas in Figure 8 showing the 95th percentile. The seasonal boxplots also show that there is a winter increase. However, January is also shown to be a peak season. Lowest concentrations are in March and April and slightly lower on weekends.

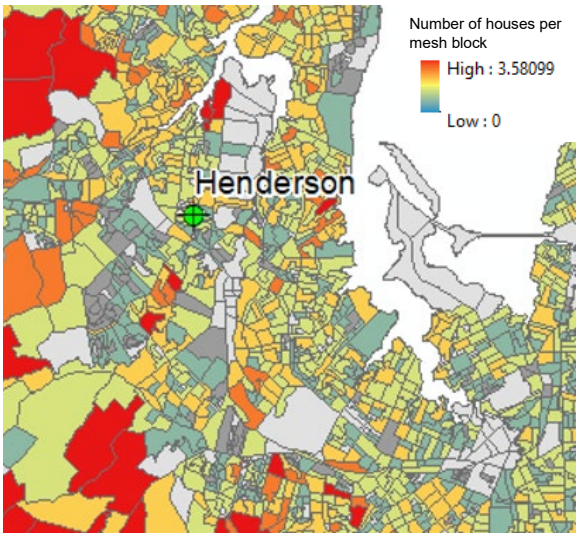

Figure 9 Density of households in Henderson that answered in the 2013 Census that they burn wood or coal for home heating.

Using source apportionment techniques to describe the key source contribution of particulate mass at the Henderson site, marine aerosol is by far the most dominant source followed by biomass burning from domestic heating (Figure 10). The distribution of housing with solid-fuel burners per mesh block is provided to help describe home heating emission variability across the area (Figure 9).

Secondary sulphate and motor vehicle sources both contribute 11% to the deseasonalised total concentration. Davy et al., 2017 reported a statistically significant decrease in sea salt contribution across Auckland during the period 2006-2013 which may help lower the total PM_{10}. These findings correspond well with the observed concentrations from Auckland Council's monitoring data. The downward trend in the long-term data would appear to be largely from reductions in secondary sulphate and marine aerosol (Figure 11) in contrast to increasing particulate contribution emanating from combustion sources.

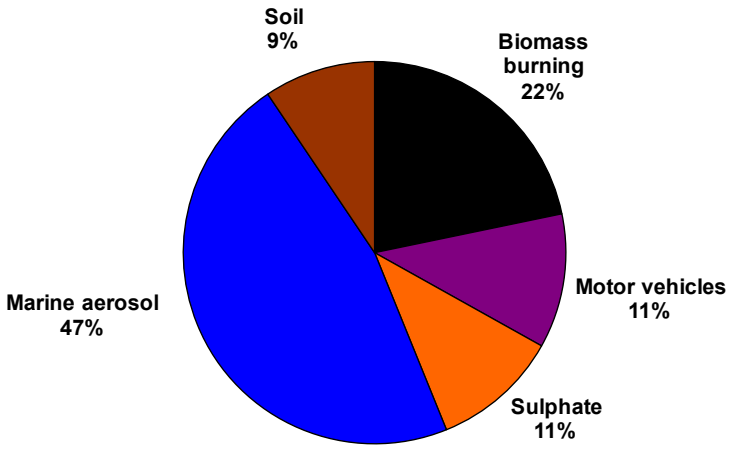

Figure 10 Source apportionment data for PM_{10} at Henderson, 2006-2013 (Davy et al., 2017).

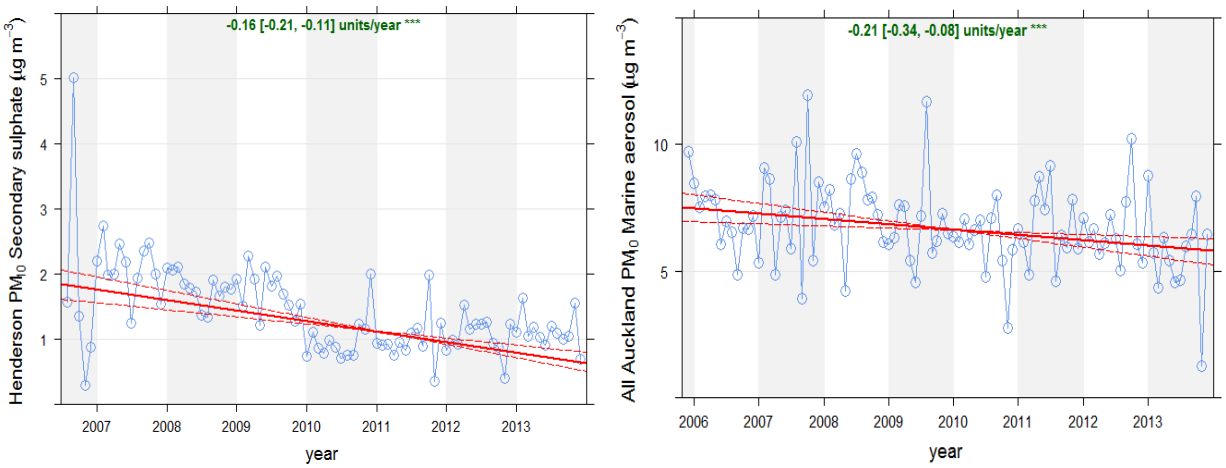

Figure 11 Temporal variability of source contributions for the PM_{10} size fraction from secondary sulphate and marine aerosol, 2006-2013 (Davy et al., 2017).

The reductions in secondary sulphate associated PM_{10} were at least partially a result of policy implementation that step-reduced the sulphur content of fuel from 50 ppm in 2007 to 10 ppm in January 2008. However, similar use of regulatory restrictions that encourage the replacement of old wood burners and limit the installation of new burners appear to be less effective, with PM_{10} contributions from home heating increasing over 2006 to 2013 (Figure 12) (Talbot et al., 2017).

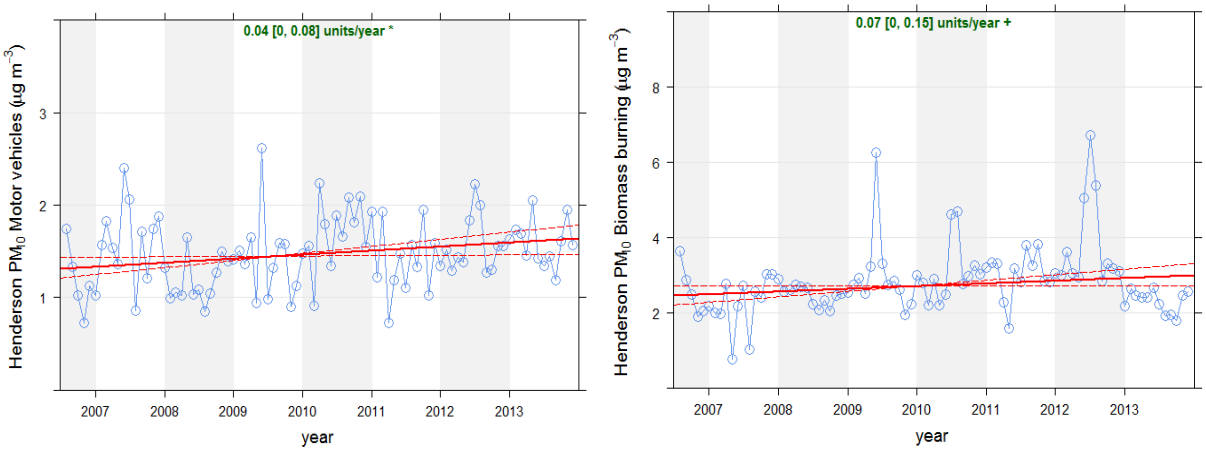

Figure 12 Temporal variability of source contributions for the PM_{10} size fraction from motor vehicles and biomass burning, 2006-2013 (Davy et al., 2017).

When describing the monitoring site data by monthly average there appears to be a baseline PM_{10} concentration of close to 12 µg/m^3. Higher concentrations occur during winter months when both biomass burning and traffic contributions are shown to increase, due to increased home heating and reduced atmospheric dispersal (Figure 13). Moreover, a smaller peak is observed in spring attributed to stronger equinox winds delivering more marine aerosol (Davy et al., 2017).

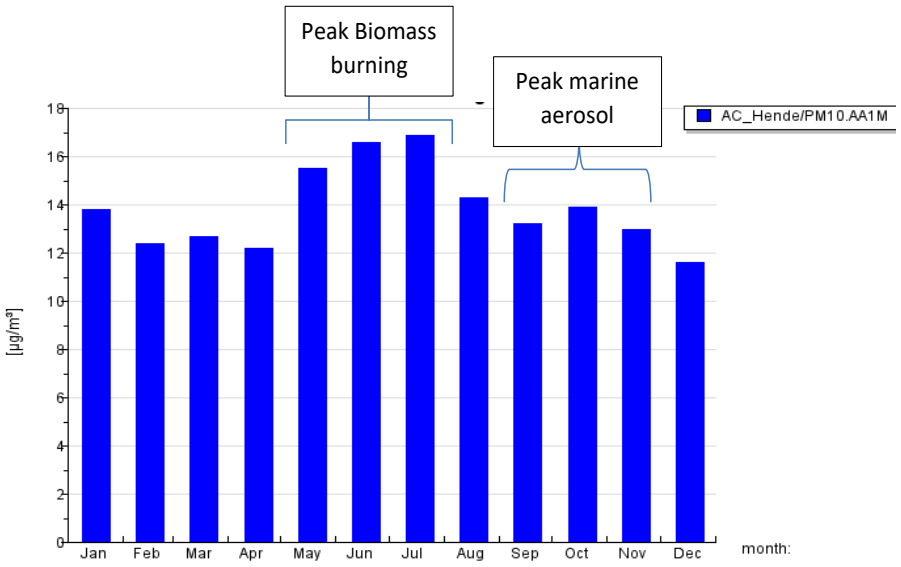

Figure 13 Monthly average PM_{10} results for 2018 from Henderson monitoring site, noting primary sources as identified by source apportionment (Davy et al., 2017).

2.1.3 Black carbon (BC) measurements

The first year of real-time BC data was recorded at Henderson in 2018. BC can be source-apportioned in real-time by measuring the light-absorbance of the particles at differing wavelengths of light. BC emitted from wood combustion has a greater proportion of organic content (sometimes termed ‘brown carbon’) than that emitted from diesel combustion and therefore, BC within woodsmoke absorbs less light at longer wavelengths (Bond et al., 2013).

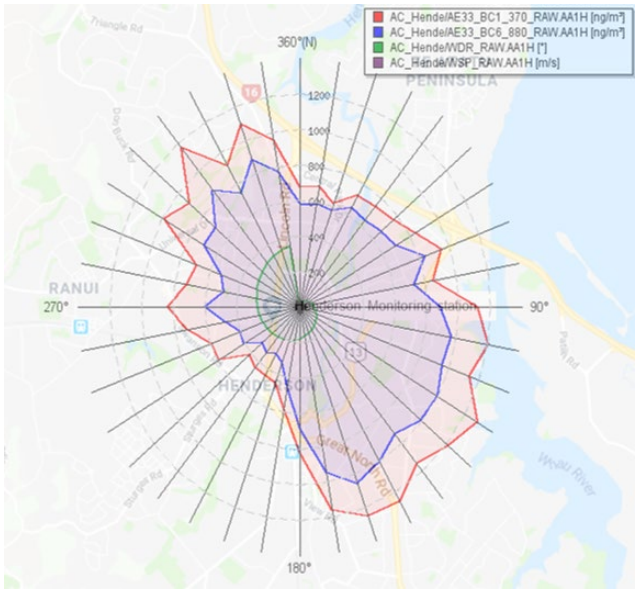

Figure 14 Concentration rose for Black Carbon at Henderson, 2018.

The peak concentrations in BC measured at both 370 nm wavelength (red line, indicative of wood smoke emissions) and 880 nm wavelengths (blue line indicative of diesel fuel emissions) are shown in Figure 14. The greatest concentrations of BC were recorded during winds from the south-east and east (from Lincoln Rd) and the north-west (residential wood burning in Massey) (Figure 14).

Figure 15 plots reveal 880 nm wavelength (diesel combustion) BC being more consistent throughout the year while the 370 nm wavelength (woodsmoke) BC concentrations are raised during the winter months, a signature from home heating sources. The BC concentrations reported by Figure 15 are method specific so should not be compared to other BC data collected elsewhere by other methods.

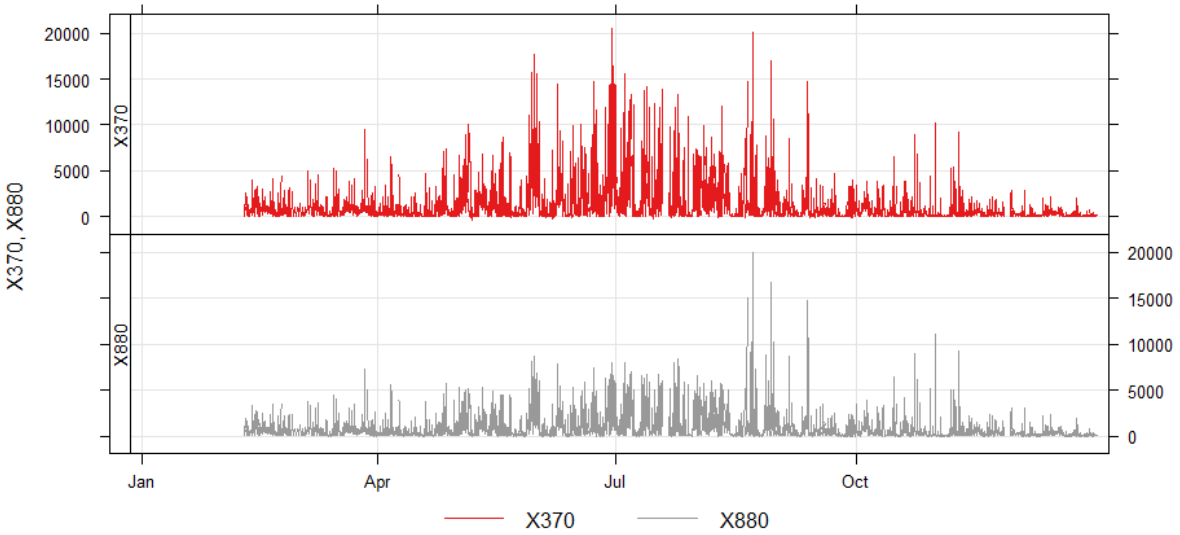

Figure 15 Temporal plot for Black Carbon concentrations (in ng/m³) measured at 370 nm (woodsmoke, top) and 880 nm (diesel, bottom) wavelengths at Henderson.

2.1.4 NO_2 trends and analysis

The long-term deseasonalised trend for NO_2 at Henderson (Figure 16 – top plot) shows a strong decrease in concentrations between 2006 and 2018 (P=<0.001). This trend is not apparent on the short-term 2013-2018 assessment (Figure 16 – lower plot) which shows no trend. The dominance of on-road vehicle emissions for NO_2 across Auckland implies that these emissions are directly from the motorway or adjacent roads (Xie et al., 2014). Lincoln Rd is a major arterial route carrying approximately 30,000 vehicles per day. There may also be significant NO_2 emissions from construction work at this site, construction activity being another major source of NO_2, globally (Font et al., 2014). The seasonal statistics provided in Table 4 agrees with the deseasonalised trends with long-term statistically significant decreases set against no statistical trend in the short-term dataset from 2013-2018.

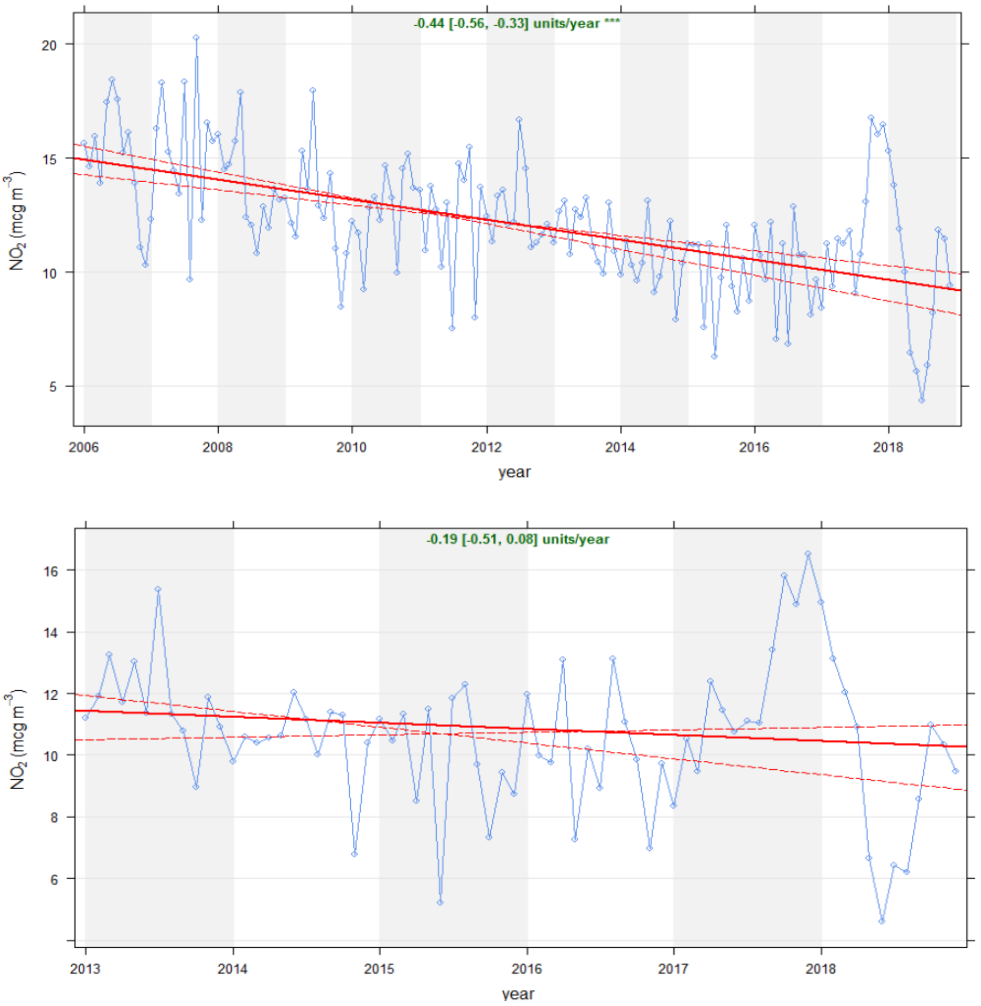

Figure 16 Theil-sen deseasonalised trends for NO_2 at Henderson, from 2006-2018 (top) and 2013-2018 (bottom).

Table 4 Mann-Kendall seasonal statistical test for NO_2 at Henderson.

Stats		***NO_2***		***Stats***		***NO_2***
probability		0.988		probability		0.719
Z		-2.241		Z		-0.635
p		0.025		p		0.525
Theil-Sen deseasonal p		<0.001		Theil-Sen deseasonal p		No trend

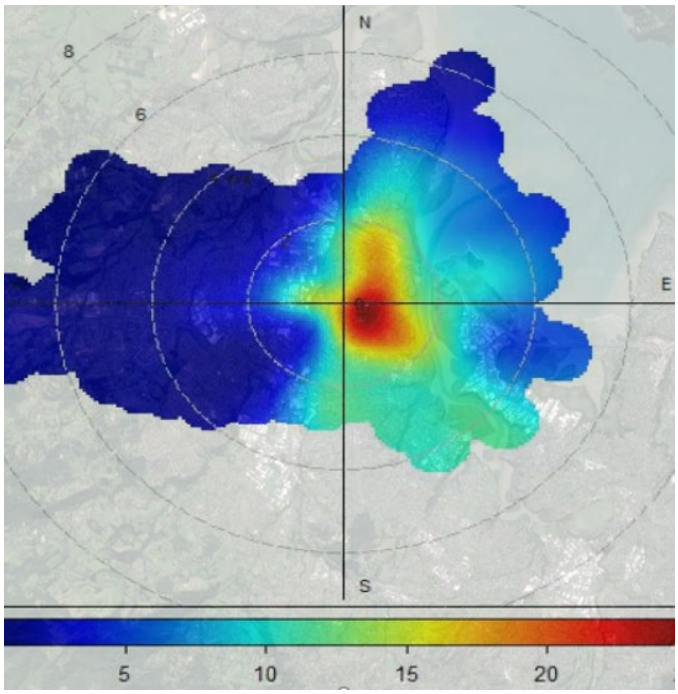

Figure 17 Polar plot showing NO_2 concentrations at Henderson in relation to wind speed and direction, 2018.

The key contributor for NO_2 at Henderson originates from the eastern side of the station (Figure 17). The busy Lincoln Rd, the north-western motorway and Auckland City are all situated to the east and are therefore likely sources. Unlike PM_{10} data, there is very little NO_2 originating from the western section indicative of the different source contribution to NO_2.

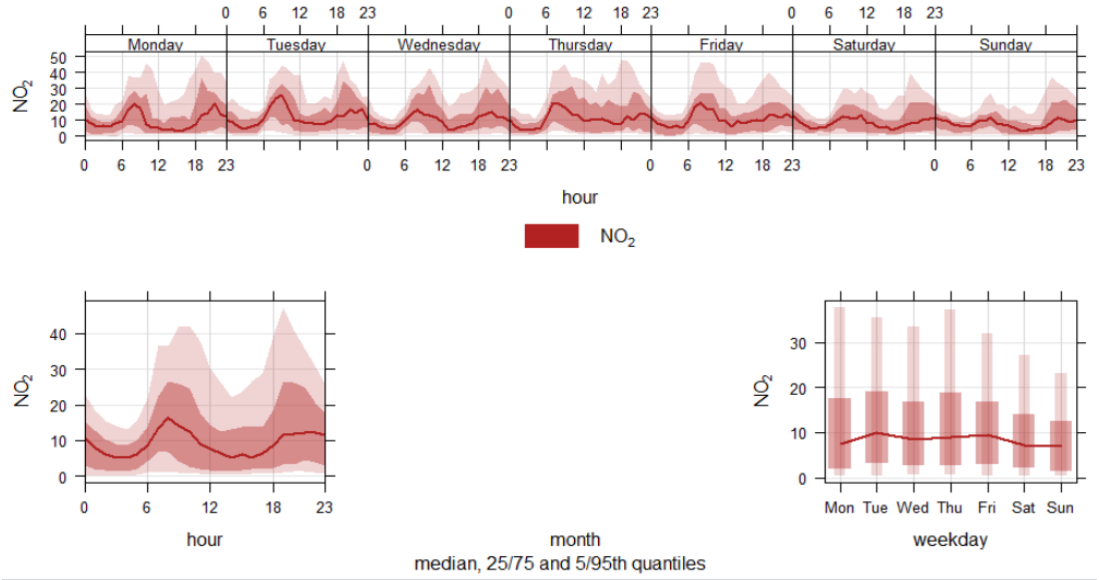

Figure 18 Temporal variability for NO_2 at Henderson, including hourly and weekday plots, 2018.

There is a clear diurnal trend for NO_2 coinciding with times of heaviest traffic volumes with morning and afternoon peaks evident (Figure 18). Higher NO_2 concentrations are also observed on weekdays compared to weekends. This is not necessarily due to less traffic on weekends, but it might be that people make their journeys later when the air is more mixed and therefore, there are not the same the increases in NO_2 concentrations. Due to lost data in 2018, monthly plots are not available for 2018 in Figure 18. The hourly plots exemplify the strong NO_2 source contribution from the east (Figure 19). There are also clear daily demarcated NO_2 concentration peaks during heavily trafficked periods.

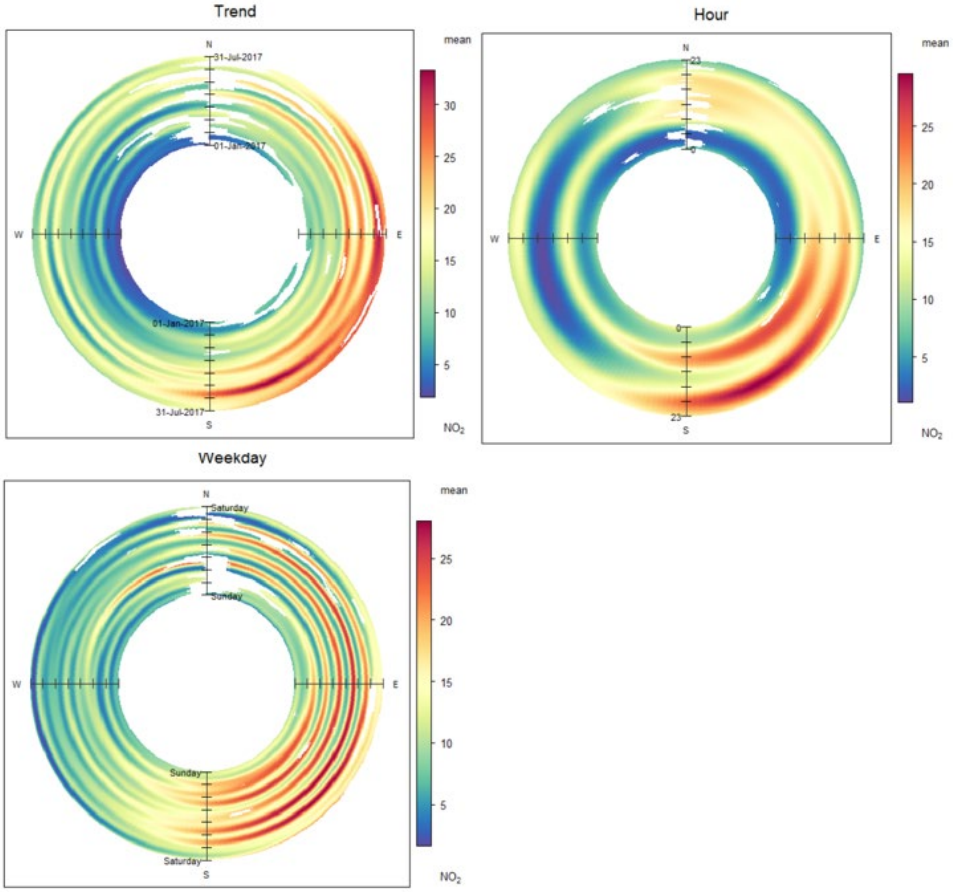

Figure 19 PolarAnnulus plots for NO_2 at Henderson, 2018.

2.2 Takapuna

2.2.1 Site description

Takapuna air quality monitoring station is located within the grounds of Westlake Girls High School, off Taharoto Road, Takapuna (Figure 20) and is approximately 3.5 km northwest of the Takapuna shopping and commercial centre and 50 m east of the Northern Motorway. Land use in the area is a mixture of residential and commercial activities with the Wairau industrial area (mainly warehousing and light industrial activities). During 2011, the fields around the monitoring stations were substantially redeveloped to provide a netball facility and artificial turf surfaces for hockey fields. Site changes and meteorological considerations for Takapuna are provided in the appendix (Figures A2 and A3).

Figure 20 Map of the location of Takapuna air quality monitoring site (Google Maps 2018).

2.2.2 PM_{10} trends and analysis

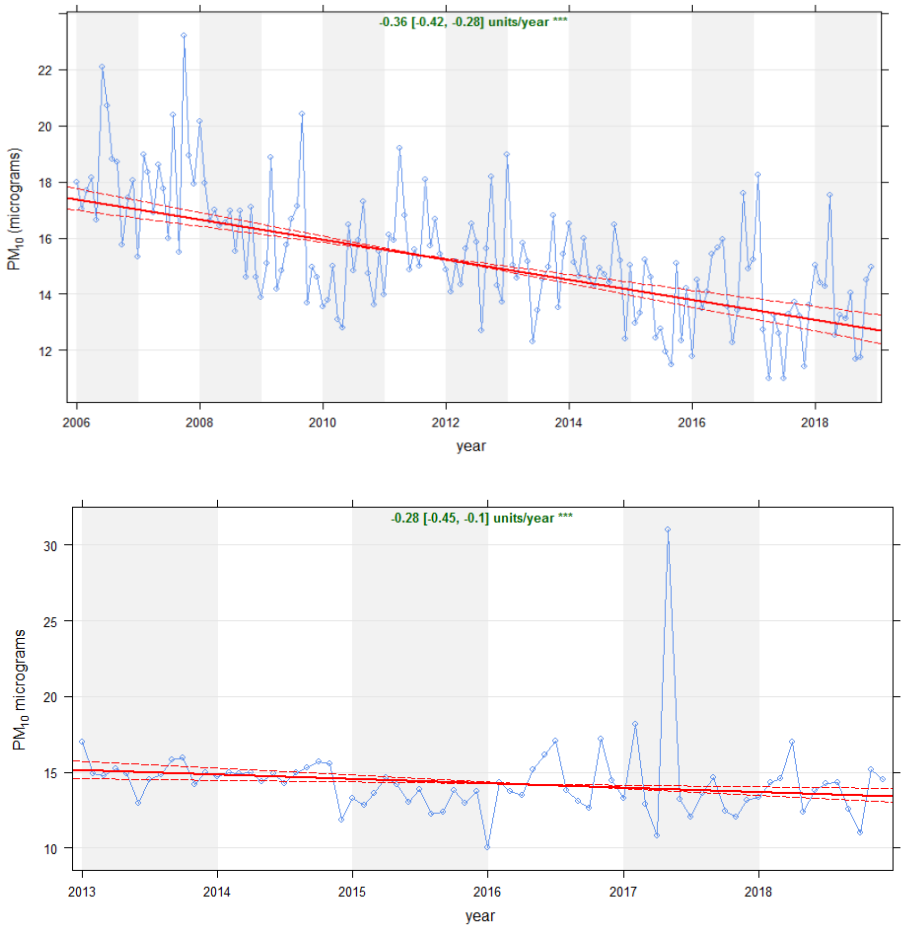

Figure 21 Theil-sen deseasonalised trends for PM_{10} at Takapuna, 2006-2018 (top) and 2013-2018 (bottom).

Long term deseasonalised trends for Takapuna PM_{10} are shown in Figure 21 (top). An overall downward trend is observed (p=<0.001). The decrease appears to be non-linear throughout the period. There appears to be a strong downward change between 2008 and 2010, a period of stability between 2010 and 2014 and then a slower but still significant downward trend between 2014 and 2018. The lower plot in Figure 21 shows the data from 2013 and 2018. Again, a strong downward trend is recorded (p=<0.001). The seasonal Mann-Kendall analysis shows a slightly lower P value (P=0.027) in the short-term analysis than the deaseasonalised Theil-sen P value (Table 5).

Table 5 Mann-Kendall seasonal statistical test for PM_{10} at Takapuna.

Takapuna: Mann-Kendell Seasonal						
2006- 2018				2013 - 2018		
Stats		***PM10***		***Stats***		***PM10***
probability		1.000		probability		0.9987
Z		-3.661		Z		-2.218
p		0.000		p		0.027
Theil-Sen deseasonal p		<0.001		Theil-Sen deseasonal p		<0.001

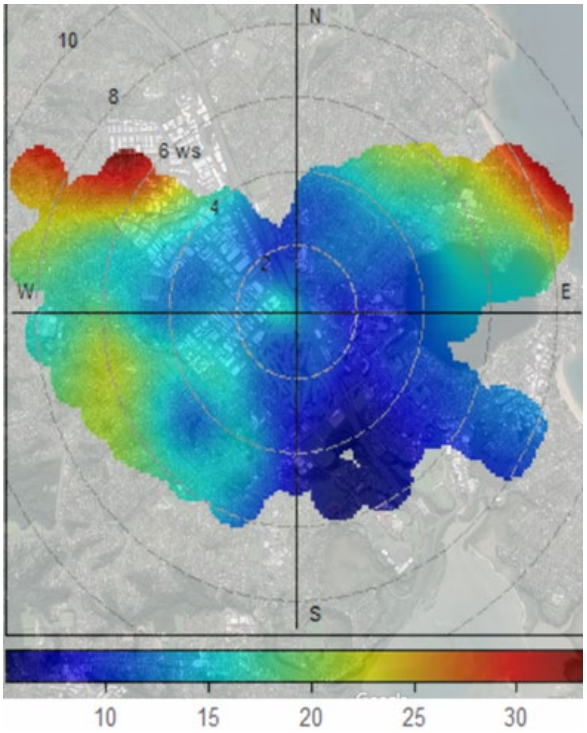

Figure 22 Polar plot showing PM_{10} concentrations at Takapuna in relation to wind speed and direction, 2018.

The polar plot (Figure 22) shows that there are two key locations where the PM_{10} concentrations are originating from, the northeast and northwest sectors (denoted by the red within the plot). The distance of the red from the apex of the circle indicates the highest concentrations occur during windy conditions. The strong winds indicate that sea salt is likely major contributing factor. This is supported by source apportionment data from Davy et al., 2017 which indicates that almost half of all PM_{10} at Takapuna comes from marine aerosol (Figure 23).

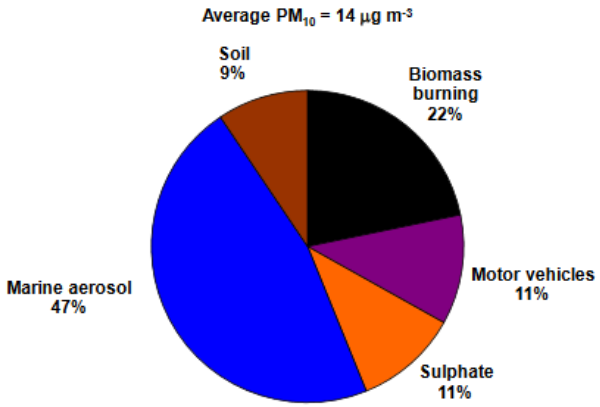

Figure 23 Source apportionment data for PM_{10} at Takapuna, 2006-2013 (Davy et al., 2017).

Biomass burning is the second largest contributing factor for PM_{10}. Given the temporal variability profile of PM_{10} shown in Figure 24 (Hour plot) it is likely that the downward trend is being created by changes in home heating emissions from the area, given that home heating is the single largest anthropogenic contribution to PM_{10} in this location. Interestingly, there is a weaker signal from the adjacent motorway on the PM_{10} Polar Plot indicative of the lower significance of vehicle emissions on the PM_{10} size fraction.

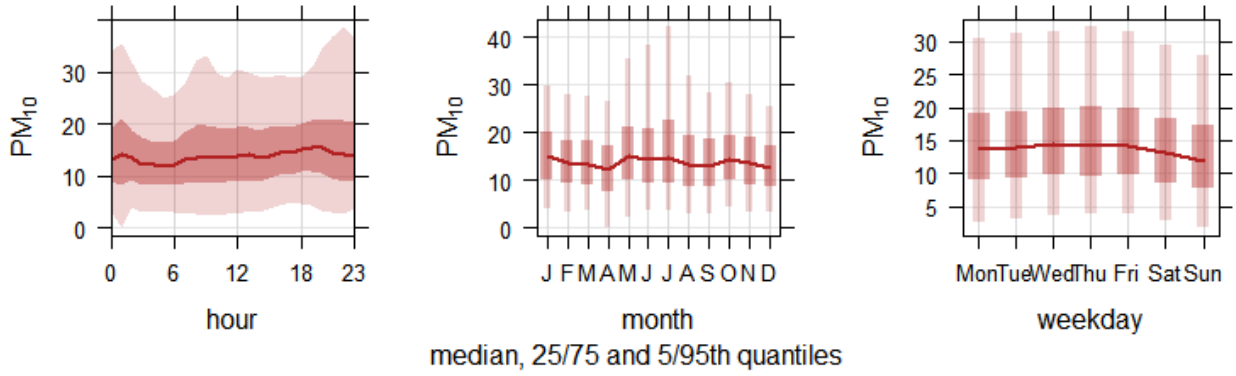

Figure 24 Temporal variability for PM_{10} at Takapuna, including hourly, weekday and monthly plots, 2006-2018.

The polar plots in Figure 26 offers broader temporal and spatial analysis. The Hourly plot (top right) supports Figure 23 showing highest concentrations arriving at the measurement site from the northwest during evening periods. The northwest area has the highest density of wood burners (Figure 25).

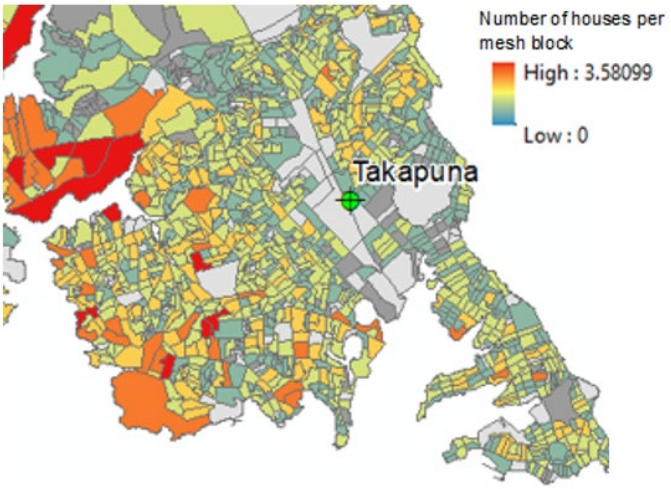

Figure 25 Density of households in Takapuna that answered in the 2013 Census that they burn wood or coal for home heating.

Given the seasonal profile for peak PM_{10} concentrations is autumn and winter, home heating combustion is a likely source. During January, there is the strongest easterly concentration. This is like Henderson's PM_{10} results, further supporting sea salt over the region delivered by seasonal storms. The weekday profile (Figure 26 – bottom left) clearly shows daily variability in PM_{10}, with the strongest signal from the west /northwest segment.

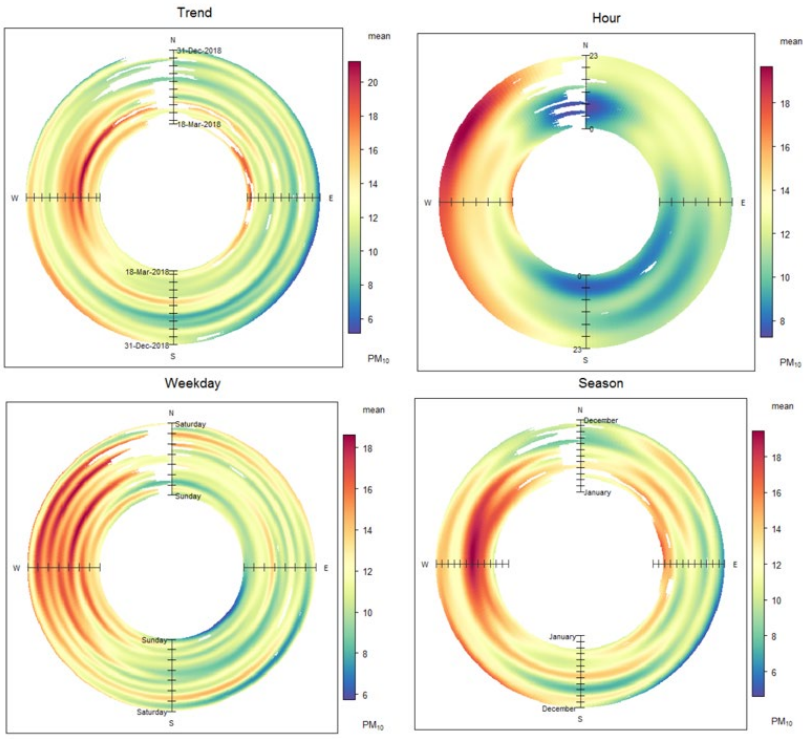

Figure 26 PolarAnnulus plots for PM_{10} at Takapuna, 2018.

2.2.3 $PM_{2.5}$ trends and analysis

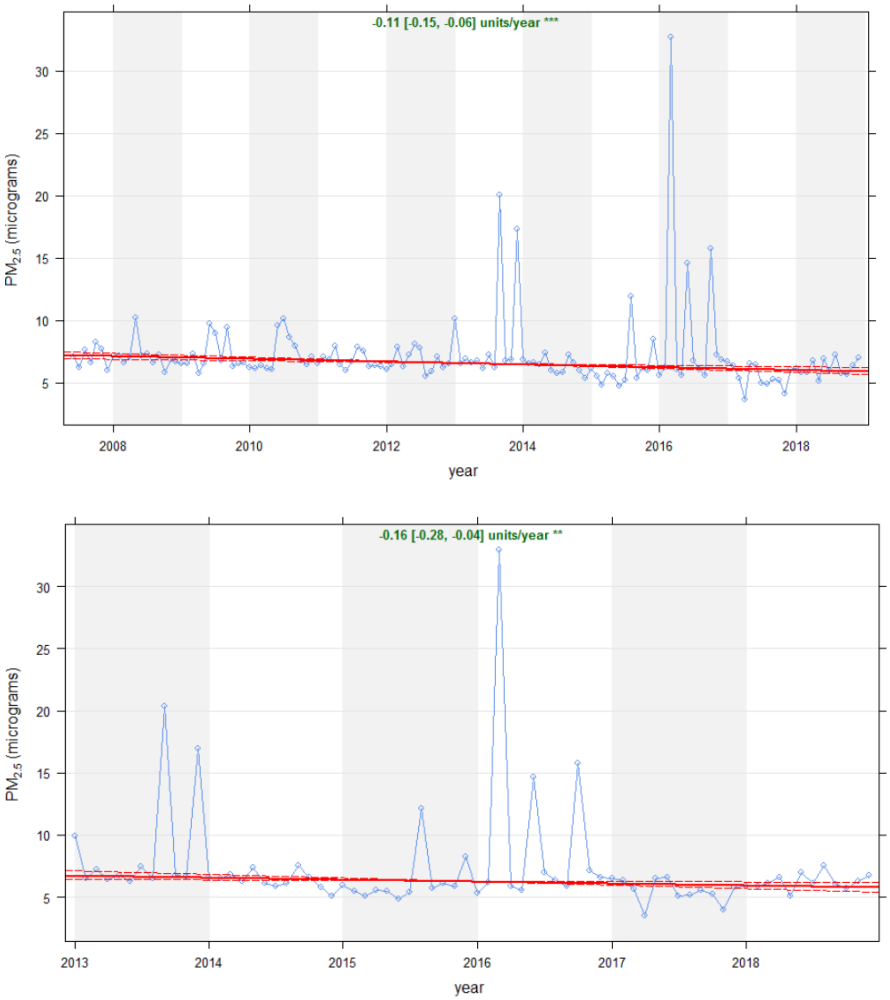

Figure 27 Theil-sen deseasonalised trends for $PM_{2.5}$ at Takapuna, 2006-2018 (top) and 2013-2018 (bottom).

The deseasonalised $PM_{2.5}$ trends for Takapuna are presented in Figure 27. The long-term trend shows a strong decrease in concentrations (P=<0.001). The spikes in data from 2016 are unexplained. Since 2013 the decrease has slowed somewhat with a still significant trend (P=<0.01). Since 2017, concentrations have levelled off and may now be showing signs of increasing slightly. When looking at a seasonal variability in Table 6 the trend is not observed with a weak trend (P= 0.319) for the 2013-2018 data.

Table 6 Mann-Kendall seasonal statistical test for $PM_{2.5}$ at Henderson.

Takapuna: Mann-Kendell Seasonal						
2006- 2018				2013 - 2018		
Stats		***PM2.5***		***Stats***		***PM2.5***
probability		0.988		probability		0.820
Z		-2.224		Z		-0.997
p		0.026		p		0.319
Theil-Sen deseasonal p		<0.001		Theil-Sen deseasonal p		<0.01

The polar plot for $PM_{2.5}$ shows a different dominant source to that of PM_{10} with a very strong west-south-westerly signal, most notable at highest wind speeds. This would strongly signal a marine aerosol source given that this is the prevailing wind direction. Interestingly, there is very little signal for increased concentrations from the east showing little impact from Pacific sea salt. Unlike PM_{10}, there is a clear signal from road traffic, denoted by the very localised hotspot adjacent/immediately east of the site in Figure 28. There is also a high concentration plume to the southeast, with the city and shipping the likely origin. As south-easterly winds are rare for Takapuna (Figure A3) the strength of the southeast concentrations might be based on only a couple of data-points.

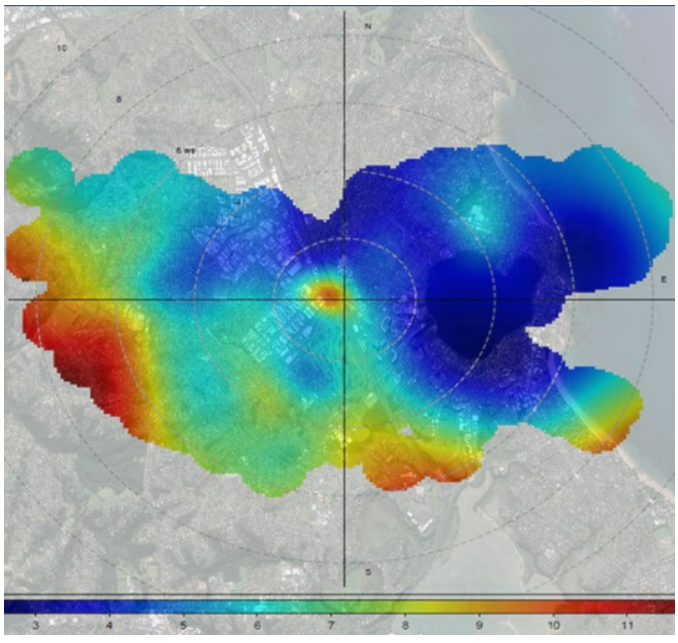

Figure 28 Polar plot showing $PM_{2.5}$ concentrations at Takapuna in relation to wind speed and direction, 2018.

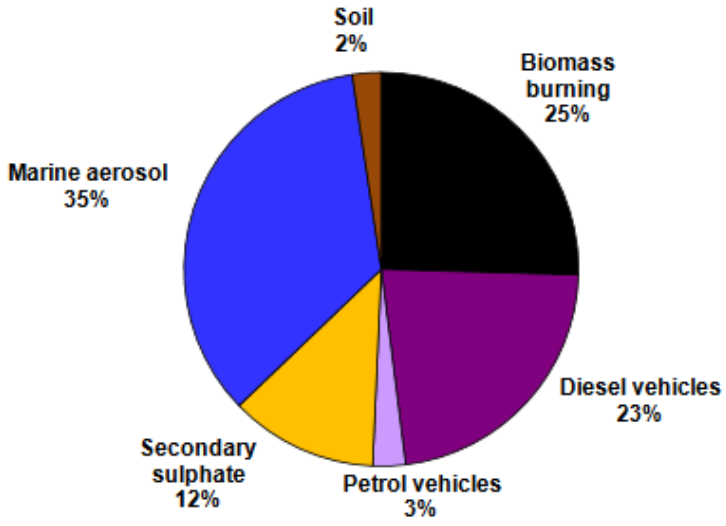

Figure 29 Source apportionment data for $PM_{2.5}$ at Takapuna, 2006-2013 (Davy et al., 2017).

Source apportionment data for $PM_{2.5}$ is available from Takapuna for the period 2006-2013 (Figure 29). Marine aerosol is the primary contributor to $PM_{2.5}$ with anthropogenic emissions split almost evenly between diesel emissions and biomass burning from home heating.

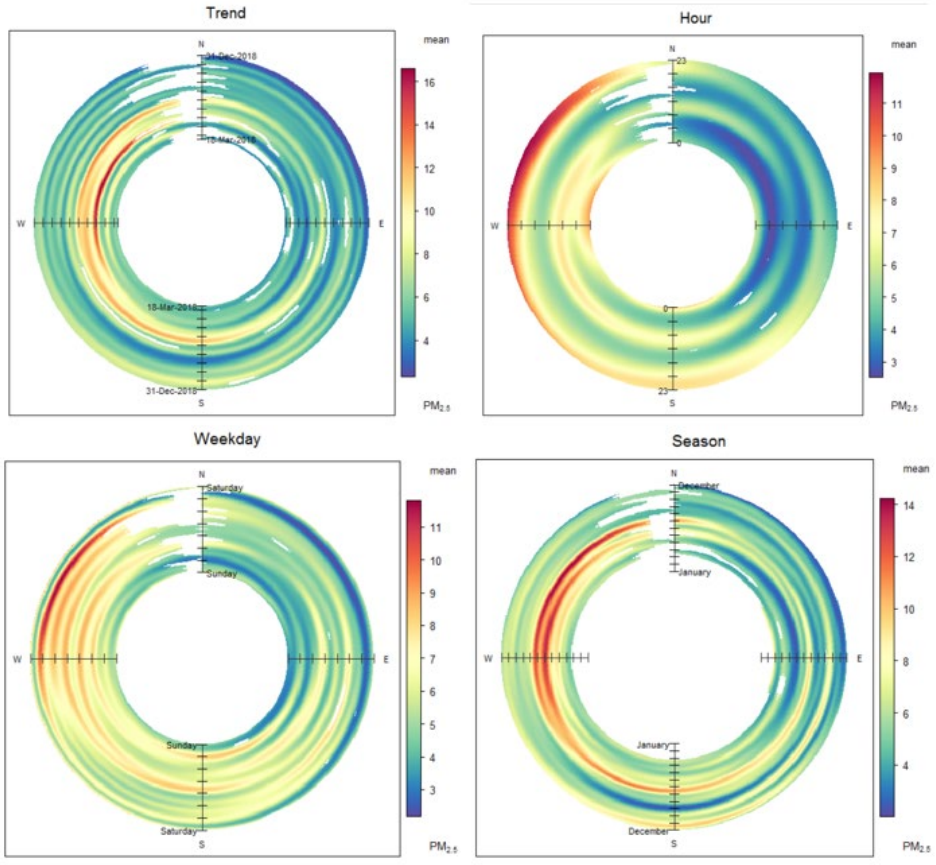

Figure 30 PolarAnnulus plots for $PM_{2.5}$ for Takapuna, 2018.

Weekday concentrations peak on Friday afternoons (Figure 30), the busiest day for vehicle traffic. Monthly concentrations peak in June and July, indicating that there may also be a substantial home heating contribution to $PM_{2.5}$. (Figure 28). This is further supported by the high north-westerly contributions during late evening. It is notable that there are very low concentrations across the northeast section indicating very little Pacific origin sea salt or shipping emissions from the inbound/outbound channel as reported by Davy et al., 2017.

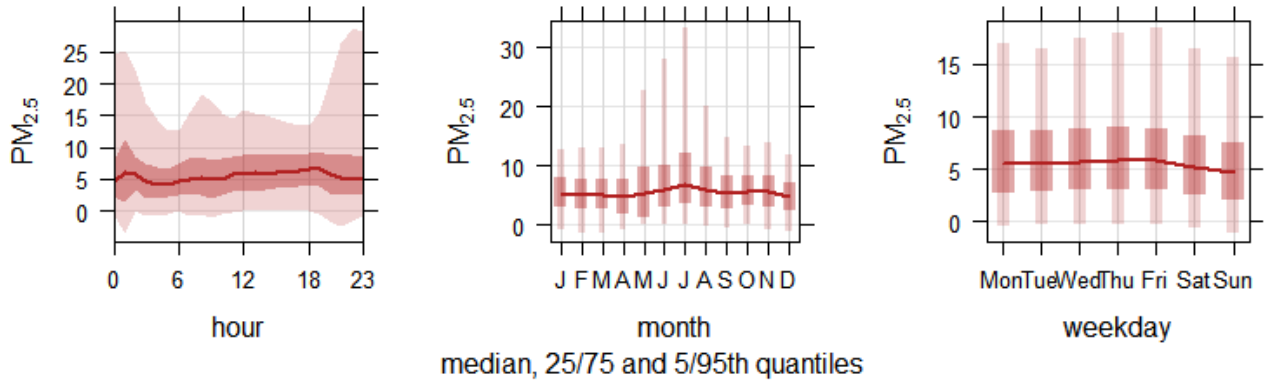

Figure 31 Temporal variability for $PM_{2.5}$ at Takapuna, including hourly, weekday and monthly plots, 2006-2018.

The contribution of home heating is evident from the wintertime peak observed in the in-depth temporal analysis shown in Figure 31. The weekday anomaly that shows Friday with significantly higher concentrations (Figure 30 – bottom right) is less evident in the boxplots (Figure 31), with only slightly higher peak concentrations observed in the 95th quartile (light shaded line). The hour plot also shows significant increases both early and late in the day.

2.2.4 NO_2 trends and analysis

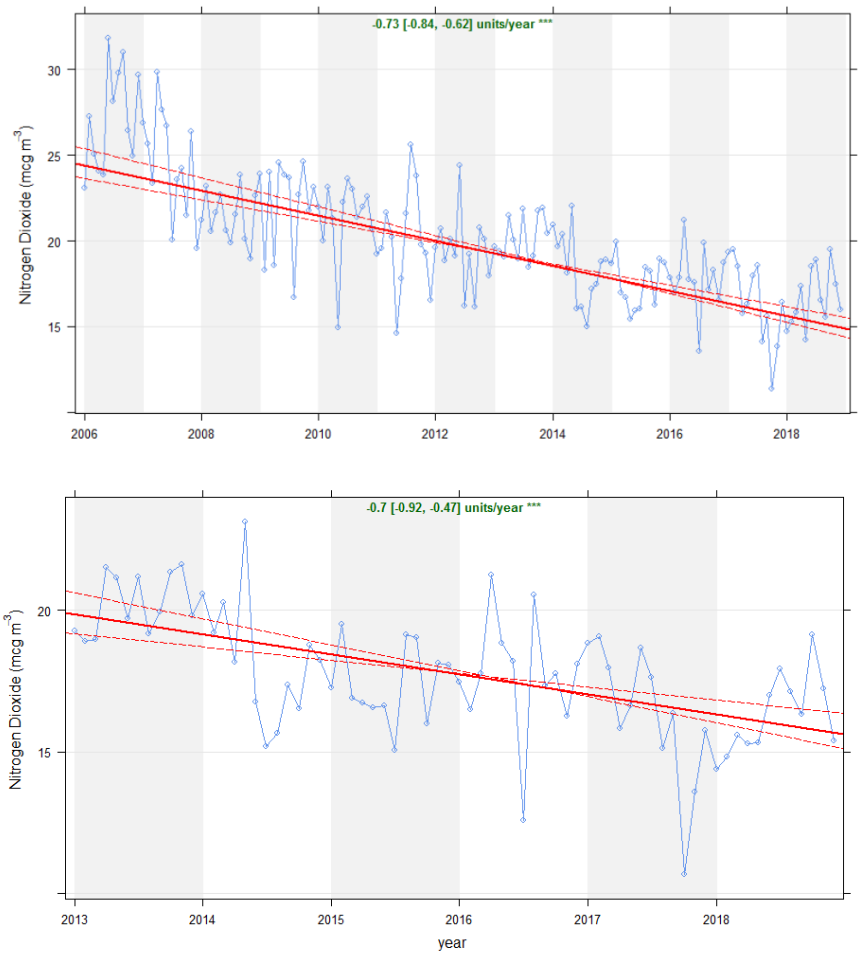

Figure 32 Theil-sen deseasonalised trends for NO_2 at Takapuna, 2006-2018 (top) and 2013-2018 (bottom).

For Takapuna, deseasonalised NO_2 concentrations have been lowering at a rapid rate (Figure 32). Interestingly, the gradient of reduction is similar for both long term 2006-2018 (0.73 µg/m^3 per annum) and short term 2013-2018 (0.7 µg/m^3 per annum). Like the PM_{10} concentrations, NO_2 concentration reductions are non-linear and can be defined in two step changes occurring in 2007/2008 and 2014. The 2007-2008 change coincides with regulatory changes in fuel quality, focusing on the reduction in sulphur content. However, 2008 also saw the opening of the northern busway, and therefore, some of the NO_2 observed in 2006-2007 may have been associated with construction emissions (Font et al., 2014). Note that since 2014, there is no statistical trend for NO_2 at Takapuna indicating that increasing emissions through increased traffic volume might be balancing reductions due to engine/fleet improvements (Sridhar and Metcalfe, 2019).

Table 7 Mann-Kendall seasonal statistical test for NO_2 at Henderson.

Takapuna: Mann-Kendell Seasonal						
2006- 2018				2013 - 2018		
Stats		***NO_2***		***Stats***		***NO_2***
probability		1.000		probability		0.923
Z		-4.567		Z		-1.446
p		0.000		p		0.148
Theil-Sen deseasonal p		<0.001		Theil-Sen deseasonal p		<0.001

The polar plot shown in Figure 32 for NO_2 illustrates the dominance of on-road vehicle traffic to concentrations. The trace of the adjacent motorway is clearly defined by the bright colours aligned southeast to northwest. There are very low NO_2 concentrations arising from the east of the site.

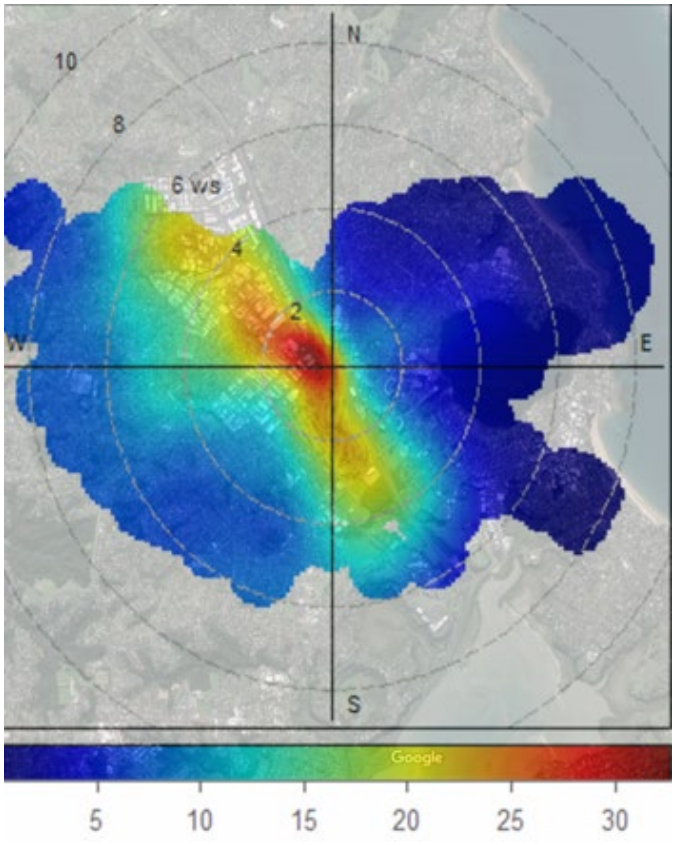

Figure 33 Polar plot showing NO_2 concentrations at Takapuna in relation to wind speed and direction, 2018.

NO_2 concentrations are raised when the winds come from the north westerly segment (Figure 34). Higher concentrations of NO_2 also occur during morning peak traffic when the winds come from the west and south, with lowest concentrations from the north

east (Figure 34). The winter season is clearly driving high NO_2 concentrations at this site. Reduced pollution dispersion during the cold winter months are known to increase overall concentrations along with increased emissions from colder engines (Sridhar and Metcalfe, 2019). Concentrations of NO_2 tend to increase later in the week with highest concentrations typically seen Wednesday to Friday, with traffic volume is the likely contributing factor.

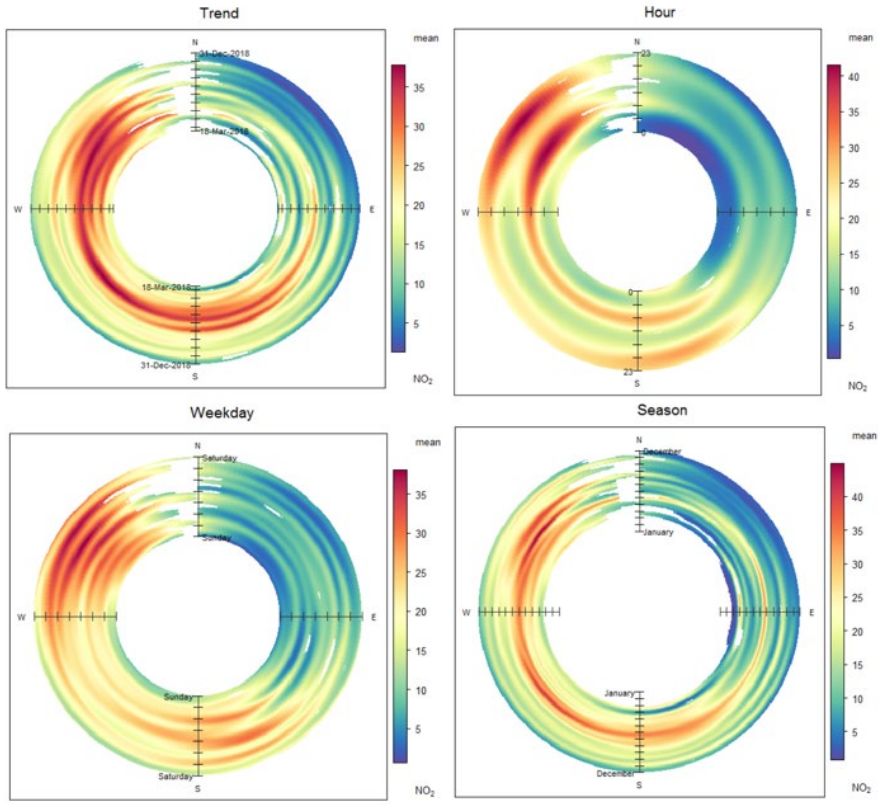

Figure 34 PolarAnnulus plots for NO_2 at Takapuna, 2018.

2.3 Penrose

2.3.1 Site description

The Penrose air quality monitoring site is within the Gavin Street substation, 106 m to the eastern side of the Southern motorway, aligned north-west to south-west (Figure 35). To the north-west and south are industrial premises including concrete batching facilities and glass manufacturing. Residential suburbs are located to the north and beyond the industrial area to the southwest. Houses date from 1930s onward; about 50% with chimneys. Meteorological conditions are provided in the appendix (Figure A4).

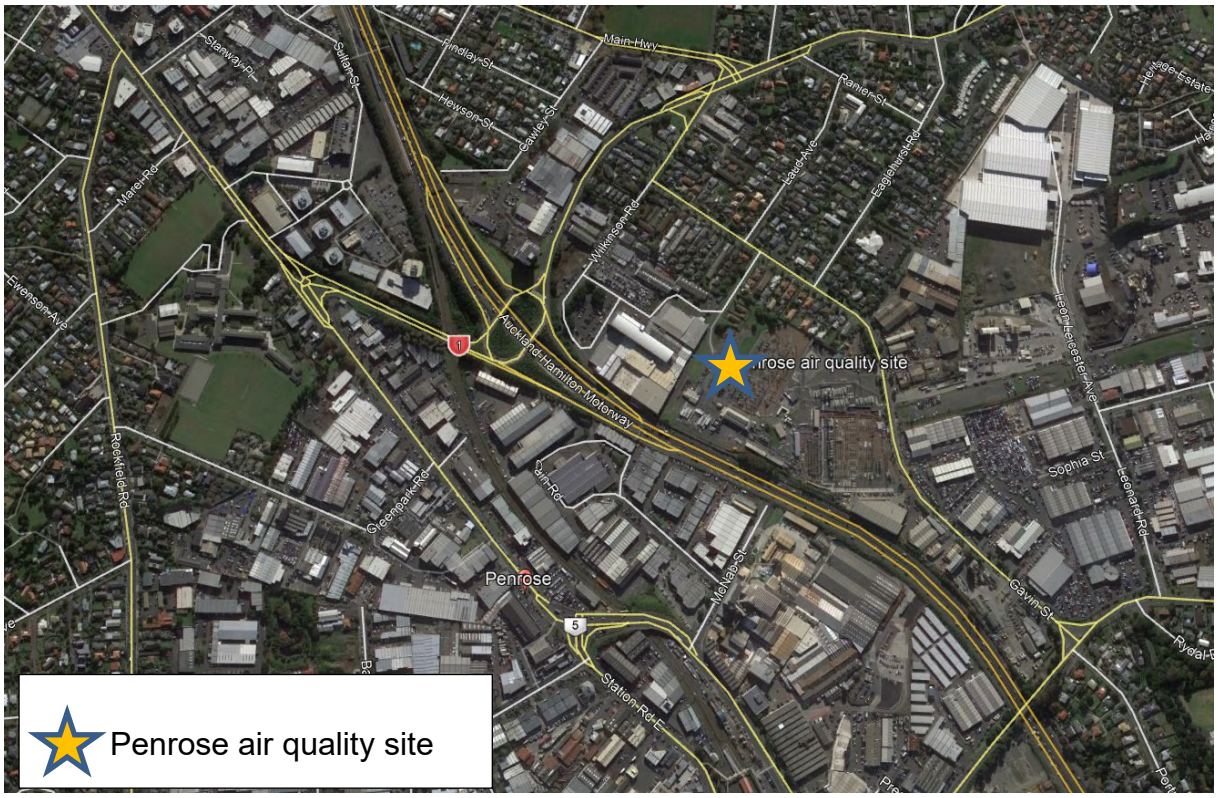

Figure 35 Map of the location of Penrose air quality monitoring site (Google Maps 2018).

2.3.2 PM_{10} trends and analysis

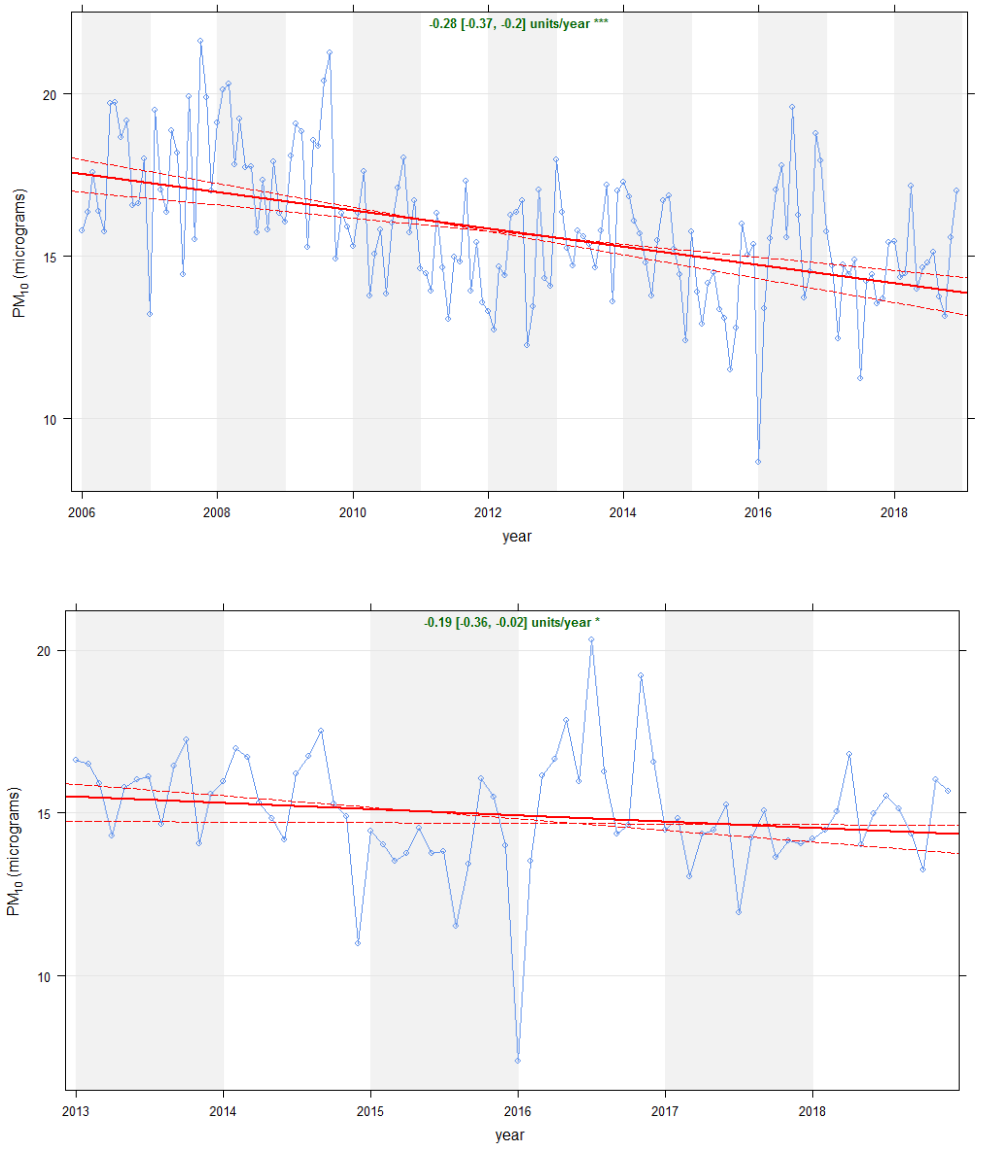

Figure 36 Theil-sen deseasonalised trends for PM_{10} at Penrose, 2006-2018 (top) and 2013-2018 (bottom).

The long-term deseasonalised trend for PM_{10} at Penrose shows significant decrease in PM_{10} concentrations (P=<0.001) (Figure 36). There is a step-change in concentration around year 2010 that drives this decease and was most likely a result the relocation of the monitoring shed slightly further away from the motorway, although still located within the same area of Gavin St.

The short-term trend analysis from 2013-2018 (Figure 36 – lower plot) shows only slight decrease in concentrations. (P= 0.1). There is an unexplained dip in concentrations during summer 2016; however, annual-average concentrations are largely stable since 2015 at around 15 µg/m^3.

Table 8 Mann-Kendall seasonal statistical test for PM_{10} at Penrose.

Penrose: Mann-Kendell Seasonal						
2006- 2018				2013 - 2018		
Stats		***PM_{10}***		***Stats***		***PM_{10}***
probability		1.000		probability		0.842
Z		-3.925		Z		-0.980
p		0.000		p		0.327
Theil-Sen deseasonal p		<0.001		Theil-Sen deseasonal p		<0.05

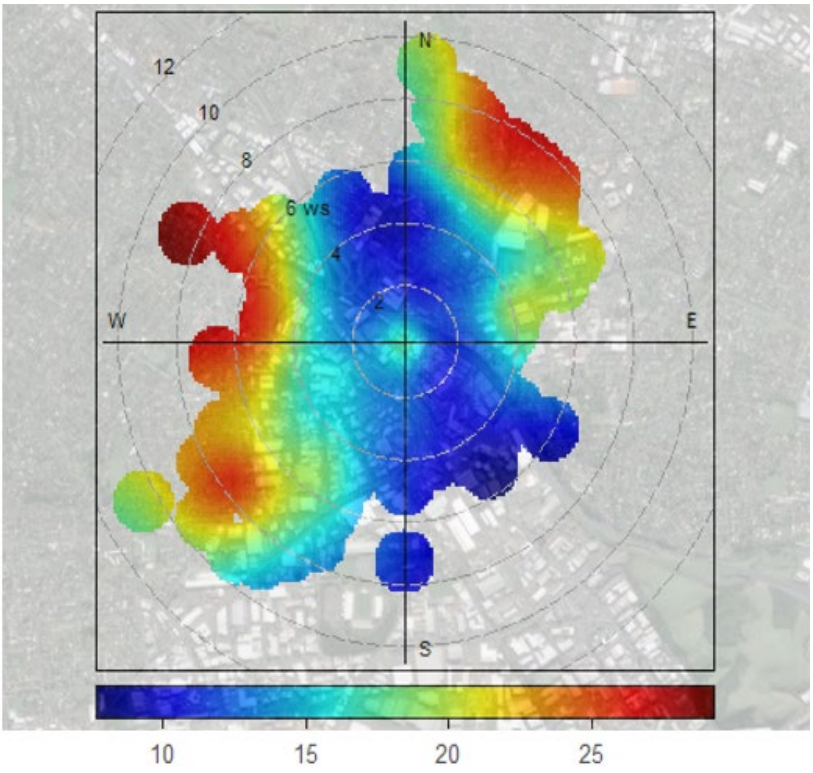

Figure 37 Polar plot showing PM_{10} concentrations at Penrose in relation to wind speed and direction, 2018.

A bi-directional nature of PM_{10} peak concentration for Penrose is evident (Figure 37). However, there is more of a westerly origin rather than south-westerly. The directional bias shows that the Tasman Sea and Pacific Ocean might also be sources of PM_{10} at this site when westerly and north-easterly winds are prevalent.

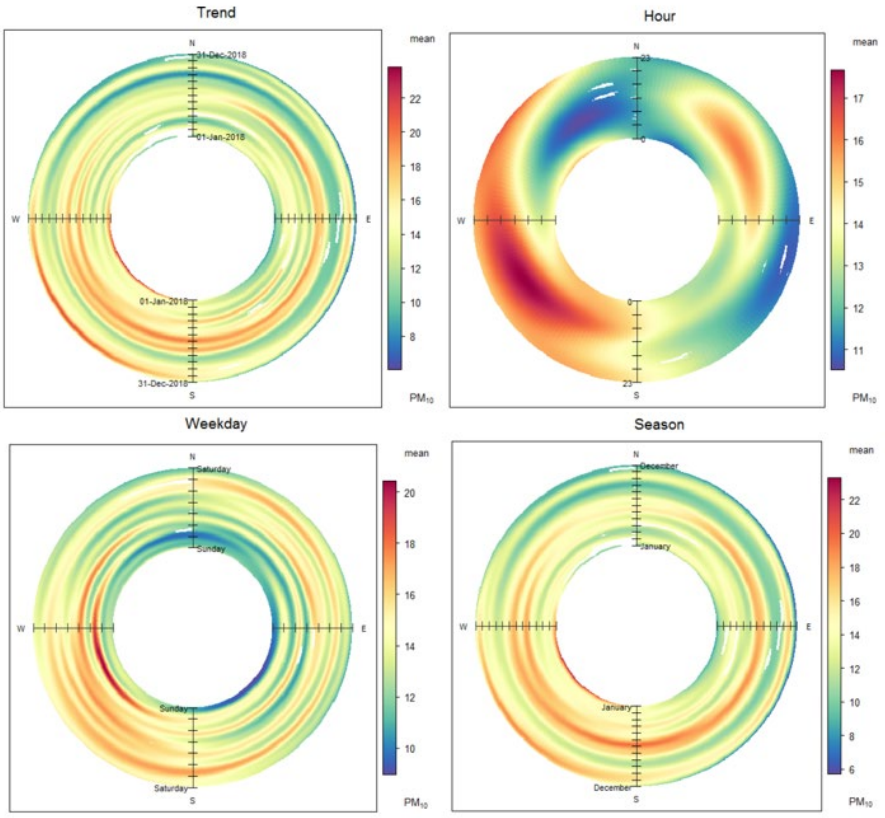

Figure 38 PolarAnnulus plots for PM_{10} at Penrose, 2018.

Temporal analysis show that almost every hour brings high concentrations when the winds come from a southwest direction (Figure 38). This wind direction draws on-road emissions from the Sothern motorway and coincides with the direction of the Manukau Harbour. The weekday plots show that Mondays typically have the highest PM_{10} concentrations. The reason for this is unknown. Both winter and summer also show higher concentrations than spring and autumn.

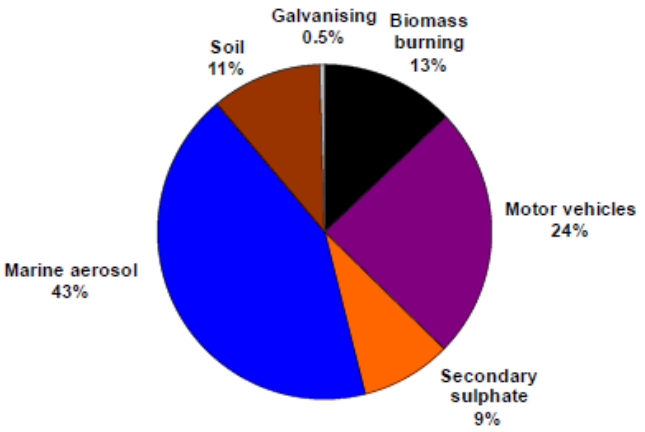

Figure 39 Source apportionment data for PM_{10} at Penrose, 2006-2013 (Davy et al., 2017).

Source apportionment data from Davy et al., 2016 shows that marine aerosol accounts for almost half of PM_{10} at the Penrose site (Figure 39). This is like most of the Auckland airshed. The proximity of the motorway seems to influence PM_{10} more at Penrose than Takapuna, Auckland's other motorway-adjacent site. This might be a result of lower residential biomass burning influence at Penrose increasing, proportionally, the influence of on-road traffic on the Sothern motorway.

2.3.3 $PM_{2.5}$ trends and analysis

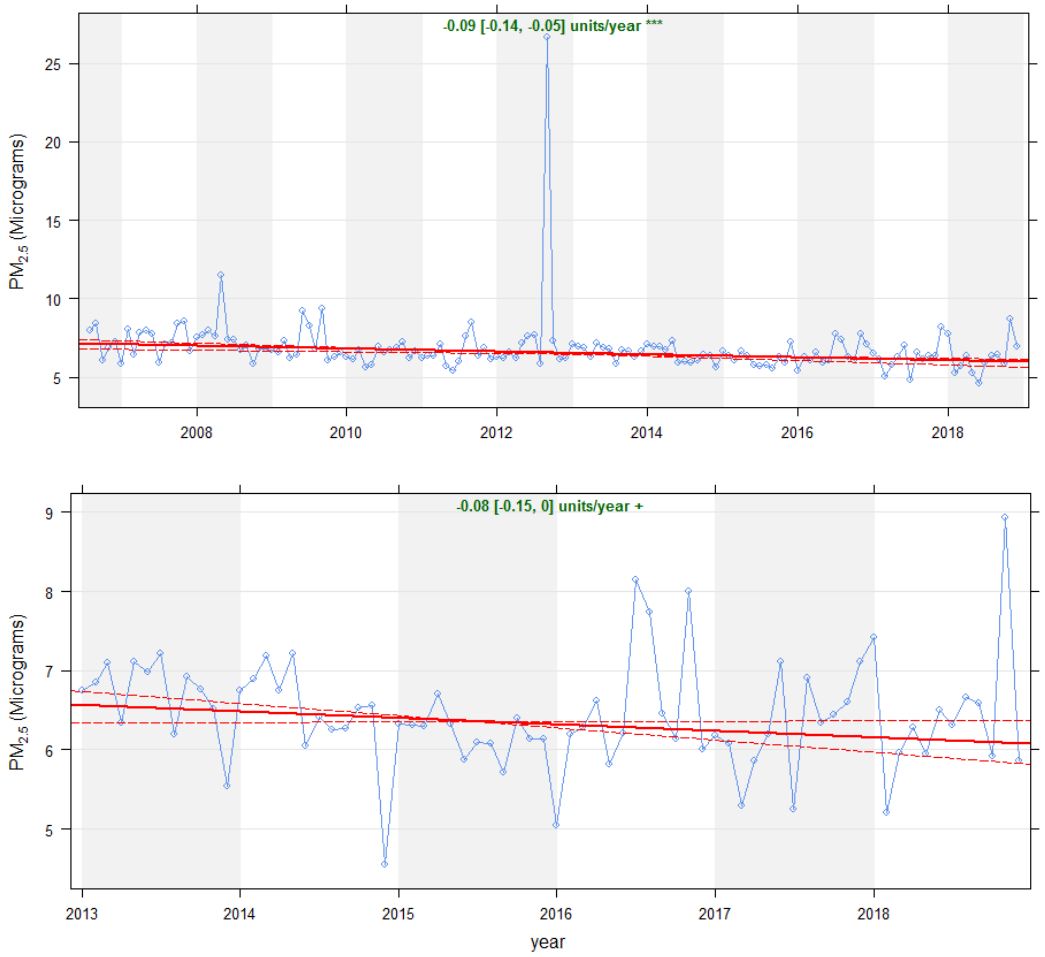

Figure 40 Theil-sen deseasonalised trends for $PM_{2.5}$ at Penrose, 2006-2018 (top) and 2013-2018 (bottom).

The long-term deseasonalised trends for $PM_{2.5}$ shows a significant decrease for the period 2006-2018 (P=<0.001) (Figure 40 – top plot). For 2013-2018 period the decrease is less pronounced but still significant (P=<0.1) (Figure 40 – lower plot). The similarity in both long-term and short-term trends between PM_{10} and $PM_{2.5}$ at Penrose indicates that $PM_{2.5}$ size fraction is contributing to the decrease.

Table 9 Mann-Kendall seasonal statistical test for $PM_{2.5}$ at Penrose.

Penrose: Mann-Kendell Seasonal						
2006- 2018				2013 - 2018		
Stats		***$PM_{2.5}$***		***Stats***		***$PM_{2.5}$***
probability		0.966		probability		0.692
Z		-1.815		Z		-0.458
p		0.070		p		0.647
Theil-Sen deseasonal p		<0.001		Theil-Sen deseasonal p		<0.05

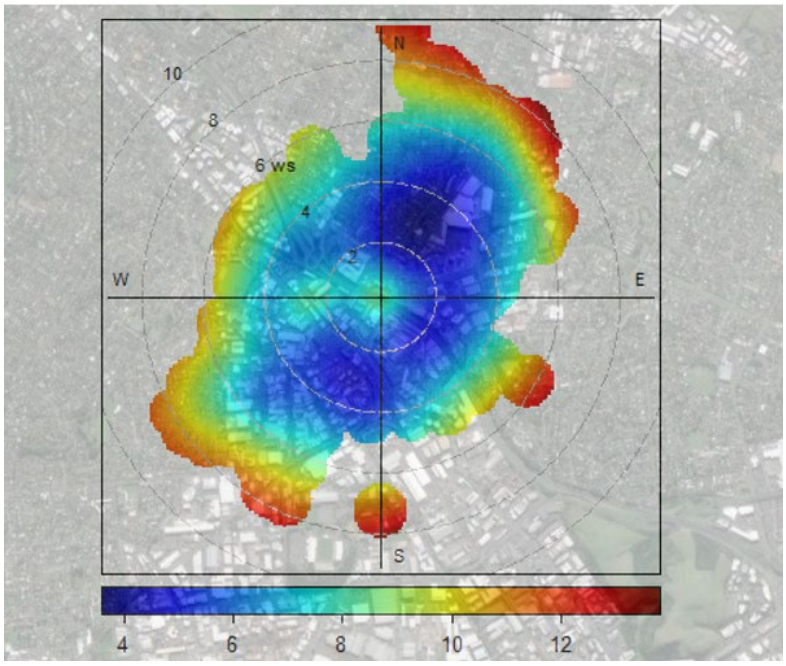

Figure 41 Polar plot showing $PM_{2.5}$ concentrations at Penrose in relation to wind speed and direction, 2018.

There is little distinct concentration peak observed from the southern motorway (Figure 41), with most elevated concentrations of $PM_{2.5}$ coming during the windiest conditions and from the southwest and northeast, implying a sea salt contribution from the Tasman Sea and Pacific Ocean. However, source apportionment data for this site, shown in Figure 42, does not agree with this conclusion with motor vehicles being the major contributor to $PM_{2.5}$ (Davy et al., 2016). This might be a result of peak concentrations coming from sea salt, but mean concentrations are emitted from on-road vehicles.

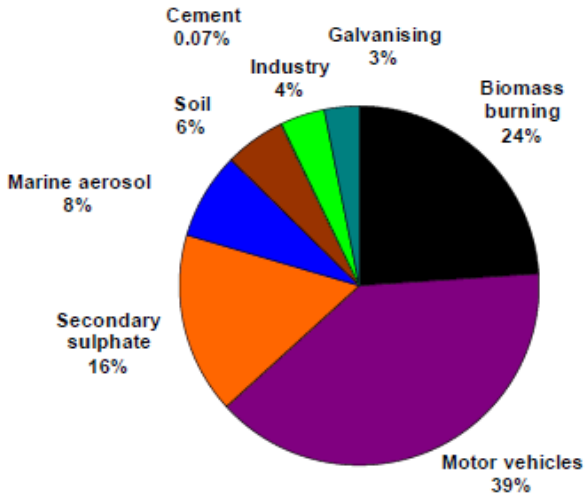

Figure 42 Source apportionment data for $PM_{2.5}$ at Penrose, 2006-2013 (Davy et al., 2017).

Biomass burning is found to have a higher contributing factor to the $PM_{2.5}$ at Penrose than for PM_{10}. To further test traffic influence at Penrose an intensity plot for $PM_{2.5}$ is plotted against NO_2 (Figure 43). The plot shows that as NO_2 increases (x-axis) $PM_{2.5}$ does not increase at a similar rate. As NO_2 is not emitted from wood burning to the same degree as other combustion activities, it would imply that $PM_{2.5}$ has other key sources. Simple linear regression modelling agrees with this assumption with a poor correlation of R=0.003 between NO_2 and $PM_{2.5}$ using 2018 data.

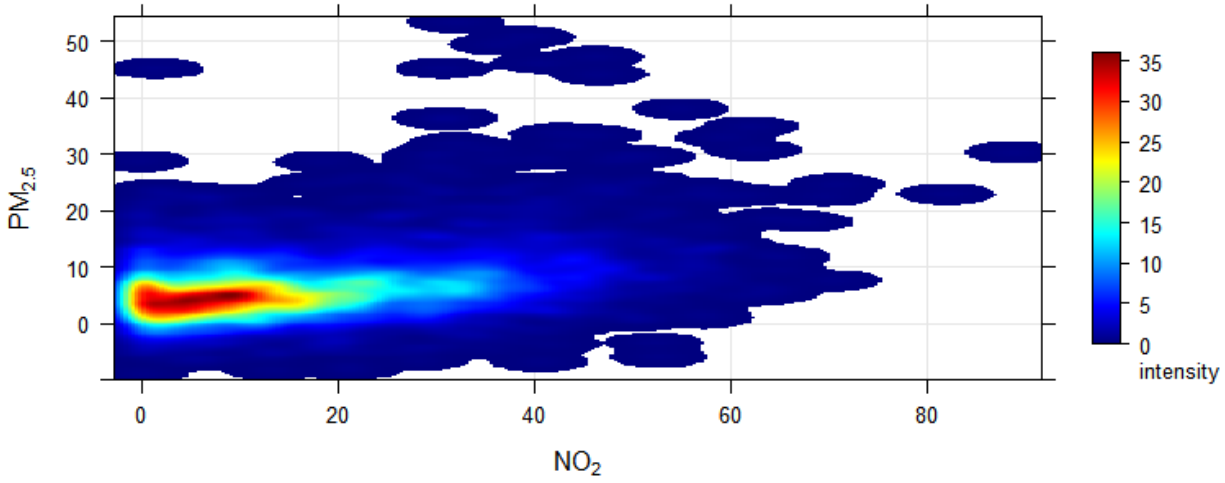

Figure 43 Comparison of hourly $PM_{2.5}$ concentrations and NO_2 concentrations at Penrose, 2018.

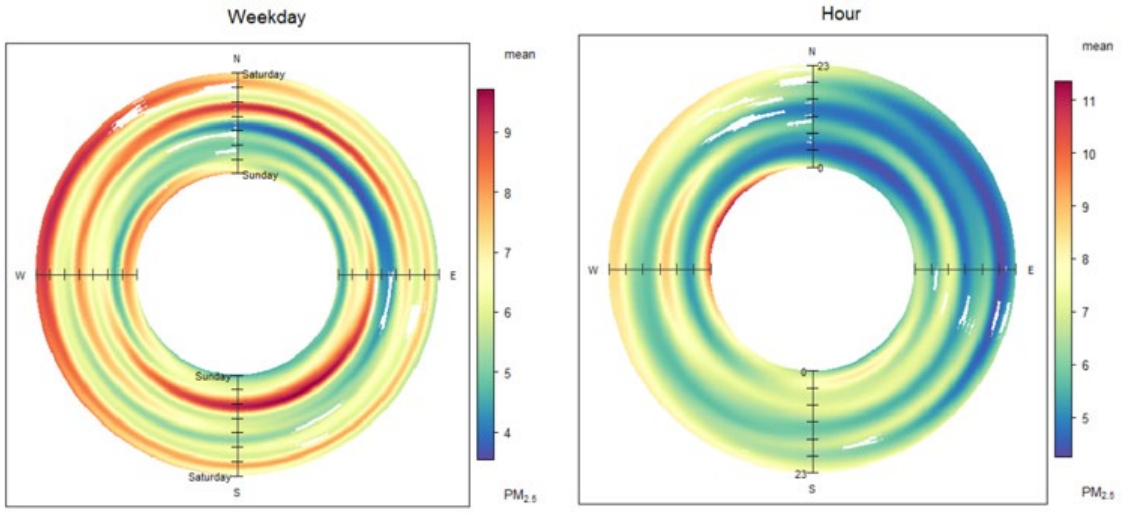

Figure 44 PolarAnnulus plots for $PM_{2.5}$ at Penrose, 2018.

The plots in Figure 44 show that Fridays have the highest $PM_{2.5}$ concentrations from the southeast, whilst weekend concentrations peak when the air flow is from the northwest. Hourly concentrations show late night peaks in concentrations from the west with a lower morning peak.

2.3.4 NO_2 trends and analysis

The long-term deseasonalised trend analysis for NO_2 taking in the period 2006-2018 presented in Figure 45 shows a clear plateau shift at the beginning of 2012. The reduced NO_2 concentration at the Penrose site was likely caused by the monitoring station being moved within the Gavin Street substation. The short-term trends (Figure 45 – lower plot) 2013-2018 shows no trend and is slightly increasing year on year. This is commensurate with traffic volume increases on the motorway during this period (Sridhar & Metcalfe, 2019).

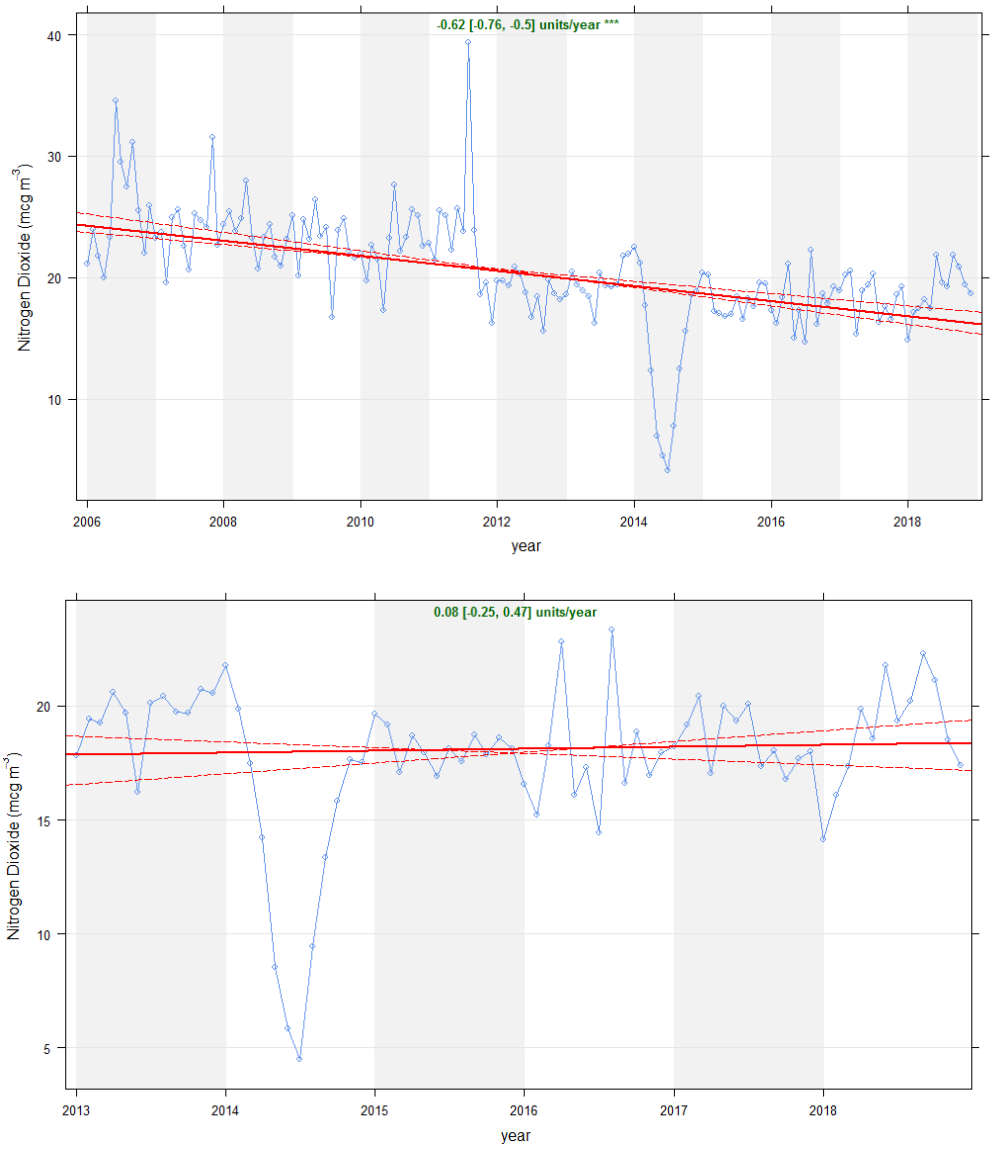

Figure 45 Theil-sen deseasonalised trends for NO_2 at Penrose, 2006-2018 (top) and 2013-2018 (bottom).

Table 10 Mann-Kendall seasonal statistical test for NO_2 at Penrose.

Penrose: Mann-Kendell Seasonal						
2006- 2018				2013 - 2018		
Stats		***NO_2***		***Stats***		***NO_2***
probability		0.999		probability		0.758
Z		-3.084		Z		-0.741
p		0.002		p		0.459
Theil-Sen deseasonal p		<0.001		Theil-Sen deseasonal p		No trend

Time dependent analysis showed a strong morning peak in concentration from the southerly and westerly sectors (Figure 46). City-bound traffic along the Sothern motorway is the likely emission source. There is a weaker evening traffic peak also evident. The weekday analysis shows strong weekday concentrations/patterns when the winds come from the southerly and westerly sectors. There is also a large peak in winter concentrations likely caused by colder engines releasing more NO_2 and more stable morning meteorology allowing for pollutants to build up.

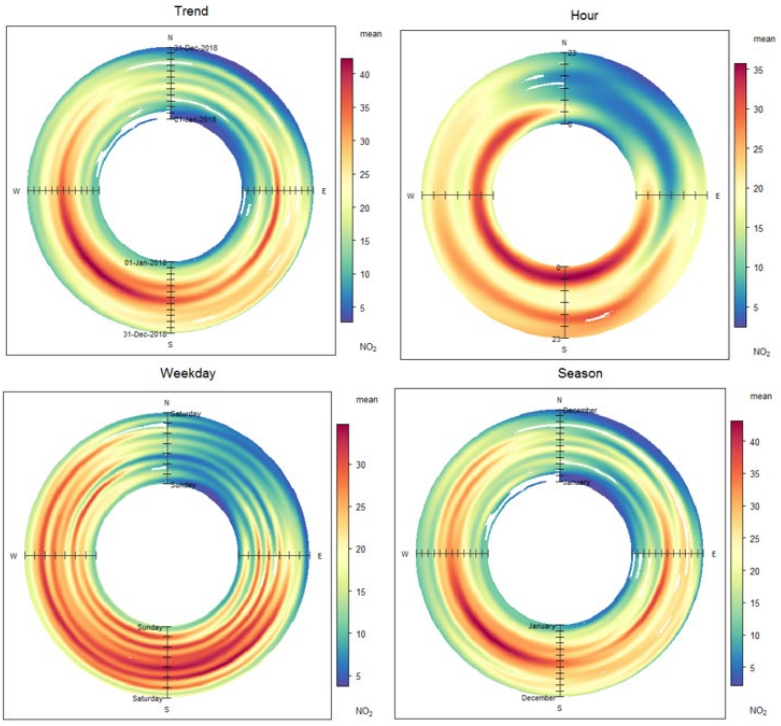

Figure 46 PolarAnnulus plots for NO_2 at Penrose, 2018.

The polar plot confirms the influence of the motorway at the Penrose site with the southeast -northwest NO_2 trajectory clearly aligned with the Southern motorway (Figure 47). There is also a clear trajectory to the Southwest following prevailing wind direction. From this direction, there is probable NO_2 source from Onehunga, Penrose town, and further downwind there is the SH20 south western motorway.

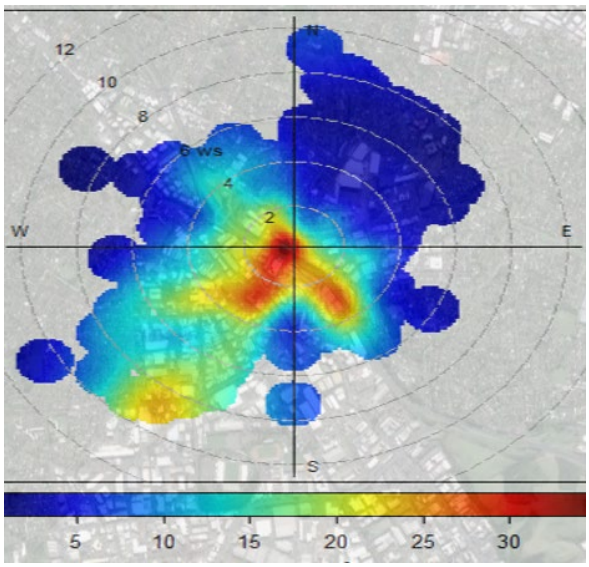

Figure 47 Polar plot showing NO_2 concentrations at Penrose in relation to wind speed and direction, 2018.

2.3.5 Sulphur dioxide trends and analysis

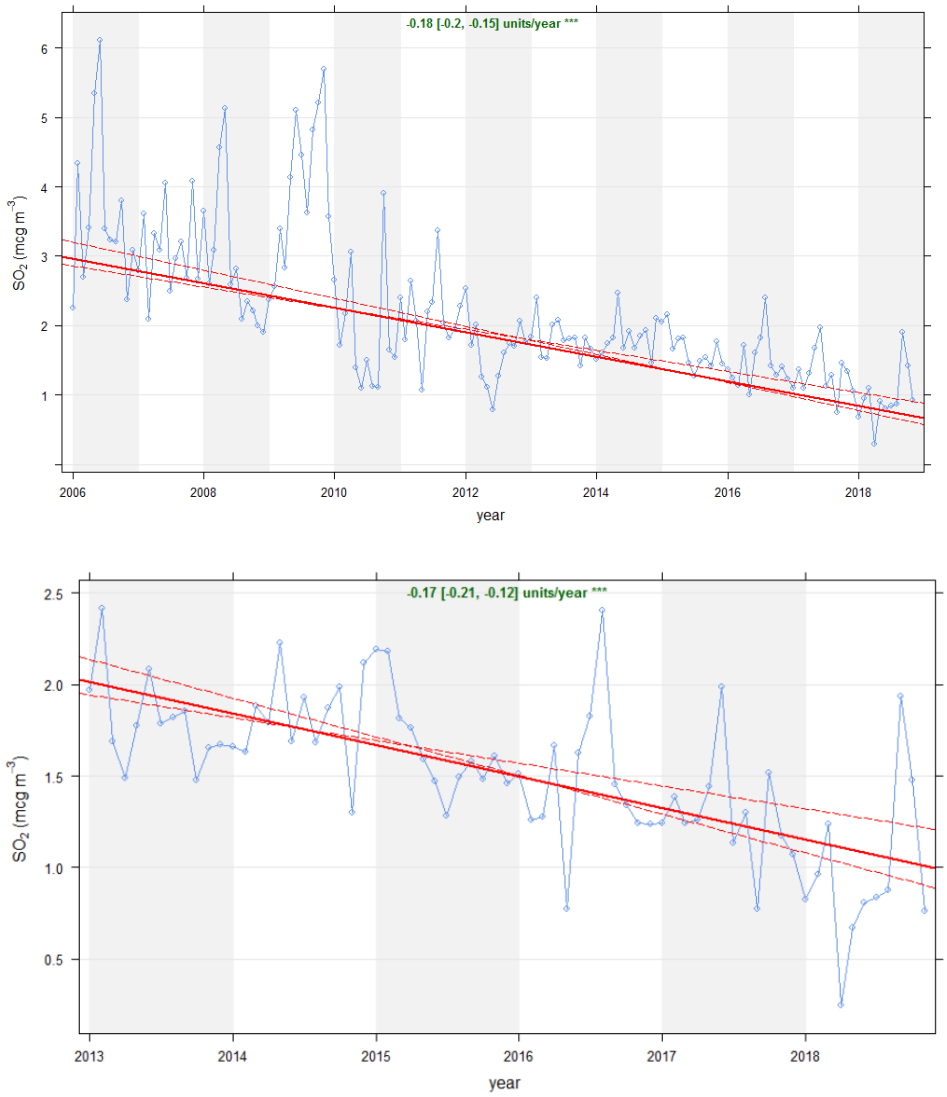

Figure 48 Theil-sen deseasonalised trends for SO_2 at Penrose, 2006-2018 (top) and 2013-2018 (bottom).

Penrose is the only site across the Auckland network where SO_2 has been continuously monitored. Figure 48 (top) shows the long-term trend (2006 -2018). There has been a steep decline in concentrations (P=<0.001) initiated by the reductions in sulphur in transport fuel in 2006-2011 (Sridhar & Metcalfe, 2019). The short-term trends in Figure 48 (lower) continues the steep decline in concentrations indicative of improvements in vehicle performance.

Table 11 Mann-Kendall seasonal statistical test for SO_2 at Penrose.

Penrose: Mann Kendell Seasonal						
2006- 2018				2013 - 2018		
Stats		***SO_2***		***Stats***		***SO_2***
probability		1.000		probability		0.993
Z		-5.327		Z		-2.376
p		0.000		p		0.017
Theil-Sen deseasonal p		<0.001		Theil-Sen deseasonal p		<0.001

The polar plots in Figure 49 it is evident that the southern motorway still contributes SO_2 from the southerly direction. However, there appears to be a secondary SO_2 source during higher winds from the south-easterly sector. This concentration peak could be localised industry including a glass factory, situated southeast of the monitoring site. This peak could also be a signature of SO_2 emissions from White Island volcano, located in the Bay of Plenty (Davy et al., 2017).

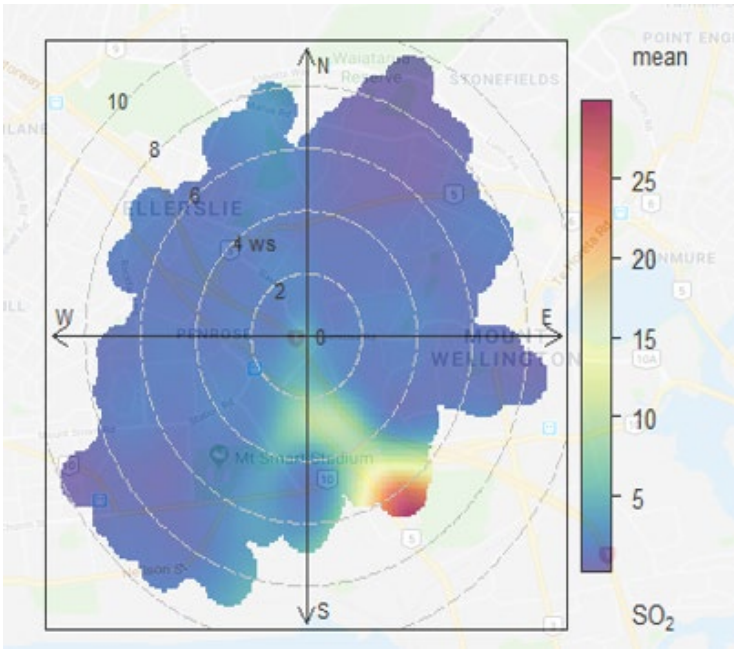

Figure 49 Polar plot showing SO_2 concentrations at Penrose in relation to wind speed and direction, 2018.

2.4 Queen Street

2.4.1 Site description

Queen Street monitoring station is located on a first-floor canopy on the corner of Queen Street and Wyndham Street (Figure 50). The key emission source measured at this site is combustion emissions from vehicle exhausts (Talbot et al., 2017). This site is the most central site providing information on possible personal exposure in one of the most densely populated areas of Auckland with several million people walking below the monitoring site every year (Talbot & Lehn, 2018). Wind speed and direction data has been recorded at the Queen Street monitoring site since late 2017 only and is presented in the appendix (Figure A6).

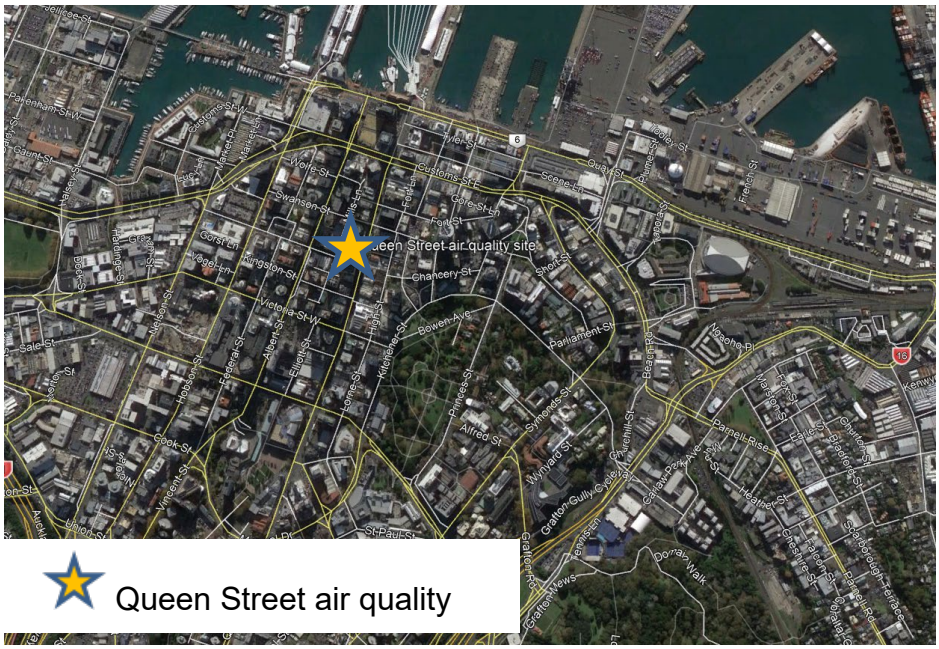

Figure 50 Map of the location of Queen Street air quality monitoring site (Google Maps 2018).

2.4.2 PM_{10} trends and analysis

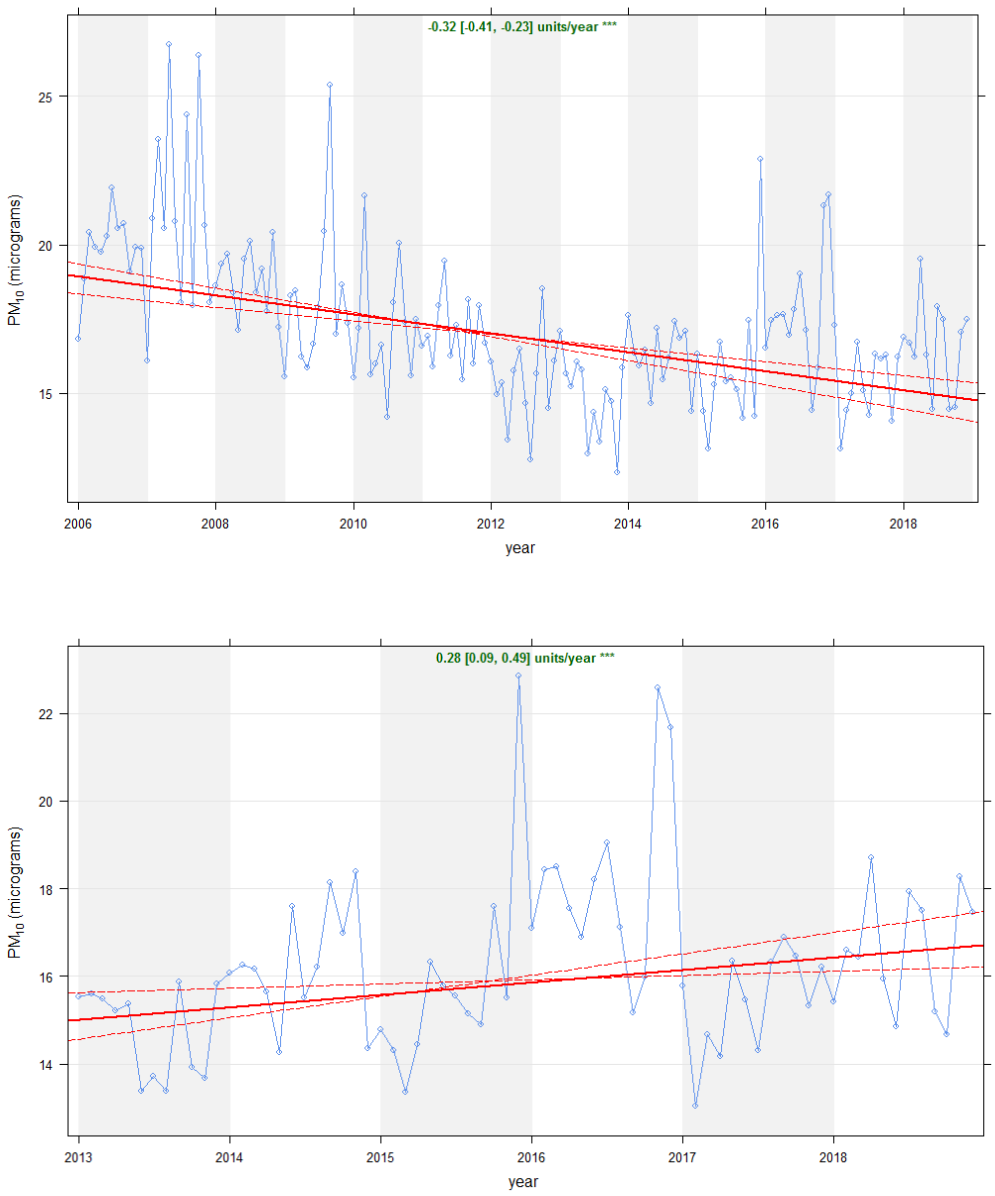

Figure 51 Theil-sen deseasonalised trends for PM_{10} at Queen Street, 2006-2018 (top) and 2013-2018 (bottom).

The long-term trend for PM_{10} at Queen Street shows a statistically steep decline in concentrations (P=<0.001) Figure 51 (top). This decrease was most notable between 2008-2012 when changes to Queen Street layout and reduction in speed to 30 km/h was introduced. Since 2013, there has been a statistically significant increase in concentrations (P=<0.001) (Figure 51 – lower). Davy et al., 2017 noted that decreases shown in the 2006-2013 PM_{10} trend were driven by reduction in diesel and marine aerosol during this period. Since 2013, the causes of the increases in concentrations

are yet to be determined; however, Talbot and Lehn 2018 discuss contributing factors to air pollution increases on Queen Street.

Table 12 Mann-Kendall seasonal statistical test for PM_{10} at Queen Street

Queen Street: Mann-Kendell Seasonal						
2006- 2018				2013 - 2018		
Stats		**PM_{10}**		**Stats**		**PM_{10}**
probability		1.000		probability		0.915
Z		-4.279		Z		1.354
p		0.000 (<0.001)		p		0.176 (<0.001)

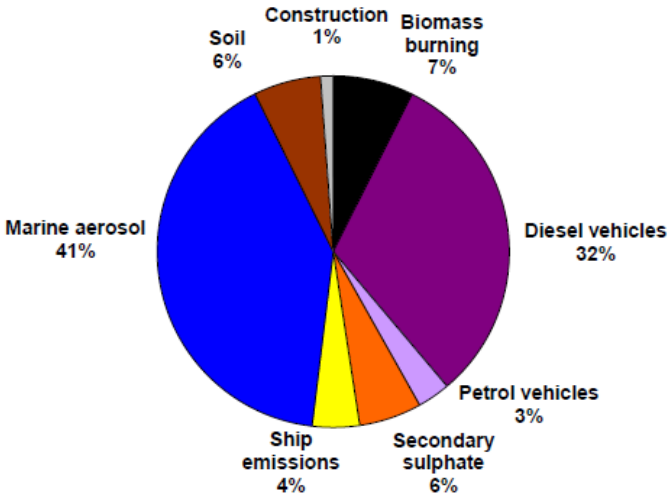

Figure 52 Source apportionment data for PM_{10} at Queen Street, 2006-2013 (Davy et al., 2017).

Source apportionment data for Queen Street is shown in Figure 52. Marine aerosol dominates the PM_{10} size fraction, with diesel emissions being the only other major source. Peak PM_{10} concentrations recorded at Queen Street come when the wind is from an easterly direction (Figure 53). The directional bias of PM_{10} is largely due to the shielding effect of the neighbouring buildings to the west, with the monitoring station on the western side of the street. The increased concentrations with higher wind speeds would imply that larger particulates might be responsible for elevated PM_{10}. Road dust resuspension, construction work and marine aerosol are likely contributors to this observed trend.

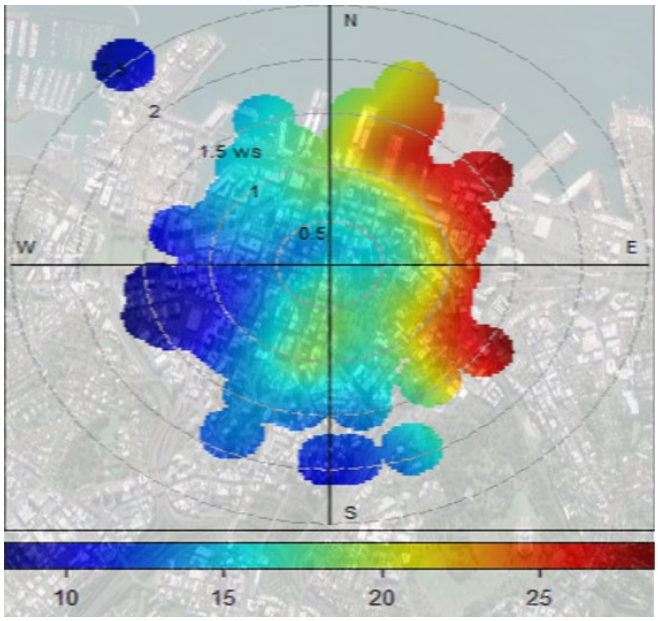

Figure 53 Polar plot showing PM_{10} concentrations at Queen Street in relation to wind speed and direction, 2018.

Temporal analysis shows highest concentrations during the daytime, rather than a distinct morning rush-hour peak, typical of other roadside monitoring stations (Figure 54). This is due to Queen Street being a major shopping street with most people visiting during the day and early evening. Winter season shows the highest concentrations (bottom right); however, there is a second peak in concentration around October. This is a period around the spring equinox when wind speeds tend to be highest in Auckland, which may well increase PM_{10} concentrations due to marine aerosol.

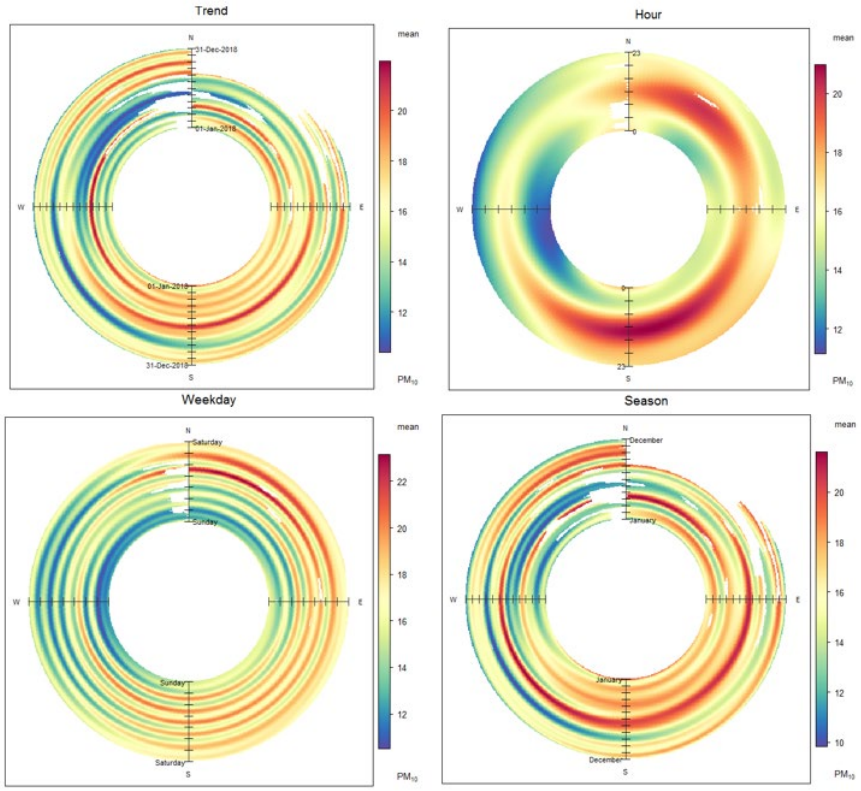

Figure 54 PolarAnnulus plots for PM_{10} at Queen Street, 2018.

2.4.3 $PM_{2.5}$ trends and analysis

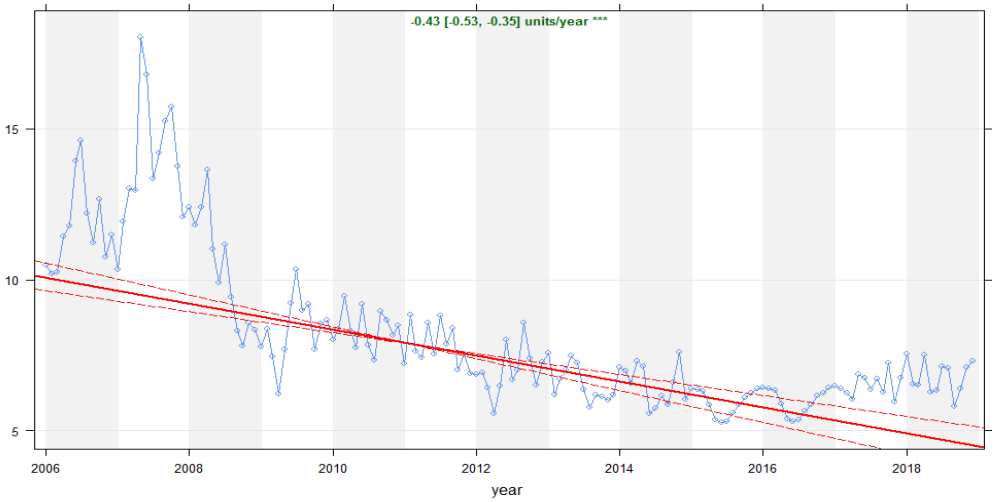

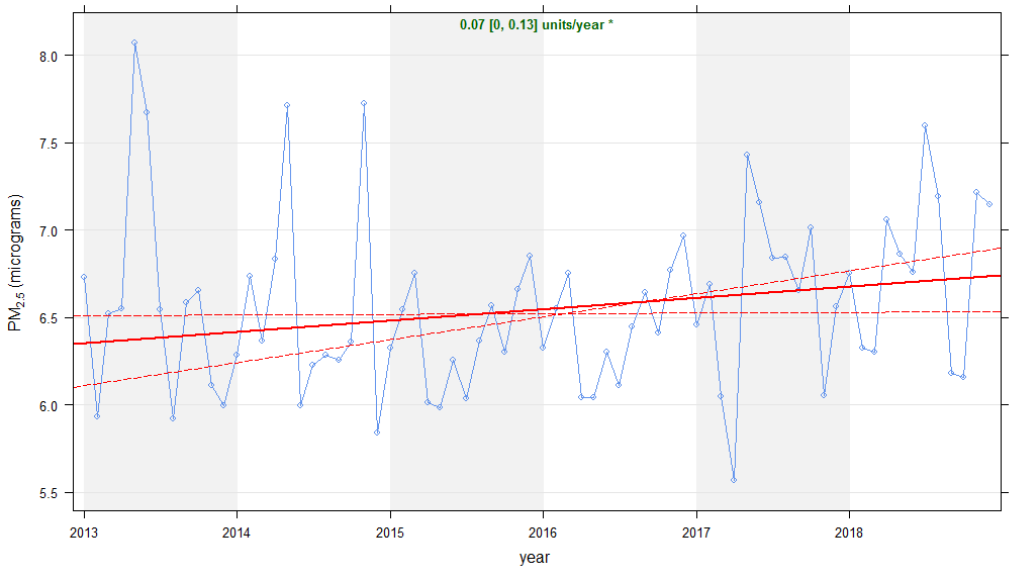

Figure 55 Theil-sen deseasonalised trends for $PM_{2.5}$ at Queen Street, 2006-2018 (top) and 2013-2018 (bottom).

Like PM_{10}, concentrations in $PM_{2.5}$ rapidly decreased during the period 2006-2010 (Figure 55 – top). This reduction is also likely to be a result of fine sea salt and diesel emissions on Queen Street. Since 2013, concentrations are increasing slowly (P=0.1) (Figure 55- lower plot). Traffic numbers have remained steady on Queen Street; however, there has been an increase in bus numbers and construction vehicles with a new downtown mall and commencement of the City Rail Link underground railway in the adjacent street.

Table 13 Mann-Kendall seasonal statistical test for $PM_{2.5}$ at Queen Street

Queen Street: Mann-Kendell Seasonal						
2006- 2018				2013 - 2018		
Stats		**$PM_{2.5}$**		**Stats**		**$PM_{2.5}$**
probability		1.000		probability		0.560
Z		-5.608		Z		-0.136
p		0.000		p		0.892
Theil-Sen deseasonal p		<0.001		Theil-Sen deseasonal p		<0.05

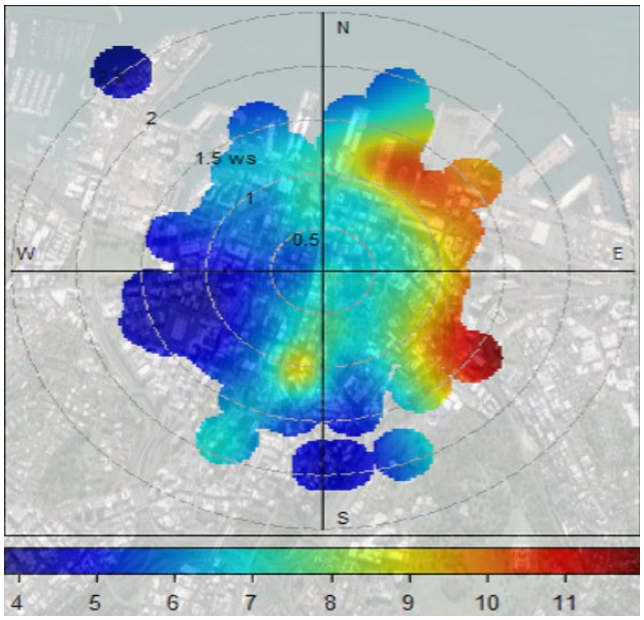

Figure 56 Polar plot showing $PM_{2.5}$ concentrations at Queen Street in relation to wind speed and direction, 2018.

Figure 56 shows the polar plot for $PM_{2.5}$ describing possible origin of fine particulate in relation to wind speed and direction. Like PM_{10}, $PM_{2.5}$ originates to the east of the monitoring site. This is explained by the Queen Street monitoring station set against buildings to the west of the busy road.

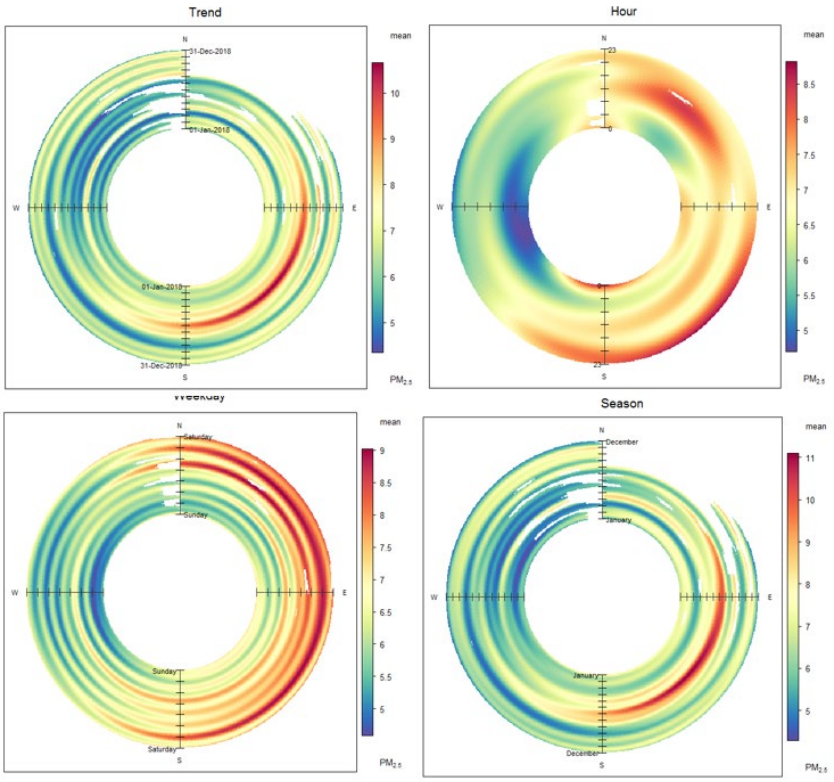

Figure 57 PolarAnnulus plots for $PM_{2.5}$ at Queen Street, 2018.

There is a subtle difference for $PM_{2.5}$ that shows a preference for raised $PM_{2.5}$ from a south-easterly direction rather than north-easterly as with PM_{10}. This is indicative of finer particulate coming from diesel emissions and secondary suspended road dust. This is a supposition that is supported by source apportionment data for $PM_{2.5}$ (Figure 58). Temporal analysis (Figure 57) for $PM_{2.5}$ at Queen Street shows key periods when fine particulates increase. When the winds come from the north east (from the port and Waitemata Harbour) concentrations tend to increase during the afternoon, when the winds are from the southeast there is a trend to increase during the evening (Figure 57).

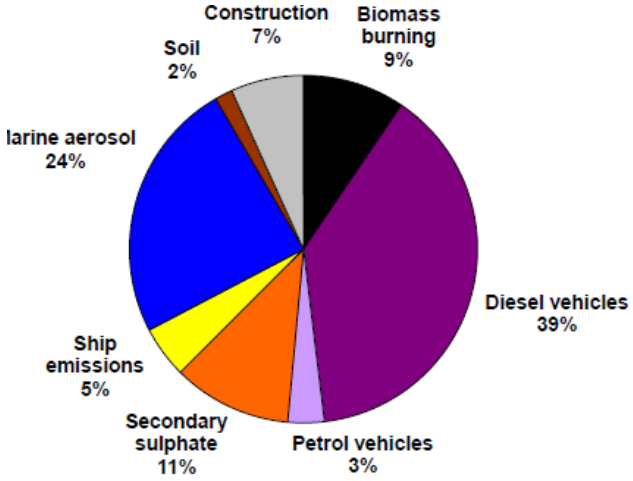

Figure 58 Source apportionment data for $PM_{2.5}$ at Queen Street 2006-2013 (Davy et al., 2017).

The weekday plots show a strong trend towards later in the week. This corresponds to visitor numbers on Queen Street. However, when looking at the time of day data and factoring in seasonal changes which has a strong winter anomaly (Figure 57 lower right) wood smoke from home heating might also contribute to $PM_{2.5}$ along with less winter-time dispersion and contributions from regional sources. Finally, for $PM_{2.5}$ it is notable how much higher $PM_{2.5}$ and NO_2 are at Queen Street when compared to other sites across the Auckland air quality network (Figure 46). Mean concentrations taken over a 10-year period at Queen Street show $PM_{2.5}$ to be over 2µg/m^3 higher than the citywide average (derived from the average of Penrose, Takapuna and Henderson) and almost double for the citywide NO_2 average.

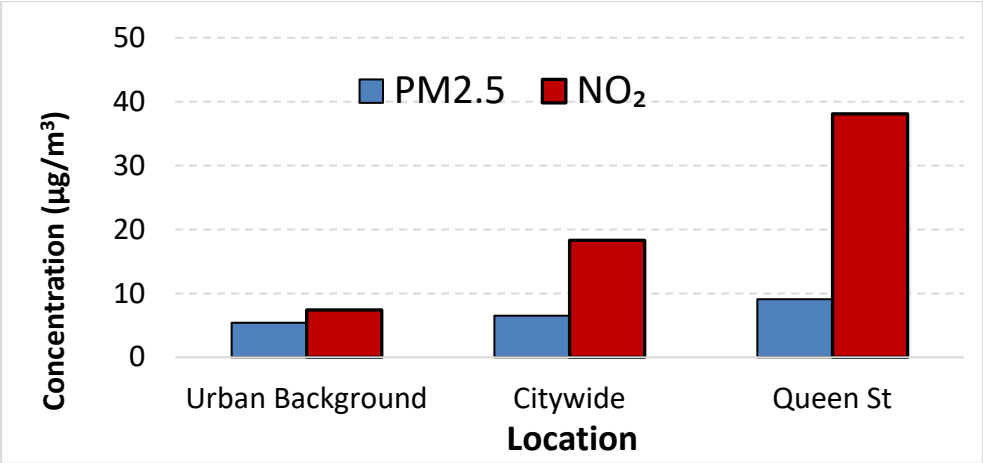

Figure 59 Comparison of mean $PM_{2.5}$ and NO_2 concentrations for Urban Background (Glen Eden), Citywide (Penrose/Takapuna/Henderson) and Queen Street sites, 2008-2018.

2.4.4 NO_2 trends and analysis

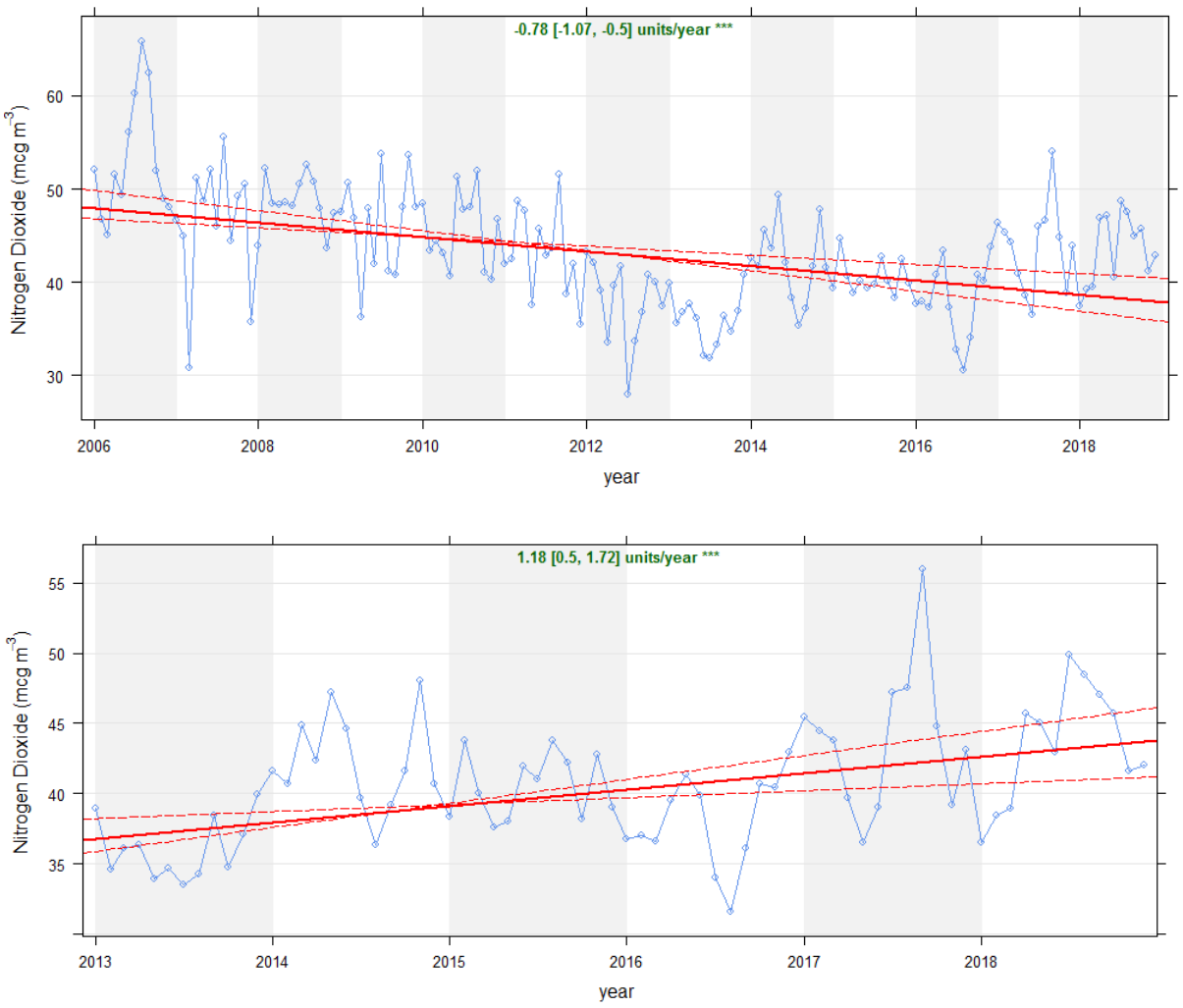

Figure 60 Theil-sen deseasonalised trends for NO_2 at Queen Street, 2006-2018 (top) and 2013-2018 (bottom).

There was a step change decrease in NO_2 between 2011 and 2012 within the deseasonalised data (Figure 60). This was likely due to the reconfiguration of buses along Queen Street, reducing NO_2 emitting diesel vehicles (Talbot & Lehn, 2018). Since, 2013 NO_2 concentrations are increasing at a statistically significant rate (P=<0.001). Importantly, annual NO_2 levels have exceeded the Auckland ambient air quality guidelines of 40 µg/m^3 for the past two years.

Table 14 Mann-Kendall seasonal statistical test for NO_2 at Queen Street

Queen Street: Mann-Kendell Seasonal						
2006- 2018				2013 - 2018		
Stats		**NO_2**		**Stats**		**NO_2**
probability		0.999		probability		0.911
Z		-3.051		Z		1.342
p		0.002		p		0.179
Theil-Sen deseasonal p		<0.001		Theil-Sen deseasonal p		<0.001

The trend plot shows that the strong drop-off in NO_2 during the winter months after Queen Street was reconfigured in 2008 and the speed limited to 30 km/h shortly after. There has been significant increase in wintertime NO_2 since 2016; Figure 61 shows these winter peaks with monthly mean concentrations now approaching 60 µg/m^3, levels not seen since 2010.

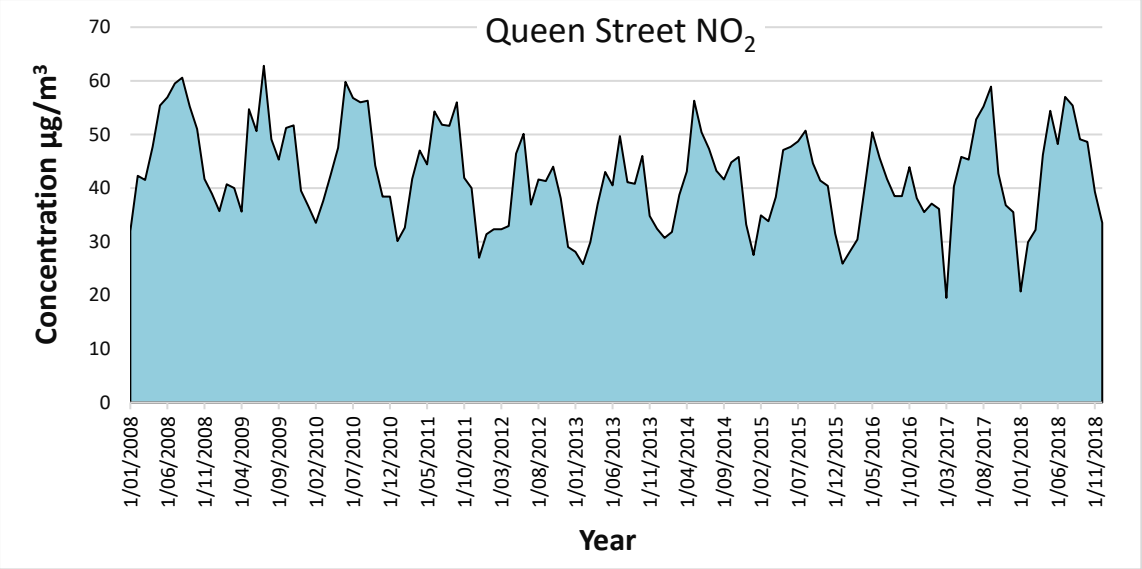

Figure 61 Monthly NO_2 concentrations at Queen Street, 2008-2018.

PolarAnnulus plots in Figure 62 for NO_2 at Queen Street show peak concentrations commencing late morning and continuing into the evening. Only summer months tend to show reduced concentrations while there is also a diurnal trend with Sunday showing the lowest concentrations. A directional bias for NO_2 is observed with peak concentrations coming from the southeast sector (Figure 62). The higher wind speeds at this time imply that the NO_2 is being brought into the downtown area from upper Queen Street, with the possibility that the motorway further up Queen Street is also contributing to NO_2.

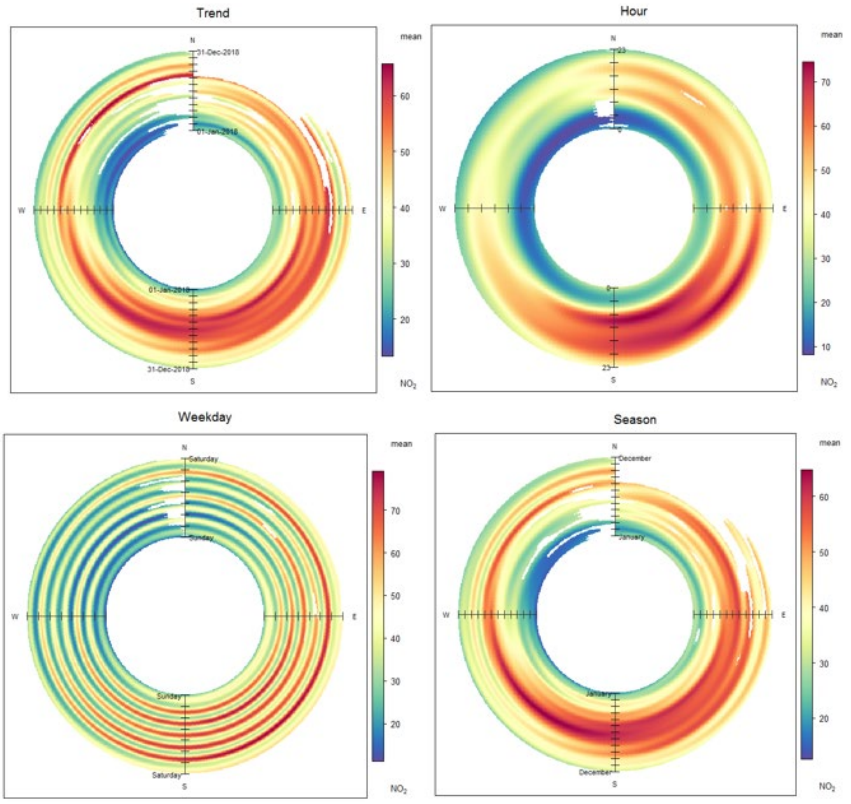

Figure 62 PolarAnnulus plots for NO_2 at Queen Street, 2018.

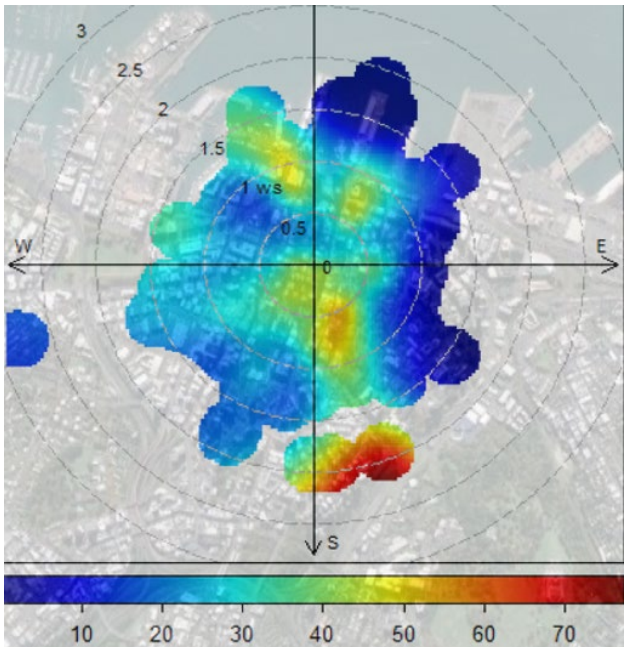

Figure 63 Polar plot showing NO_2 concentrations at Queen Street in relation to wind speed and direction, 2018.

In-depth research of city centre traffic pollution carried out by Talbot and Lehn 2018 revealed that 12% of weekday on-road fleet on upper Queen Street are diesel-powered buses. It is likely that these buses, plus the increase in construction vehicles, is driving up concentrations, along with increased building height and the blocking off Queen Street at the lower end, decreasing ventilation when the wind comes from the southerly sector.

2.5 Glen Eden

2.5.1 Site description

The Glen Eden monitoring site is set away from immediate air pollution sources and as such, can be referred to as an urban background site (Figure 64). Most houses in the immediate area date from the 1980s and newer (medium-sized sections, few chimneys), but the area to the north has more older houses (1960s) on larger sections, approximately 75% with chimneys. Meteorological data is provided in the appendix (Figure A7).

Figure 64 Map of the location of Glen Eden air quality monitoring site (Google Maps 2018).

2.5.2 PM_{10} trends and analysis

Figure 65 Theil-sen deseasonalised trends for PM_{10} at Glen Eden, 2006-2018 (top) and 2013-2018 (bottom).

Table 15 Mann-Kendall seasonal statistical test for PM_{10} at Glen Eden

Glen Eden: Mann-Kendell Seasonal						
2006- 2018				2013 - 2018		
Stats		**PM10**		**Stats**		**PM10**
probability		0.560		probability		0.870
Z		0.237		Z		-1.121
p		0.813		p		0.262
Theil-Sen deseasonal p		<0.05		Theil-Sen deseasonal p		<0.01

The deseasonalised long-term plots for Glen Eden for PM_{10} show a small but statistically significant downward trend (P<0.1). The Mann-Kendall seasonal analysis shows a slight increase that is not statistically significant. Both show a downward trend

when for the short -term trend 2013-2018 (Figure 66 – lower). Theil Sen shows a stronger trend (P<0.01).

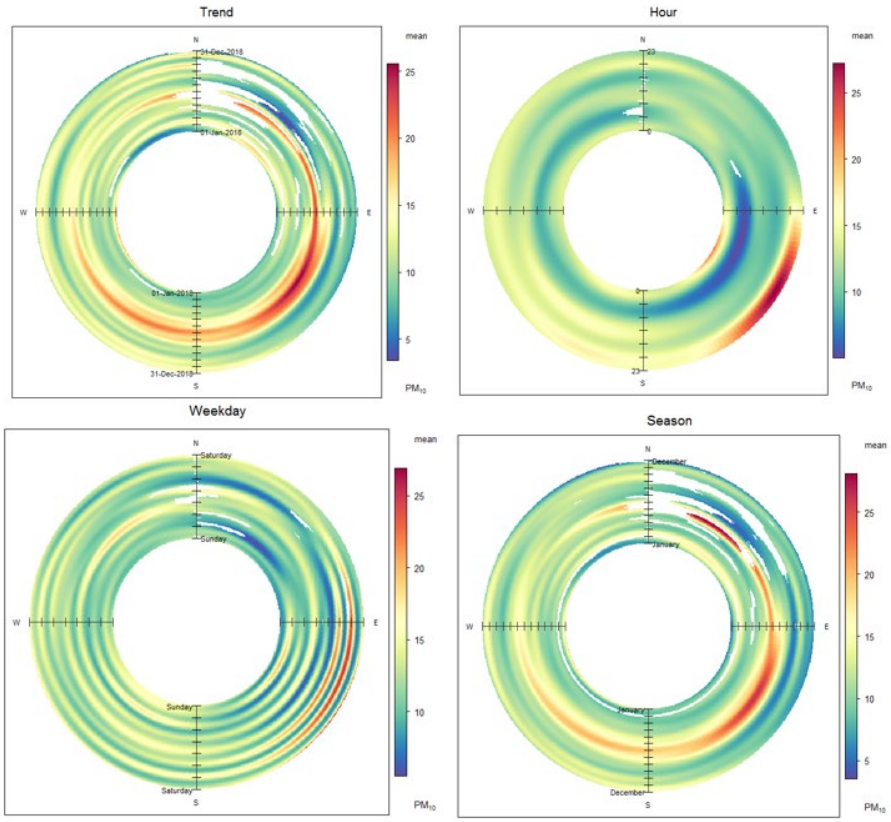

Figure 66 PolarAnnulus plots for PM_{10} at Glen Eden, 2018.

Both seasonal and annual variability are evident at Glen Eden (Figure 66). Winter shows the highest concentrations with the period between June and August showing notably higher concentrations of PM_{10} (Lower plot). Seasonal trends show that when winds come from the southeast sector and later in the evening during winter, PM_{10} concentrations are highest (Figure 67). This suggests that woodsmoke from home heating is likely to be a key component of peak PM_{10} concentrations at Glen Eden. Marine aerosol will also contribute to total PM_{10}, although source apportionment data is not available at Glen Eden.

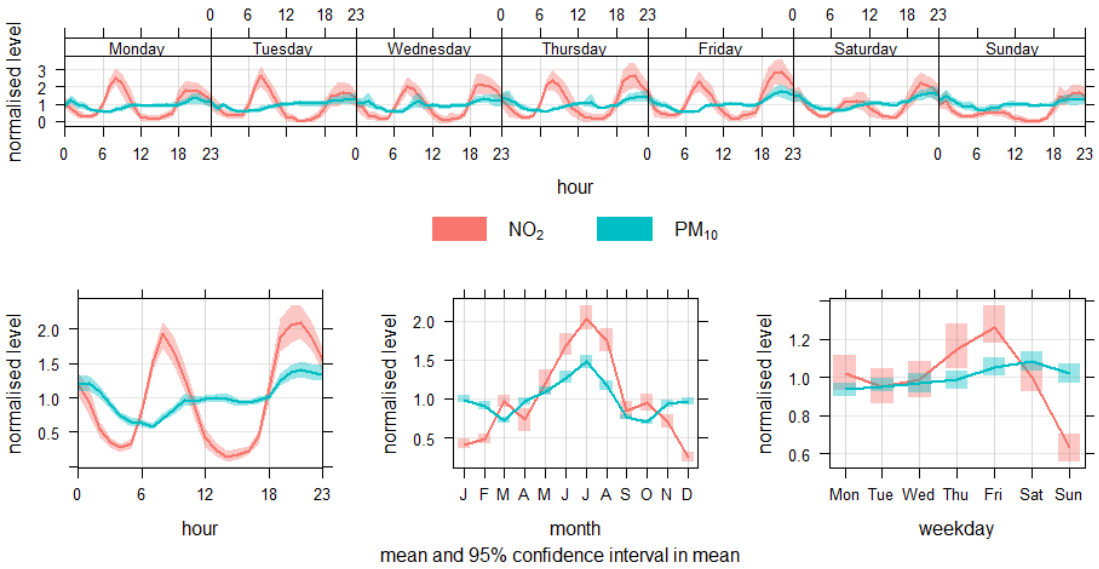

Figure 67 Time trend plots for PM_{10} and NO_2 at Glen Eden, 2006-2018.

Figure 67 plots show increases in both PM_{10} and NO_2 during the evening, later in the week and during the winter months. This would appear to confirm that the main but not only contributor to PM_{10} is wood smoke. Despite Glen Eden's representation as an urban background air quality monitoring station there is still a notable contributing factor for NO_2 emitted from on-road local combustion sources, evident by the morning and evening peaks in concentrations (Figure 67 lower left).

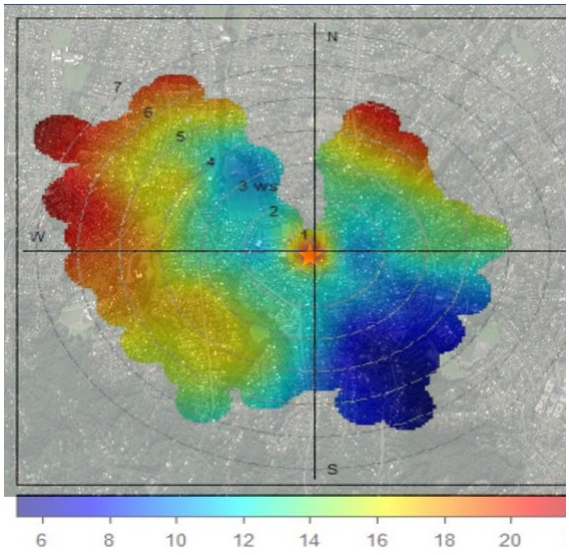

Figure 68 Polar plot showing PM_{10} concentrations at Glen Eden in relation to wind speed and direction, 2018.

When wind speed and direction are considered alongside PM_{10} concentrations, the likely influence of marine aerosol from the west becomes apparent (Figure 68). The

strongest winds bring sea salt across from the west coast. There is also a PM_{10} bulge from the northeast during high wind speeds, this is likely from Waitemata harbour or the Pacific.

2.5.3 NO_2 trends and analysis

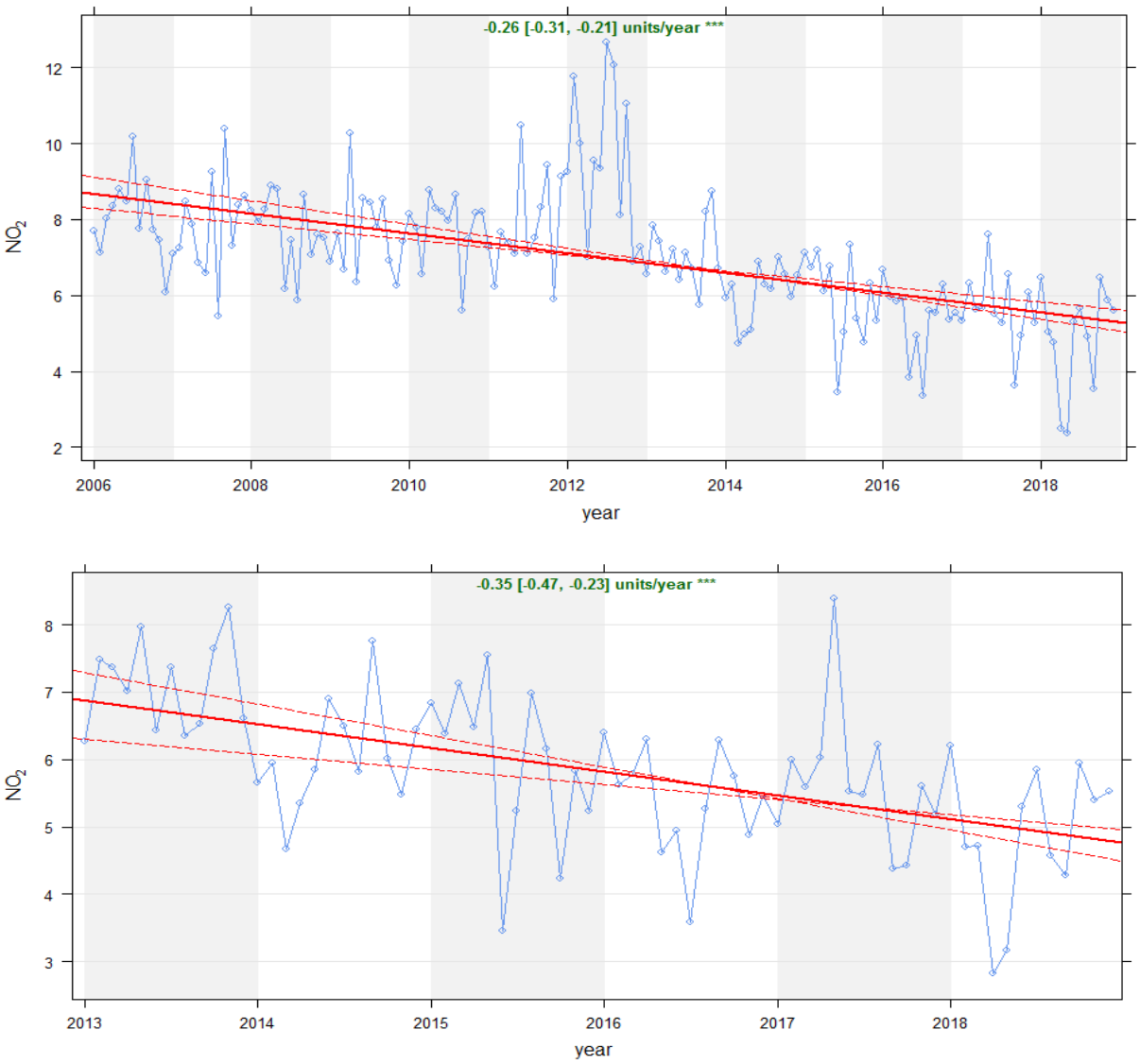

Figure 69 Theil-sen deseasonalised trends for NO_2 at Glen Eden, 2006-2018 (top) and 2013-2018 (bottom).

The deseasonalised long-term trend analysis 2006-2018 (Figure 69-top) shows a strong downward trend (P=<0.001). The rate of NO_2 decline has remained consistent at around 0.3 µg/m^3. The seasonal Mann-Kendall trends are similar but show that a more significant downward trend in the long-term data (Table 16 P=0.005) than in the 2013-2018 trend (P=0.013).

Table 16 Mann-Kendall seasonal statistical test for NO_2 at Glen Eden

Glen Eden: Mann-Kendell Seasonal						
2006- 2018				2013 - 2018		
Stats		**NO_2**		**Stats**		**NO_2**
probability		0.997		probability		0.994
Z		-2.811		Z		-2.490
p		0.005		p		0.013
Theil-Sen deseasonal p		<0.001		Theil-Sen deseasonal p		<0.001

The NO_2 polar plot shows that the NO_2 concentrations at Glen Eden are dominated by local sources which are most notable at periods of low wind speed most likely due to diffuse NO_2 emitted from surrounding roads (Figure 70).

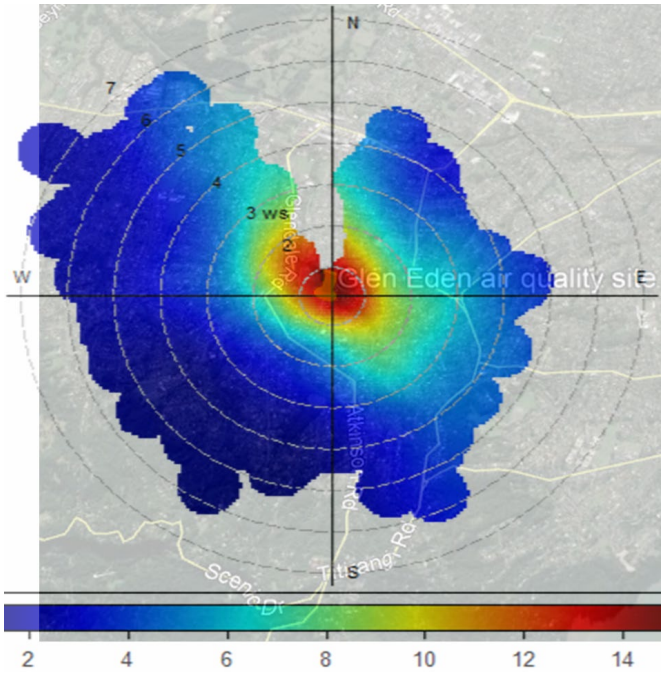

Figure 70 Polar plot showing NO_2 concentration at Glen Eden in relation to wind speed and direction 2018.

Analysis at Glen Eden shows that most weekdays have strong diurnal pattern of concentrations for NO_2 (Figure 71). Seasonality is strongly biased towards winter months and again come largely from the southeast sector. Although higher in winter, peak NO_2 concentrations are less focused on winter months and are spread across the year from March – October (Figure 71 – bottom right); evening NO_2 concentrations are higher than those of the morning.

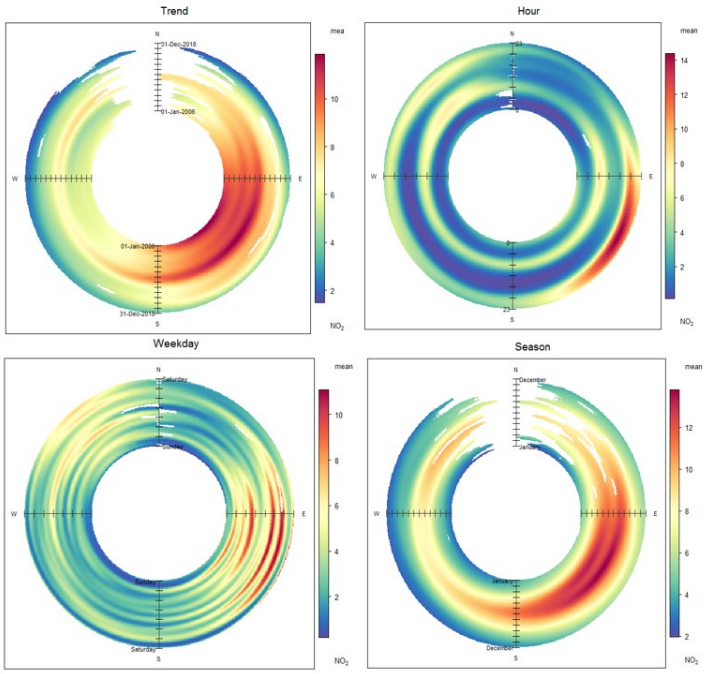

Figure 71 PolarAnnulus plots for NO_2 at Glen Eden, 2018.

2.6 Pakuranga

2.6.1 Site description

The Pakuranga air quality monitor is in the southwest corner of Bell Reserve about 75 m from Pakuranga Road (Figure 72). The Pakuranga monitor only measures PM_{10} and meteorology. Houses in the area are of mixed age - from 1960s to <5 years old, mostly on medium sized sites. About 50% of houses have chimneys. Pakuranga Road is a major arterial road carrying around 25,000 vehicles per day. The wind speed and direction for Pakuranga air quality monitoring site is dominated by a south-westerly flow (Figure A8).

Figure 72 Map of the location of Pakuranga air quality monitoring site (Google Maps 2018).

2.6.2 PM_{10} trends and analysis

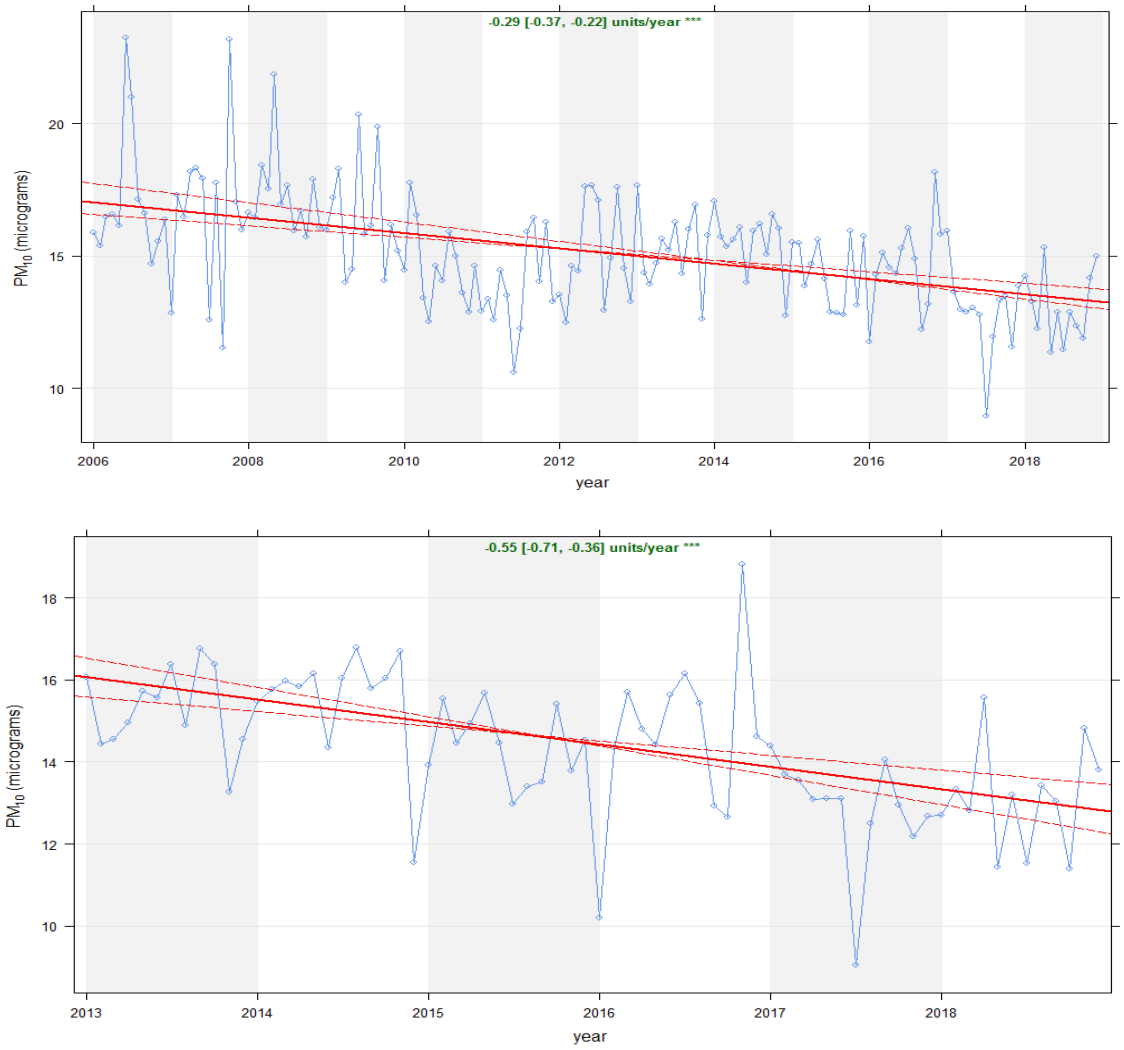

Figure 73 Theil-sen deseasonalised trends for PM_{10} at Pakuranga, 2006-2018 (top) and 2013-2018 (bottom).

Both deseasonalised long and short-term trend plots show statistically significant decreases in PM_{10} concentrations at Pakuranga (P=<0.001) (Figure 73). There is a notable plateau shift at the end of 2009-2010 which is shown across most of the air quality sites and is likely due to improvements in on-road fuel during this period. There is another fall in PM_{10} concentrations during 2017 which has helped to continue to lower concentrations. There is no source apportionment data for PM_{10} at Pakuranga.

Table 17 Mann-Kendall seasonal statistical test for PM_{10} at Pakuranga

Pakuranga: Mann-Kendell Seasonal						
2006- 2018				2013 - 2018		
Stats		**PM10**		**Stats**		**PM10**
probability		1.000		probability		0.999
Z		-4.426		Z		-3.008
p		0.000		p		0.003
Theil-Sen deseasonal p		<0.001		Theil-Sen deseasonal p		<0.001

Pakuranga shows the highest concentrations of PM_{10} in the evening and during the working week (Figure 74). There is also a smaller increase in morning concentrations indicative of road emissions. The degree of variability within the 95% confidence interval for the early hours imply that wood smoke impacts this site on occasions.

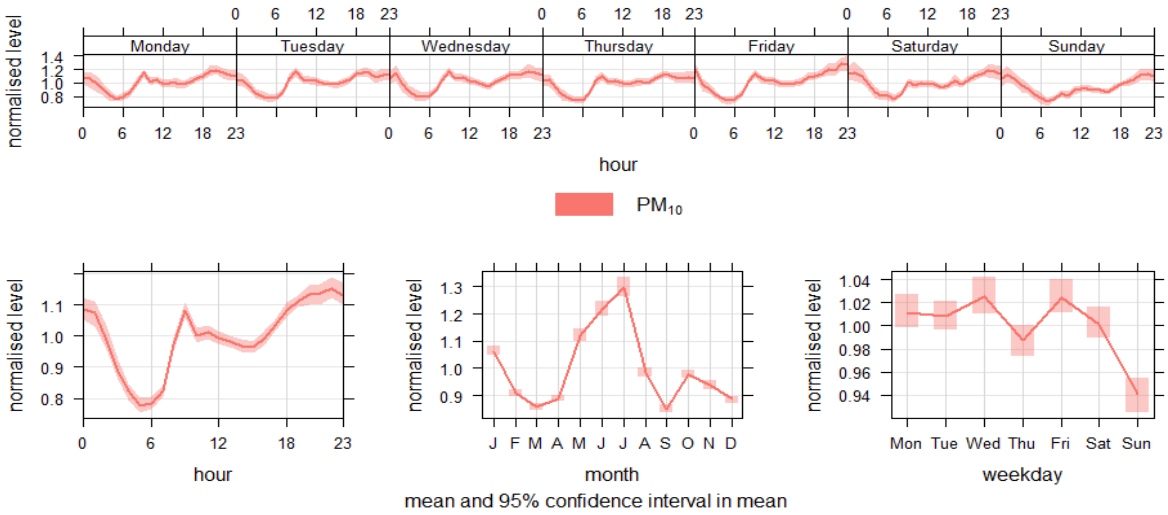

Figure 74 Temporal variability for PM_{10} at Pakuranga, including hourly, weekday and monthly plots, 2018.

A daytime source is evident at this site, while peak concentrations often occur during the evening and into the early hours of the morning. Seasonal analysis shows a strong winter component (Figure 75), and the monthly plot (Figure 74) shows the highest concentrations occur in July.

Pakuranga recorded the most recent exceedance of the National Environmental Standard for PM_{10} in the Auckland Region, with a concentration of 51.5 µg/m³ recorded on a cold and still day in the winter of 2013.

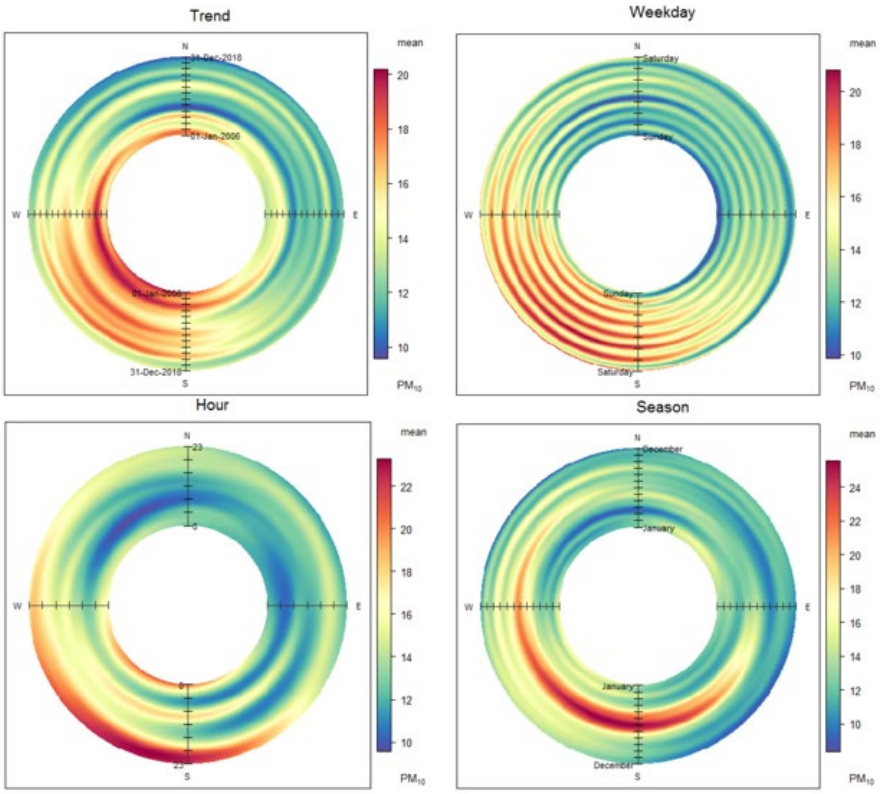

Figure 75 PolarAnnulus plots for PM_{10} at Pakuranga, 2018.

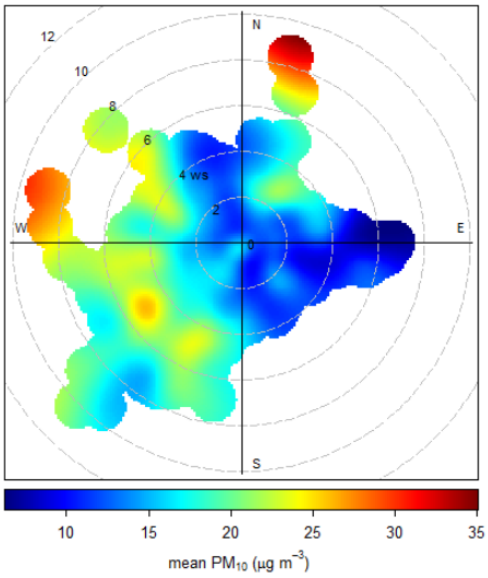

Figure 76 Polar plot showing PM_{10} concentrations at Pakuranga in relation to wind speed and direction, 2018.

The main origin of PM_{10} at Pakuranga is during moderate winds from the west and northern sectors (Figure 76). Winds from these directions would likely carry woodsmoke from the older suburbs of Point England, Panmure and Half-Moon Bay, and marine aerosol from the Tasman Sea, Pacific Ocean and nearby Waitemata Harbour.

2.7 Patumahoe

2.7.1 Site description

Located within the Crop and Food Research Station at Cronin Road (Figure 77), Patumahoe air quality station provides Auckland with regional background air quality data. The site is located approximately 2.5 km west of the Pukekohe urban area. The surrounding area is predominantly used for horticulture (market gardening) and pastoral agriculture. Occasional spikes in PM_{10} from nearby rural activities such as fertiliser application, crop tilling and green waste burning have been recorded. There are only lightly used roads immediately surrounding the monitoring station. There is no meteorological data collected at Patumahoe station.

Figure 77 Map of the location of Patumahoe air quality monitoring site (Google Maps 2018).

2.7.2 PM_{10} trends and analysis

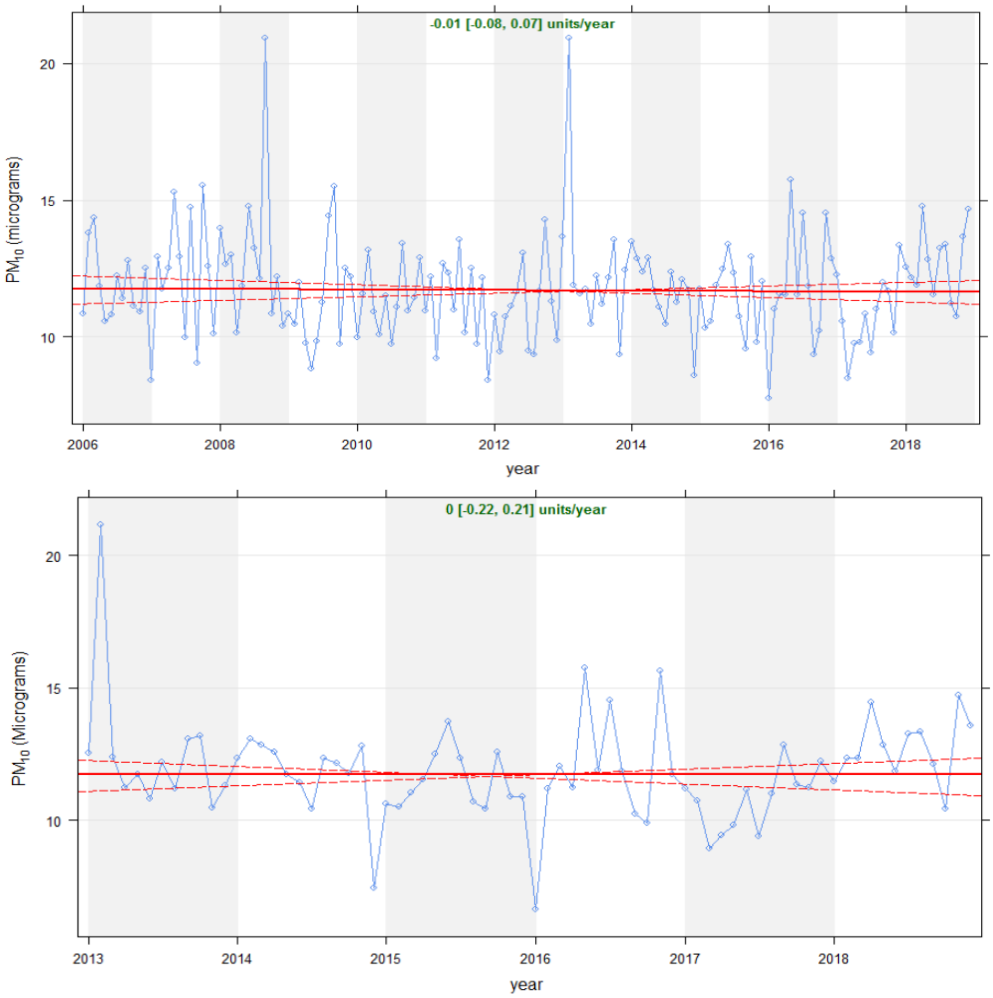

Figure 78 Theil-sen deseasonalised trends for PM_{10} at Patumahoe, 2006-2018 (top) and 2013-2018 (bottom).

The deseasonalised long-term and short-term trend for PM_{10} at Patumahoe is neutral (Figure 78). As Auckland's regional background site this indicates that there is little change in the direct source contributions around Patumahoe. However, since early 2017, there does appear to be a steady increase in PM_{10} concentrations. Whether this indicates an emerging trend resulting from residential development in Pukekohe West recently spreading to within 1.5 km of the site or is simply natural variability, is not yet understood. This recent trend is not yet statistically significant.

Table 18 Mann-Kendall seasonal statistical test for PM_{10} at Patumahoe

Patumahoe: Mann-Kendell Seasonal						
2006- 2018				2013 - 2018		
Stats		**PM10**		**Stats**		**PM10**
probability		0.702		probability		0.870
Z		-0.576		Z		0.730
p		0.564		p		0.465
Theil-Sen deseasonal p		No trend		Theil-Sen deseasonal p		No trend

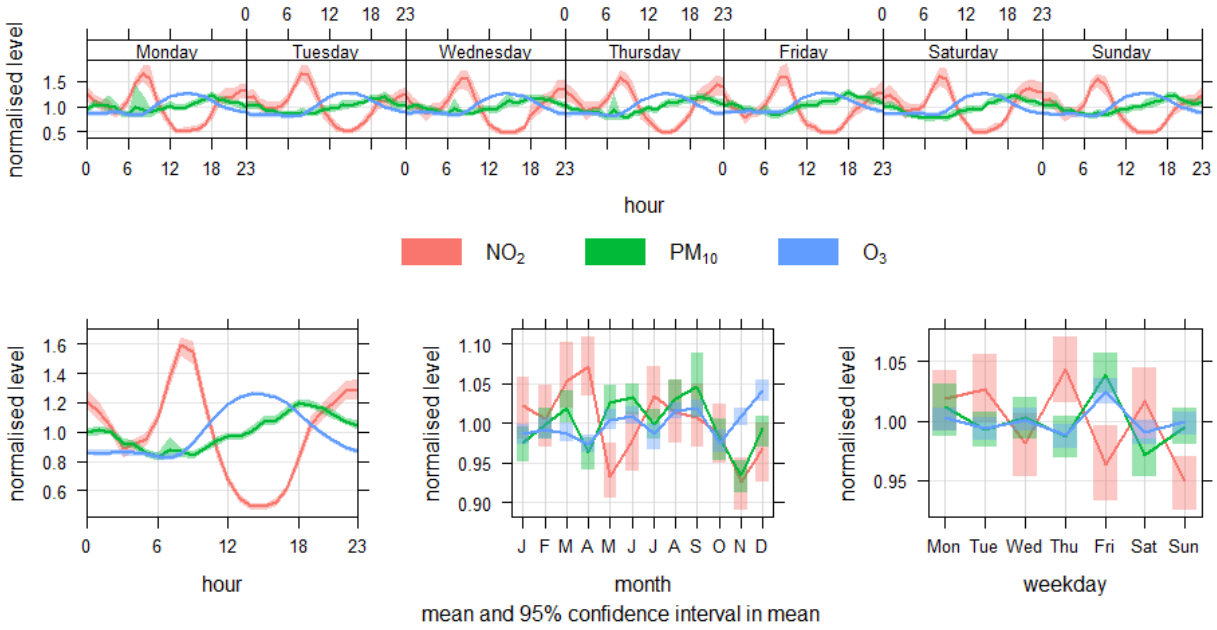

Figure 79 Temporal variability for PM_{10}, O_3 and NO_2 at Patumahoe, including hourly, weekday and monthly plots, 2006-2018.

2.7.3 NO_2 trends and analysis

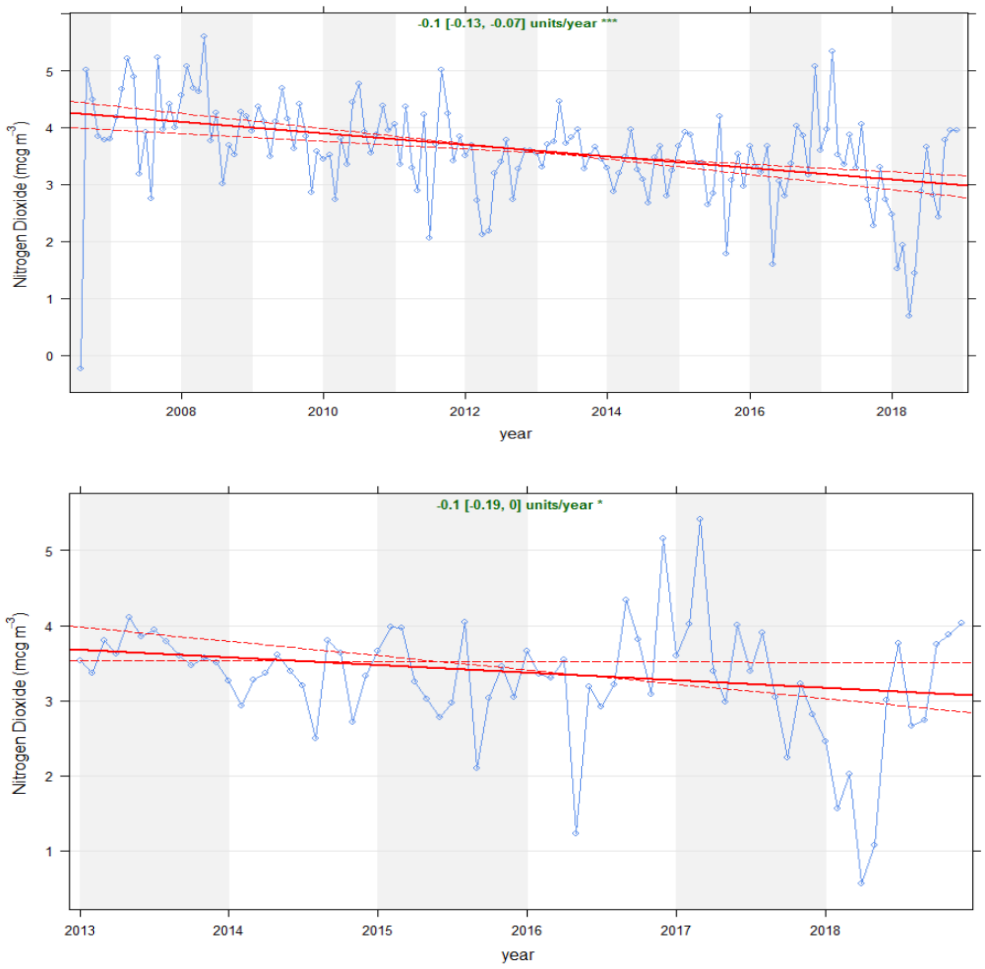

Figure 80 Theil-sen deseasonalised trends for NO_2 at Patumahoe, 2006-2018 (top) and 2013-2018 (bottom).

Interestingly, the deseasonalised long-term trend for NO_2 at Patumahoe shows a statistically significant decrease in concentrations (Figure 80 – top plot). As this site is away from direct sources such as major roads, this result indicates that the regional airshed has lowered its total NO_2 concentrations. The short-term plots (Figure 80 – lower) have a reduced rate of reduction (P=0.1).

Table 19 Mann-Kendall seasonal statistical test for NO_2 at Patumahoe.

Patumahoe: Mann-Kendell Seasonal						
2006- 2018				2013 - 2018		
Stats		**NO_2**		**Stats**		**NO_2**
probability		0.945		probability		0.802
Z		-1.651		Z		-0.772
p		0.099		p		0.440
Theil-Sen deseasonal p		<0.001		Theil-Sen deseasonal p		<0.01

2.7.4 Ozone trends and analysis

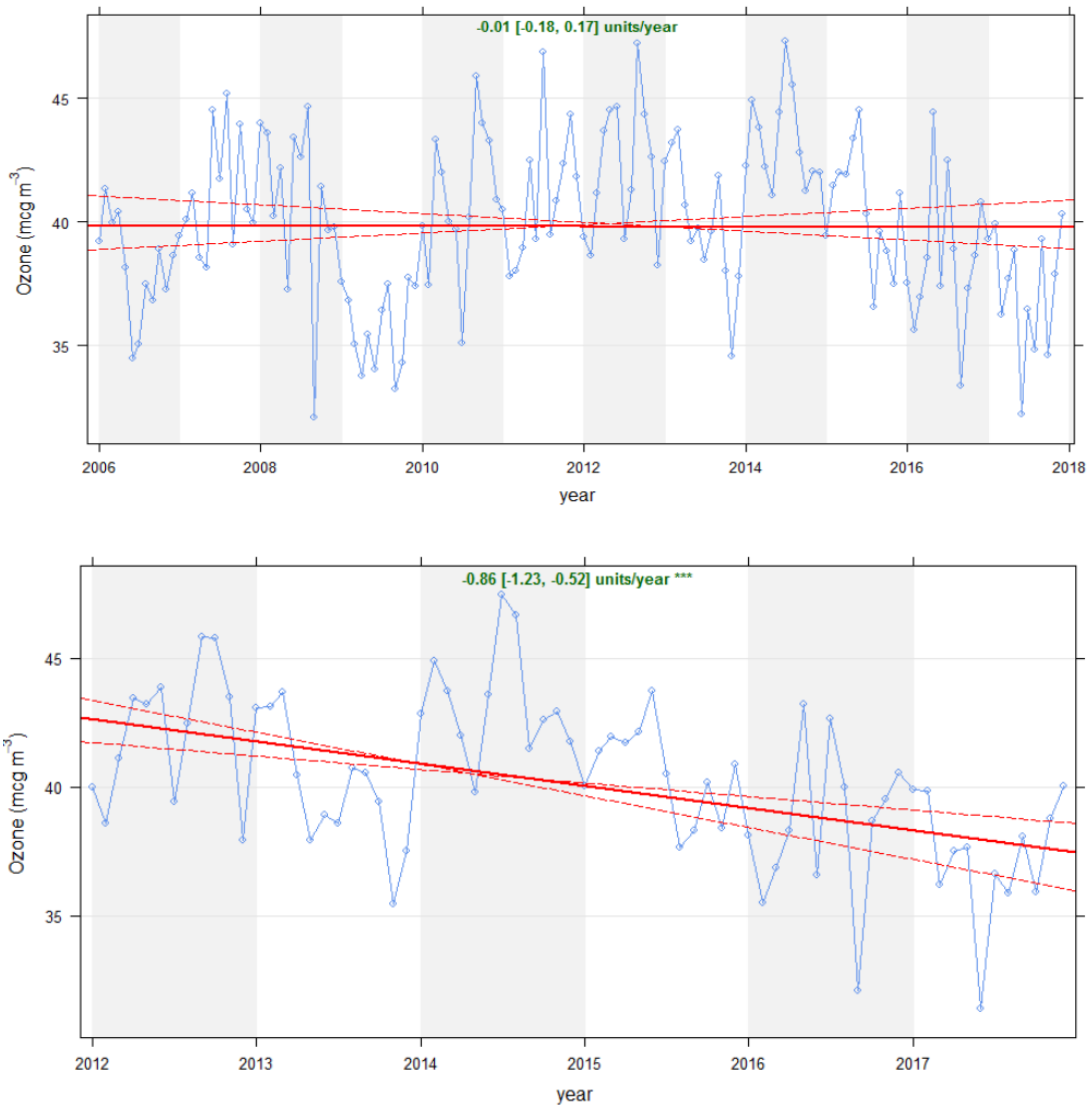

Figure 81 Theil-sen deseasonalised trends for O_3 at Patumahoe, 2006-2017 (top) and 2013-2017 (bottom).

Ground-level ozone is an air pollutant that predominantly arises from an oxidation reaction with nitrogen oxides from combustion activities. Patumahoe is the only site where ozone monitoring has been undertaken throughout the 2006 to 2018 period. The long-term ozone data from Patumahoe shows no statistically significant change; however, there has been a notable drop in the short-term deseasonalised trend analysis (P=<0.001, Figure 81).

Table 20 Mann-Kendall seasonal statistical test for O_3 at Patumahoe

Patumahoe: Mann-Kendell Seasonal						
2006- 2018				2013 - 2018		
Stats		**O_3**		**Stats**		**O_3**
probability		0.985		probability		0.600
Z		0.463		Z		-0.299
p		0.643		p		0.765
Theil-Sen deseasonal p		No trend		Theil-Sen deseasonal p		<0.001

Temporal investigations for ozone in Patamahoe reveal daily afternoon and summer increases in concentrations (Figure 79). This is expected due to the secondary processes necessary for ozone formation and its relationship with NO_2 formation and destruction. The day of week and month plots show no overlying trend. The PM_{10} concentrations show highest concentrations in the evening while ozone concentrations increase with decreasing NO_2, a predictable inverse relationship given the relationship between NO_2 and O_3 in the presence of sunlight (Xie et al., 2014).

3.0 Conclusions

Trends in air pollution datasets collected from seven sites across Auckland's air quality monitoring network are reported here. Long-term (2006-2018) and short-term (2013-2018) datasets are investigated through deseasonalised and seasonalised methods including Mann-Kendall and Theil Sen statistical methodologies. This 'broad-brush' approach enables comparison with other New Zealand councils' trend analyses which usually employ one or both methodologies.

The results for most representative monitoring locations show statistically significant decreasing trends for PM_{10} and $PM_{2.5}$ over both the short- and long-term timeframes. This downward trend is most pronounced in the earlier part of the analysed period, 2006-2010. The city centre monitoring site at Queen Street is not following this downward trend and has shown significant increases in $PM_{2.5}$ and PM_{10} for the short-term 2013-2018 deseasonalised analysis ($P<0.001$ and $P<0.1$, respectively).

Source apportionment data has been included in the analysis for PM_{10} and $PM_{2.5}$ where available from Davy et al., 2017 to help elucidate probable emission sources and compositions. It is considered likely that reductions in $PM_{2.5}$ discharged from vehicles over approximately five years from 2006 are largely responsible for the long-term PM_{10} decreases. Almost 50 per cent of annual PM_{10} across the Auckland network is marine aerosol which is generally considered as a static natural source and therefore acts to dampen upward or downward trends. However, marine aerosol concentrations across Auckland were reported by Davy et al., 2017 to be unexpectedly and significantly decreasing between 2006 and 2013 and therefore is also likely responsible for some of the total decreasing trend reported here.

NO_2 concentrations decreased significantly across the network over the long-term; however, the shorter-term trends from 2013 to 2018 at road-side sites report levels plateauing or increasing. The earlier decreases in NO_2 and $PM_{2.5}$ coincide with periods of increasing fuel and vehicle emission quality standards. However, the more-recent plateau or increase in NO_2 since approximately 2012 coincides with a period of increased traffic volumes on Auckland's roads (Sridhar & Metcalfe, 2019). This recent increasing trend in NO_2 has been so significant at peak traffic monitoring sites that Queen Street exceeded health-based ambient air quality targets for NO_2 (annual average) for 2017 and 2018.

4.0 References

Bond, Tami, S. Doherty, D. Fahey, P. Forster. et al., 2013. "Bounding the role of black carbon in the climate system: A scientific assessment." *Journal of Geophysical Research: Atmospheres*, 118, 5380-5552.

Carslaw, David, and K. Ropkins. 2012. “Openair – An R Package for Air Quality Data Analysis.” *Environmental Modelling & Software* 27-28 (January): 52-61.

Carslaw, K. S., O. Boucher, D. V. Spracklen, G. W. Mann, J. G. L. Rae, S. Woodward, and M. Kulmala. 2010. “A Review of Natural Aerosol Interactions and Feedbacks within the Earth System.” *Atmospheric Chemistry and Physics* 10 (4): 1701-37. https://doi.org/10.5194/acp-10-1701-2010.

Crimmins, Paul, K. Dirks, and J. Salmond. 2019. “The challenge of quantifying black carbon emissions: A case study from Auckland, New Zealand.” *Air Quality and Climate Change*, 53(1) 12-18.

Davy, Perry, T. Ancelet, A. Markwitz, and W. Trompetter. 2017. *Source Apportionment and Trend Analysis of Air Particulate Matter in the Auckland Region.* Auckland Council Technical Report TR2017/001. GNS Science.

Dirks, Kim, J. Scarfe, N. Talbot, R. Marshall, and J. Salmond. 2017. “A Statistical Analysis of the Relationship between Brown Haze and Surface Air Pollution Levels on Respiratory Hospital Admissions in Auckland, New Zealand.” *Climate* 5 (4).

Font, Anna, T. Baker, I. Mudway, E. Purdie, C. Dunster, and G. Fuller. 2014. “Degradation in Urban Air Quality from Construction Activity and Increased Traffic Arising from a Road Widening Scheme.” *Science of The Total Environment* 497-498 (November): 123-32.

Helsel, Dennis and R. Hirsch. 2002. *Statistical Methods in Water Resources*. US Geological Survey.

Janssen, Nicole, G. Hoek, M. Simic-Lawson, et al., 2011. “Black Carbon as an Additional Indicator of the Adverse Health Effects of Airborne Particles Compared with PMx.” *Environmental Health Perspectives* 119 (12): 1691-99. https://doi.org/10.1289/ehp.1003369.

Karagulian, Federico, C. Belis, C. Dora, A. Prüss-Ustün, S. Bonjour, H. Adair-Rohani, and M. Amann. 2015. “Contributions to Cities’ Ambient Particulate Matter (PM): A Systematic Review of Local Source Contributions at Global Level.” *Atmospheric Environment* 120 (November): 475-83. https://doi.org/10.1016/j.atmosenv.2015.08.087.

Kuschel, Gerda, J. Metcalfe, E. Wilton, J. Guria, S. Hales, K. Rolfe, and A. Woodward. 2012. *Updated Health and Air Pollution in New Zealand Study.” Health Study.* Prepared for Health Research Council of New Zealand, Ministry of Transport, Ministry for the Environment and New Zealand Transport Agency.

Longely, Ian, J. Salmond, K. Dirks, D. Welch, D. Shepherd, S. Grange, G. Olivares, G. Miskell. 2014. *Personal Exposure to Noise and Air Pollution (PENAP) in the Queen Street Valley, Auckland*. Auckland Council Technical Report TR2014/036.

Metcalfe, Jayne, L. Wickham, S. Sridhar. 2018. *Auckland air emissions inventory 2016 – home heating.* Auckland Council Technical Report TR2018/018.

Sridhar, Surekha, J. Metcalfe. 2019. *Auckland air emissions inventory 2016 - transport (revised).* Auckland Council Technical Report TR2018/016-2.

Talbot, Nick and R. Lehn. 2018. *The impacts of transport emissions on air quality in Auckland's city centre*. Auckland Council Technical Report TR2018/028.
Talbot, Nick and N. Reid. 2017. *A Review of Research into the Effects of Shipping on Air Quality in Auckland: 2006-2016*. Auckland Council Technical Report TR2017/005.
Talbot, Nick, N. Reid, and P. Crimmins. 2017. *Auckland ambient air quality trends for $PM_{2.5}$ and PM_{10} – 2006-2015*. Auckland Council Technical Report TR2017/029.
World Health Organisation (WHO). 2013. *WHO/Europe Air Quality - Review of Evidence on Health Aspects of Air Pollution - REVIHAAP Project: Final Technical Report*.
Wilton, Emily, and J. Caldwell. 2017. Ambient Air Quality Monitoring Report for the Waikato Region -2016." Technical Report 03: Waikato Regional Council.
Xie, Shanju, P. Davy, S. Sridhar, and J. Metcalfe. 2016. "Quantifying Trends of Particulate Matter Emissions from Motor Vehicles in Auckland (New Zealand Collection) - Informit." *Air Quality and Climate Change* 50 (2).
Xie, Shanju, S. Sridhar, J. Metcalfe. 2014. *Auckland Air Emissions Inventory 2006*. Auckland Council Technical Report TR2014/015.

5.0 Appendix

Table A1 Comprehensive list of AUP(OP) Auckland ambient air quality targets

Contaminant	**Target**	**Averaging Time**
Particles less than 10 microns (PM10)	20 µg/m^3	Annual
Particles less than 2.5 microns (PM2.5)	25 µg/m^3	24 hour
	10 µg/m^3	Annual
Nitrogen dioxide (NO2)	100 µg/ m^3	24 hour
	40 µg/ m^3	Annual
Carbon monoxide (CO)	30 mg/ m^3	1 hour
Sulphur dioxide (SO2)	120 µg/ m^3	24 hour
Ozone (O3)	100 µg/ m^3	8 hour
Lead	0.2 µg/ m^3	3 month moving average calculated monthly
Benzene	3.6 µg/ m^3	Annual
Benzo[a]pyrene	0.0003 µg/ m^3	Annual
1,3-Butadiene	2.4 µg/ m^3	Annual
Formaldehyde	100 µg/ m^3	30 minutes
Acetaldehyde	30 µg/ m^3	Annual
Mercury (inorganic)	0.33 µg/ m^3	Annual
Mercury (organic)	0.13 µg/ m^3	Annual
Chromium VI	0.0011 µg/ m^3	Annual
Chromium metal and Chromium III	0.11 µg/ m^3	Annual
Arsenic (inorganic)	0.0055 µg/ m^3	Annual
Arsine	0.055 µg/ m^3	Annual

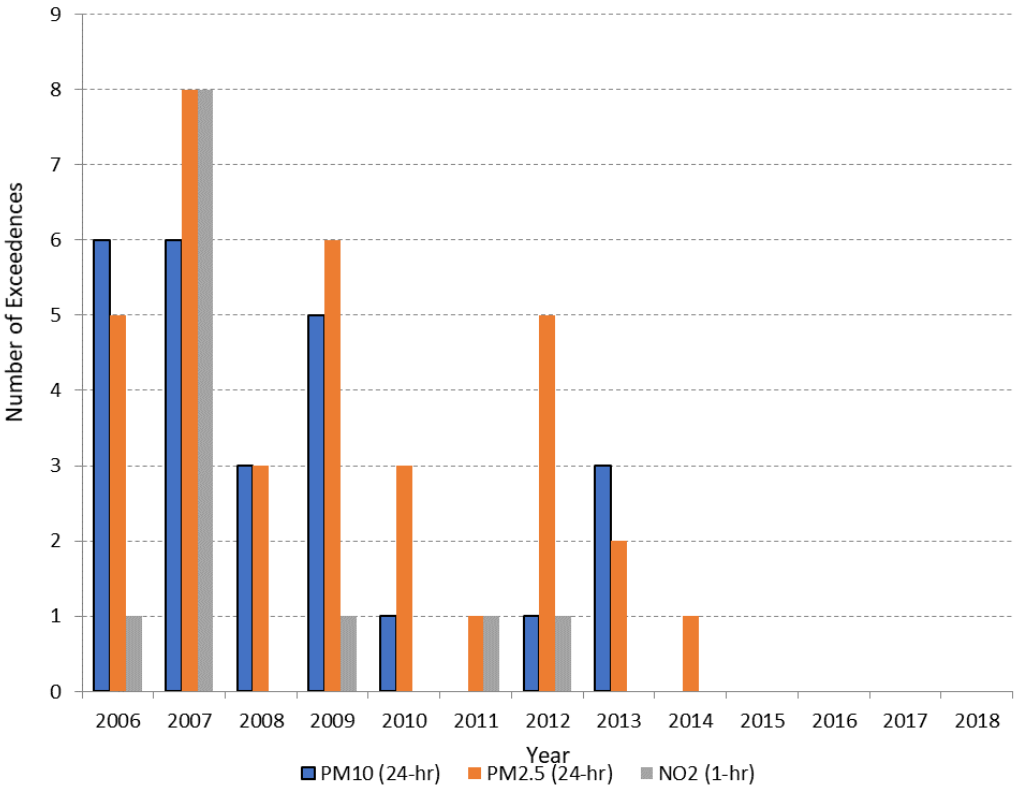

Figure A1 Exceedances of short-term ambient air quality standards recorded in Auckland 2006-2018

Henderson

Meteorology at Henderson

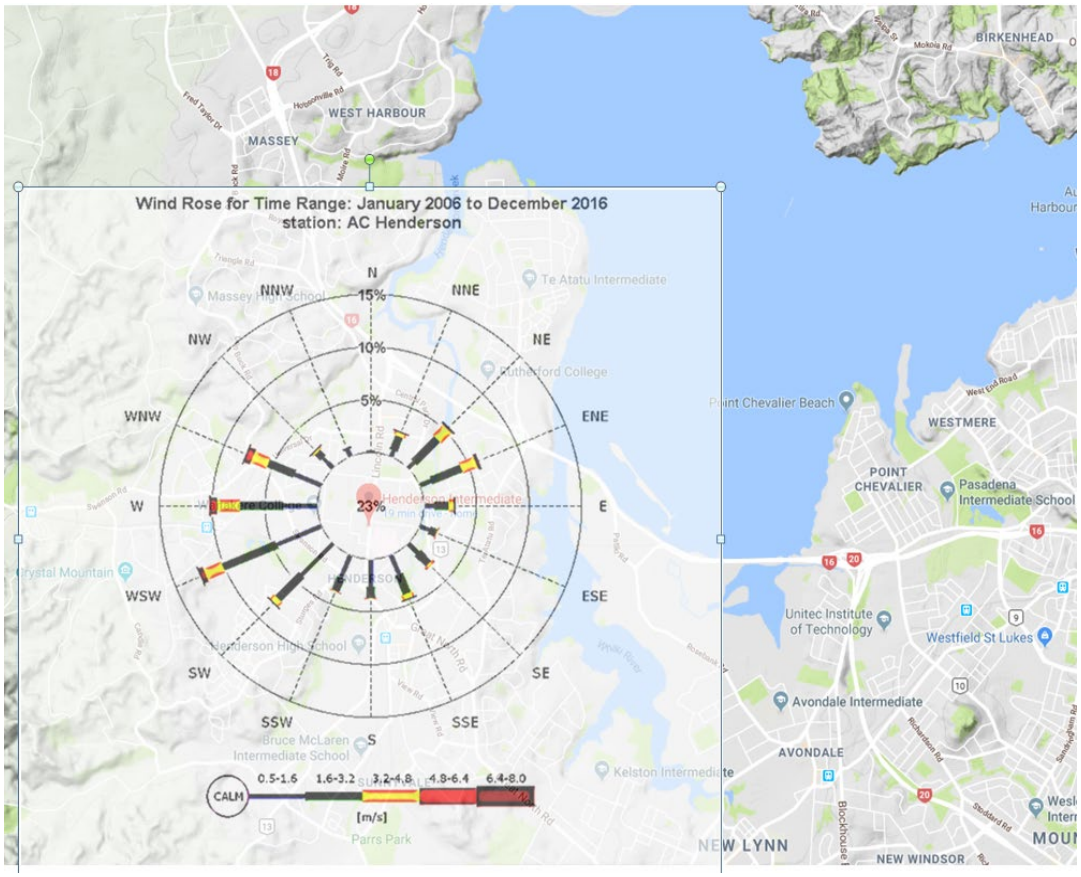

Figure A2 Wind rose for Henderson, 2006-2018.

Takapuna

Meteorology at Takapuna

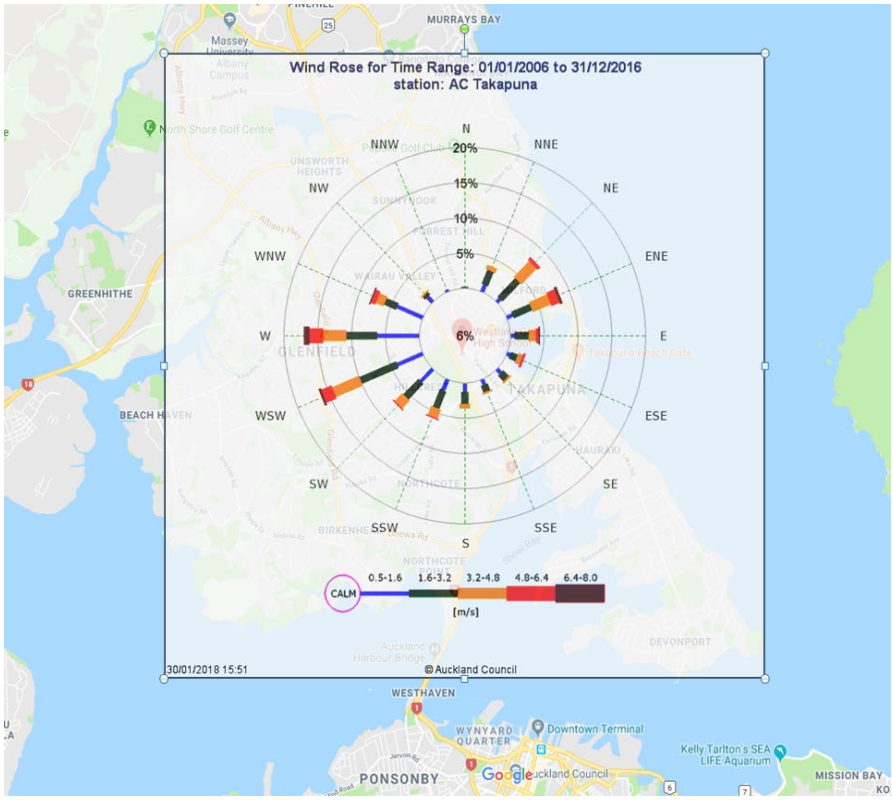

Figure A3 Wind rose for Takapuna, 2006-2018.

Figure A4 Satellite images for the Takapuna site from 2006 (left) and 2016 (right).

Penrose

Meteorology at Penrose

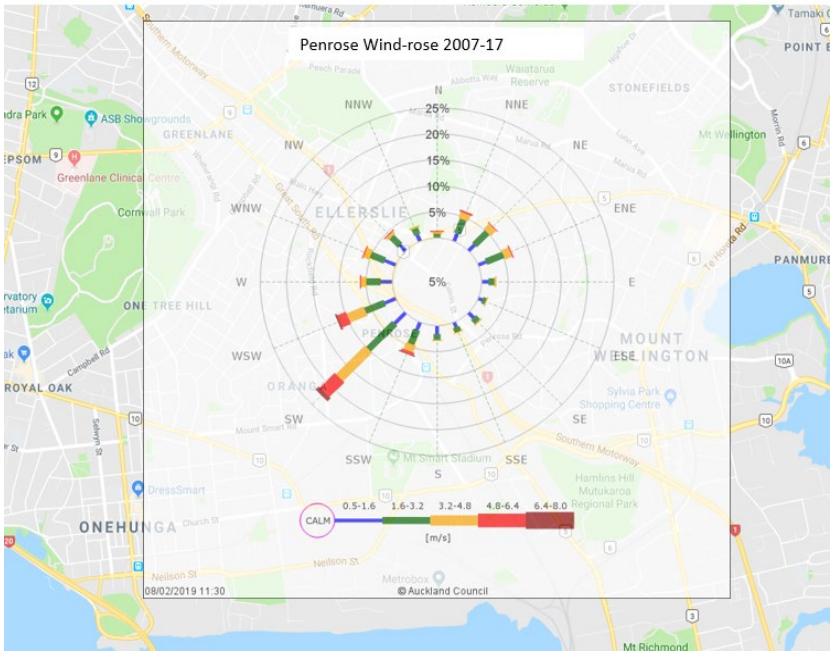

Figure A5 Wind rose for Penrose, 2006-2018.

Queen Street

Meteorology at Queen Street

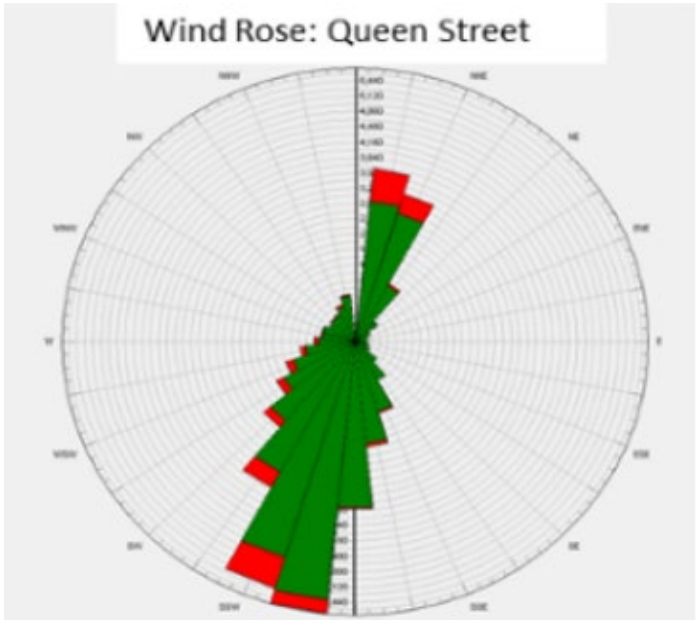

Figure A6 Wind Rose for Queen Street, 2018.

Glen Eden

Meteorology at Glen Eden

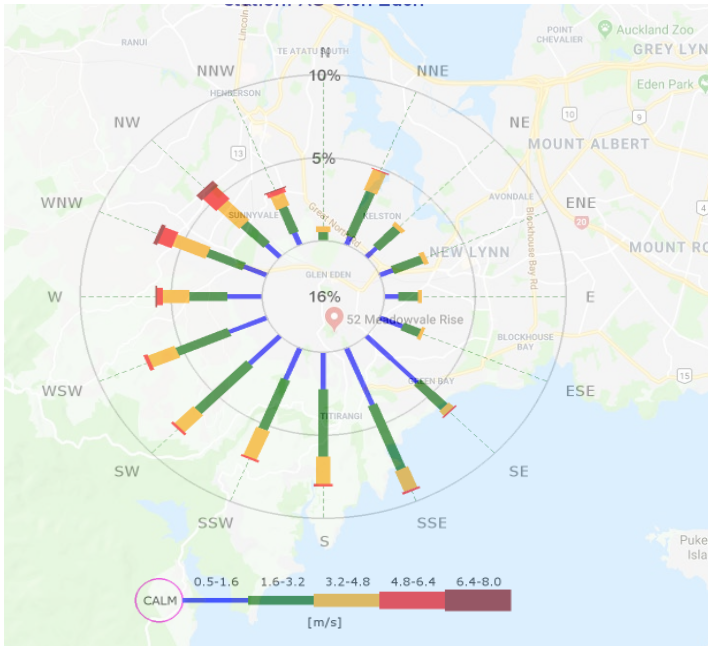

Figure A7 Wind rose for Glen Eden, 2006-2018.

Pakuranga

Meteorology at Pakuranga

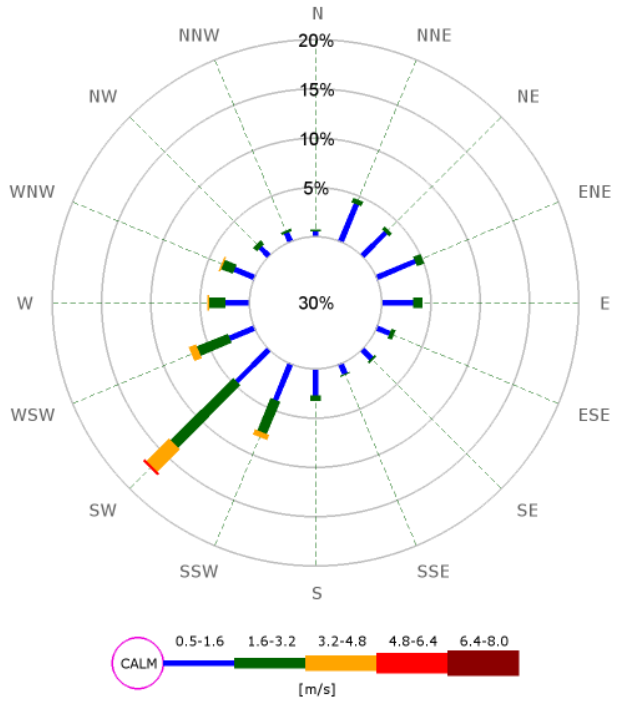

Figure A8 Wind rose for Pakuranga, 2006-2018.

Find out more: phone 09 301 0101, email rimu@aucklandcouncil.govt.nz or visit aucklandcouncil.govt.nz **and knowledgeauckland.org.nz**

Auckland Council
Te Kaunihera o Tāmaki Makaurau